GSI Helmholtzzentrum für Schwerionenforschung GmbH
Technische Universität Darmstadt

Influence of High- and Low-LET Radiation on the Cardiac Differentiation of Mouse Embryonic Stem Cells

Vom Fachbereich Biologie der Technischen Universität Darmstadt
zur
Erlangung des akademischen Grades
eines *Doctor rerum naturalium*
genehmigte Dissertation von

Dipl.-Ing. (FH) Alexander Helm
aus Erbach im Odenwald

1. Referent: Prof. Dr. Marco Durante
2. Referent: Prof. Dr. Paul Layer

Tag der Einreichung: 30.04.2013
Tag der mündlichen Prüfung: 19.07.2013

Darmstadt 2013
D17

Zusammenfassung

Eine Strahlenexposition *in utero* stellt ein Risiko für den sich entwickelnden Embryo dar. Die Effekte von Niedrig-LET Strahlung auf verschiedene Embryonalstadien sind aufgrund von *in vivo*-Studien und epidemiologischen Daten weitestgehend bekannt. Daten für Effekte auf das früheste Stadium, die Präimplantationsphase, und speziell für Effekte von Hoch-LET Strahlung sind dagegen kaum verfügbar. Eine unbeabsichtigte Bestrahlung des frühen Embryos kann jedoch bei diagnostischen oder therapeutischen Anwendungen von ionisierender Strahlung oder bei Strahlenunfällen auftreten. Des Weiteren werden Protonen und Kohlenstoffionen vermehrt in der Strahlentherapie eingesetzt. Eine bessere Risikoabschätzung zur Wirkung von Hoch-LET Strahlung besonders auf den sehr frühen Embryo ist daher von Interesse. Um hierzu beizutragen, wurden in der vorliegenden Arbeit pluripotente embryonale Mausstammzellen verwendet, die mit dem frühen Embryonalstadium der Blastozyste vergleichbar sind. Im Anschluss an die Bestrahlung der Stammzellen mit Kohlenstoffionen (Hoch-LET Strahlen) und Röntgenstrahlen (Niedrig-LET Strahlen) wurden diese als Modell für die frühe Embryonalentwicklung differenziert. Das Auftreten von spontan kontrahierenden Kardiomyozyten wurde als Marker verwendet, um den Einfluss ionisierender Strahlung auf die Differenzierung zu erfassen. Neben weiteren Endpunkten wurden Zellinaktivierung, Zelltod und Genexpression untersucht. Die Experimente zeigten eine Verzögerung der kardialen Differenzierung nach Bestrahlung. Die Resultate weisen auf einen strahleninduzierten Zelltod als Hauptursache für die verzögerte Entwicklung hin. Kohlenstoffionen sind in diesem Zusammenhang effektiver als Röntgenstrahlen.

Abstract

The *in utero* exposure to ionising radiation poses a risk for the radiosensitive developing embryo. Effects of low-LET radiation on different developmental stages of the embryo are relatively well known due to experimental studies and epidemiological data. Data for effects on the very early stage of the embryonic development, particularly the effects of high-LET radiation instead are rather limited. However, unanticipated exposures of the early embryo to ionising radiation may occur through diagnostic or therapeutic applications or through radiation accidents. Additionally, protons and carbon ions are increasingly used in radiotherapy. Thus, a risk estimation of high-LET exposure especially to the early embryo is of a certain importance. To address this topic, pluripotent mouse embryonic stem cells resembling the blastocyst stage were irradiated with high-LET carbon ions or low-LET x-rays and subsequently differentiated to mimic the early embryonic development. The occurrence of spontaneously contracting cardiomyocytes was used as a marker to asses the radiation effects on the differentiation. Among others, cell inactivation, cell death and gene expression were analysed. A delay in the cardiac differentiation after radiation exposure was found. The results point to radiation-induced cell killing as the main effector of the developmental delay. Carbon ions were found to be more effective than x-rays.

Contents

List of figures

List of tables

1. Introduction

1.1 Motivation

Humans are permanently exposed to ionising radiation from a natural background, coming from the earth itself or from space [Bundesamt fuer Strahlenschutz 2009, Hendry et al. 2009]. Ionising radiation comprises both high-LET radiation (such as α-particles or heavy ions) and low-LET radiation (for example γ- or x-rays). Additionally, a large number of people is exposed to ionising radiation coming from diagnostic and therapeutic applications [Bundesamt fuer Strahlenschutz 2001].

The health risk from an exposure to low-LET radiation is known rather well from experimental and epidemiological data. This is not the case for high-LET radiation, where only few data are available. However, risk estimations for high-LET radiation exposure are of a certain importance. Protons and carbon ions are used increasingly in modern cancer therapy due to their advantages compared to conventional radiotherapy [Weber and Kraft 2009, Durante and Loeffler 2010]. Carbon ions are even considered to be used in future for further therapeutic purposes, especially radiosurgery [Bert et al. 2012]. Along with the application of high-LET radiation for medical purposes, unanticipated exposure to it, as can happen in accidents must be considered as well. The nuclear disaster of Fukushima in March 2011 is an example for an accidental exposure of a large number of people [Shigematsu et al. 2012]. Furthermore, since September 11th 2001, nuclear terrorism is an up-to-date topic of public concern [Durante 2003, Williams and McBride 2011]. Large collectives might be exposed and inevitably will include pregnant women.

Hence, there is a certain probability of an unanticipated exposure in the very early pregnancy, when in most cases it is still unknown to the expectant mother. The developing embryo is radiosensitive during the whole prenatal period *in utero* as

indicated by experimental data and epidemiology [ICRP 2003]. However, there are less data available for exposure during the pre-implantation period (i.e. the early phase of pregnancy). They are derived mostly from experiments and suggest lethality of the embryo as the dominating effect following low-LET exposure. Data for high-LET radiation instead are limited.

These issues underpin the necessity of data on high-LET radiation for a better risk estimation during pregnancy. To contribute to this topic, in this work pluripotent mouse embryonic stem cells (mESC) were used as a model system as they resemble the embryonic development. *In vitro* differentiation then was done with cells exposed to low- or high-LET radiation. The radiation influence on pluripotency and differentiation was particularly assessed by investigating the early cardiac development, i.e. the formation of spontaneously contracting cardiomyocytes.

1.2 Physical features of ionising radiation

Radiation is referred to as ionising when the deposition of a sufficient amount of energy leads to ionisation, i.e. the ejection of an electron [Hall 2006]. These electrons are called secondary electrons [Scholz 2003]. The formation of secondary electrons, also called δ-rays crucially contributes to the distribution of the deposited energy by ionisation of further atoms. This process is an important part for all kinds of ionising radiations [ICRU 2011a]. Ionising radiation can be both, particle radiation or electromagnetic radiation (photons). X- and γ-rays are electromagnetic radiation whereas particle radiation comprises electrons, protons, α-particles, neutrons and heavy ions. Despite neutrons, all particle radiation is directly ionising, i.e. they disrupt the atomic structure producing damage by themselves. Photons and neutrons instead are indirectly ionising. Their energy is absorbed and produces charged particles that in turn produce the damage [Hall 2006, ICRU 2011b, Choppin et al. 2002].

The deposited energy (E) in a mass (m) of these processes is described as the absorbed dose (D) and has the unit *Gray* (Gy = J/kg) as shown in equation 1.1 [ICRU 2011b]. The

equivalent dose instead, measured in *Sievert* (Sv) is the absorbed dose multiplied by a quality factor [Durante and Cucinotta 2008].

$$D[Gy] = E[J] / m[kg] \quad (1.1)$$

Concerning the dose deposition radiation can be differentiated in sparsely and densely ionising radiation. Photons and electrons are sparsely ionising radiations [Hall 2006]. A single photon introduces only a small amount of energy in a microscopic volume so that a certain energy amount is deposited by the contribution of several photons. That leads to a random spatial distribution of the incident photons and the resulting secondary electrons, resulting in a homogeneous dose distribution as seen in figure 1.1. Secondary electrons are produced as well by the interaction of densely ionising radiation with matter but the spatial distribution of the deposited energy differs completely from that of photons. The main part of the energy is deposited directly along the trajectory of the particle. The probability of ionisation events rapidly decreases with the distance from the core of the trajectory resulting in a track of a locally concentrated spatial energy deposition (see figure 1.1) [Scholz 2003].

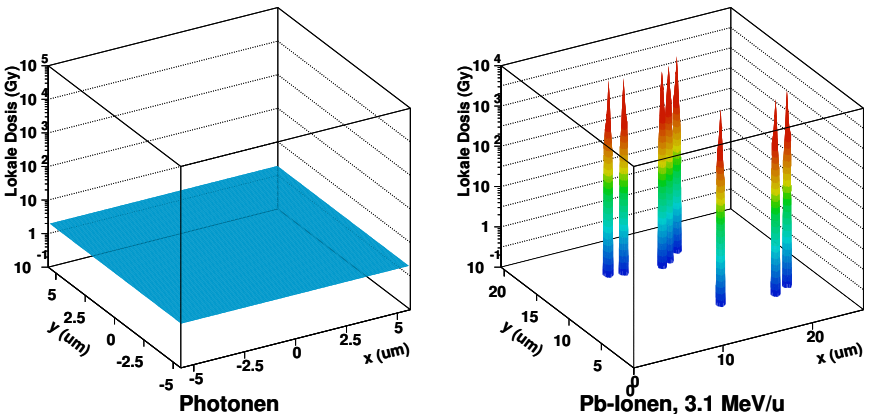

Figure 1.1 *Dose distribution of photons and particles in a microscopic volume. Photons (Photonen) exposure results in homogenously distributed dose whereas particles (here lead ions, Pb-Ionen) deposit the dose non-homogenously and locally concentrated [Courtesy of M. Scholz].*

The energy deposition of radiation is characterised by the linear energy transfer (LET), which is the ratio of deposited energy (dE) per unit track length (ds) as shown in equation 1.2 [Scholz 2003]:

$$LET = dE / ds[keV / \mu m] \quad (1.2)$$

Typically, densely ionising radiation consists of high LET-values and is therefore referred to as high-LET radiation. Sparsely ionising radiation instead has low LET-values. The dose deposition of high-LET particles also depends on the fluence, i.e. the number of incident particles per area, which is given by the equation 1.3

$$D = 1.602 \cdot 10^{-9} \cdot LET \cdot F \cdot (1/\rho) \quad (1.3)$$

where F is the fluence, i.e. number of particles per cm^2 and ρ the density in g/cm^3 [Scholz 2003].

With a decreasing energy of the particle the ionisation density and thus the LET along the trajectory of the particle increase due to the higher probability of interaction with the matter (see figure 1.2). With an increasing depth in a tissue the velocity of the ion is reduced while energy deposition increases until its maximum range. At that point most of the ion's energy is deposited. That maximum is referred to as the Bragg-peak [Scholz 2003].

The depth dose profile of particles therefore is referred to as inverted when compared to photons (see figure 1.2). Cancer therapy with ions takes advantage of that feature. Mostly carbon ions and protons are used due to their particularly advantageous depth dose profiles. Deep-seated tumours can thus be treated with a high dose while the ambient healthy tissue is spared.

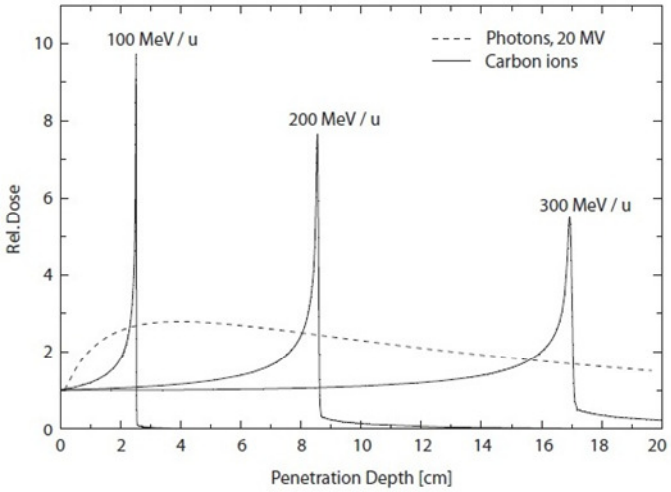

Figure 1.2 *Depth dose profiles of carbon ions versus photons [from Scholz 2003].*

By changing the initial energies of the ions, their range can be varied and the whole tumour can be irradiated using the so called spread out Bragg-peaks (SOBP) or extended Bragg-peaks (see figure 1.3). The deposited dose in the tumour is homogenously distributed due to the superimposition of the single Bragg-curves [Weber and Kraft 2009].

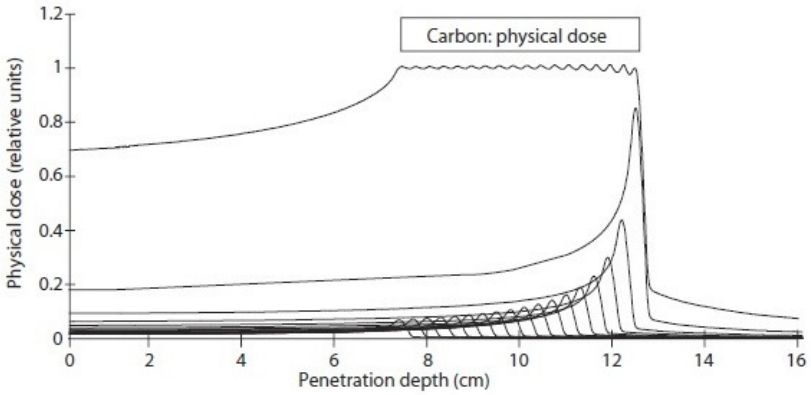

Figure 1.3 *Spread out Bragg-Peak of carbon ions [from Scholz 2003].*

1.3 Biological effects of ionising radiation

The exposure of the human body to ionising radiation can lead to cancer [Shah et al. 2012]. Radiation-induced mutations in the DNA are discussed as a reason for cancer

[Goodhead 2009]. Experimental work has indeed proven a central role for the DNA in the radiation response [Munro 1970]. DNA is considered the main target for the radiation response, however, non-targeted/bystander effects are reported leading to damage in cells that are not directly traversed by radiation [Hei et al. 2011].

Ionising radiation can damage DNA in two ways. If the photon or the particle interacts with the DNA molecule it causes ionisations that result in breaks of the DNA-strands. This is a direct effect. In contrast, the indirect effect is based on the radiolysis of water, i.e. the formation of highly reactive hydroxyl radicals (OH-radicals) that subsequently damage DNA molecules in the environment [Hall 2006]. The resulting types of DNA damage are shown in figure 1.4.

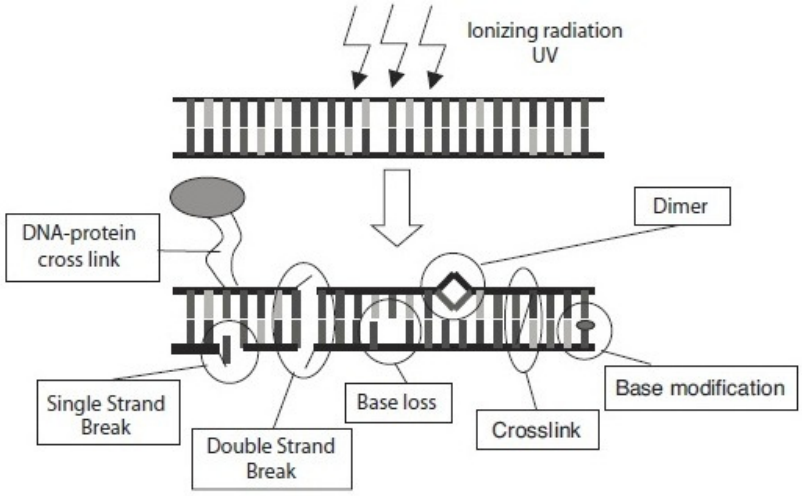

Figure 1.4 *Types of DNA damages induced by ionising radiation [from Scholz 2003].*

Among these damages the double strand breaks (DSBs) are considered the most critical events that lead to lethal lesions. Single strand breaks (SSBs) instead are less critical as they can be repaired readily using the opposite strand as template [Hall 2006]. To encounter the damage eukaryotes have evolved the so called DNA Damage Response (DDR), a complex repair mechanism pathway. It includes both the recognition of DNA damage and the subsequent signalling leading to different repair mechanisms, among them single-strand break repair (SSBR), non-homologous end joining (NHEJ) and homologous recombination (HR) that are particularly important for the repair of ionising

radiation-induced damages [Ciccia and Elledge 2010]. For embryonic stem cells (ESC), HR appears to be the predominant pathway as it conservatively repairs DNA damage using the sequence of the sister chromatid. A non-mutagenic DNA repair is pivotal for stem cells that would pass mutations to all cells they give rise to in an organism [Serrano et al. 2011].

A cell containing DNA damage undergoes cell cycle arrest in order to gain time to activate the repair mechanisms and to prevent the transmission of damaged DNA to daughter cells. Therefore, a molecular mechanism called DNA-damage checkpoints targets directly the major cell-cycle control machinery (checkpoint kinases) and a cell-cycle arrest is either triggered in G1, intra-S or G2 phase, depending on when the damage occurs. Cells thereafter may repair the damage and re-enter the cell cycle (checkpoint recovery). Cells with improperly repaired damage can experience a permanent cell cycle arrest subsequently resulting in senescence or cell death [Medema and Macurek 2012]. ESC were shown to inefficiently activate the checkpoints leading to an increased cell death rate and thus maintaining a pristine cell population [Hong and Stambrook 2004, Desmarais et al. 2012].

Several kinds of cell death can occur following damage, among them necrosis, apoptosis and autophagy. The chosen mechanism depends on the damage the cells experience [Elmore 2007]. Necrotic cell death includes cytoplasmic swelling, rupture of the plasma membrane and a subsequent release of cellular material in the surroundings. Therefore, it is accompanied by inflammation, an adverse effect for the surrounding tissue. Autophagy and apoptosis instead are controlled ways of cell death that do not involve inflammation. Morphological features of cells undergoing apoptosis are chromatin aggregation, condensation (pyknosis) and fragmentation (karyorrhexis) of cell nuclei and cytoplasm developing the so called apoptotic bodies. These criteria were used in the current work to distinguish apoptotic cells (see chapter 2.6). Through phagocytic recognition and uptake they subsequently get removed from a tissue [Kerr et al. 1972, Elmore 2007]. Especially apoptosis is of a certain relevance for radiation induced cell death [Verheij and Bartelink

2000], however, it plays important roles also in other biological processes such as embryonic development [Fuchs and Steller 2011].

Apoptosis is mediated via different complex signalling pathways that all result in the so called execution pathway. Caspases (a group of cysteine proteases), that are activated by the different signalling pathways play a major role in it. Starting from activated initiator caspases, that amplify the protease cascade, the result is the activation of effector caspases, such as caspase-3 (see chapter 2.6) that in turn activate cytoplasmic endonucleases and other proteases, that lead to the classical features of apoptosis as described above [Roos and Kaina 2006, Elmore 2007].

Despite the elimination of damaged cells via apoptosis or senescence, misrepair of DNA damage and subsequent chromosomal rearrangements can occur. Several types of chromosomal aberrations are lethal to the cell. Other types of aberrations instead are consistent with cell viability and hence can be passed to the progeny. The occurrence of these rearrangements is frequently involved in neoplasia and carcinogenesis [Hlatky et al. 2002, Hall 2006]. A transduction of chromosomal aberrations to the progeny of zygotes and mESC exposed to low-LET radiation is reported [Weissenborn und Streffer 1988, Rebuzzini et al. 2012]. In contrast to low-LET radiation, high-LET radiation leads to more complex lesions, for example clustered DSBs, due to the close vicinity of ionisation events. The repair of complex lesions is difficult and thus leads to cell death in most cases. But the residual complex damage of high-LET radiation in surviving cells is of particular concern for carcinogenesis [Maser and DePinho 2002, Cucinotta and Durante 2006]. Along with chromosomal damage, gene expression alterations after exposure to ionising radiation have been reported and are depending on the LET [Ding et al. 2005, Durante and Cucinotta 2008].

The mentioned differences between high- and low-LET radiation in inducing the damages are mainly due to their different dose distribution, leading to differences in their effectiveness, which is estimated by the so called Relative Biological

Effectiveness (RBE). Normally 200 kV or 250 kV photon radiation is used as a reference to judge the RBE for an ion according to the equation 1.4:

$$RBE = D_{photon} / D_{ion}(Isoeffect) \quad (1.4)$$

where D are the absorbed doses of the different radiations. Besides the dose, the RBE further depends on physical factors, like the energy and therefore the LET of particles, the particle type and several biological factors, such as cell type, cell cycle stage and the used endpoint [Goodhead 1999, Weyrather et al. 1999, Scholz 2003, Durante and Loeffler 2010].

1.4 Early embryonic development

Differentiation of embryonic stem cells (ESC) *in vitro* as performed in the present work is a useful tool to study the early embryonic development, especially the early cardiac development. The embryonic development of an organism is a highly complex process. Therefore this chapter gives a brief overview on the early mammalian development with a focus on the heart development. Embryonic development starts with fertilization of the oocyte in the oviduct. An early step in mammalian development, about one day after the fertilization is the cleavage.

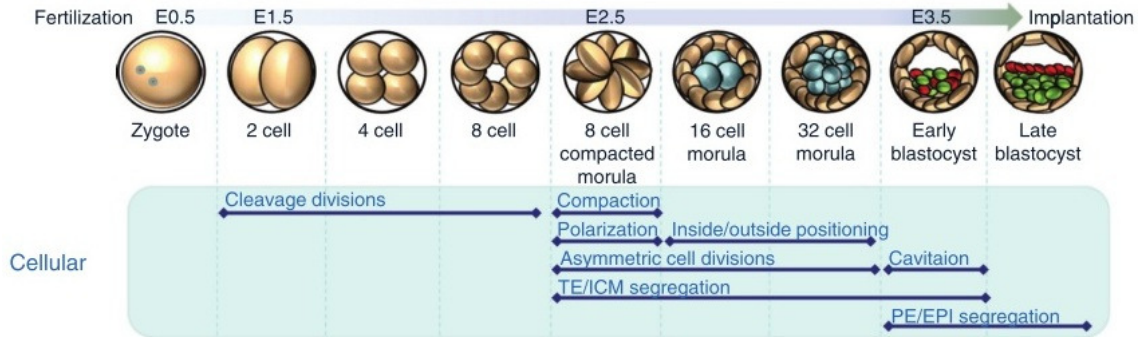

Figure 1.5 *Early development in the pre-implantation mouse embryo [from Oron and Ivanova 2012].*

A mouse zygote (the fertilized oocyte), in contrast to frog or fish zygotes, does not yet have any polarity determined by maternal factors. Thus, in the first stages of cleavage (until 8-cell stage) the blastula cells retain the potential to form all cellular lineages, i.e. they are totipotent [Wobus and Boheler 2005, Oron and Ivanova 2012]. The first cleavage of the zygote is a normal meridional divison resulting in two blastomeres (2-cell stage, see figure 1.5). The second cleavage in mammalians instead is particular as it is a rotational cleavage, meaning one of the blastomeres does not divide meridionally but equatorially [Andreuccetti et al. 2010]. The third cleavage finally results in the 8-cell stage. Zygote genome activation (ZGA) also takes place in the early stages of cleavage [Oron and Ivanova 2012]. Once having reached the 8-cell stage, the loose arrangement in which the blastomeres exist turns into a compact structure. This process, referred to as compaction is triggered by an increased expression of cell adhesion proteins such as E-cadherin that strengthen the cell-cell contacts and thus the compact arrangement of the blastomeres [Gilbert 2006, Takaoka and Hamada 2012].

The cells of the 8-cell stage further divide forming the 16-cell morula, in which they become polarized being distinct into outward- (apical) and inward-facing (basolateral) regions. This polarization is a crucial prerequisite for blastocyst lineage differentiation, as the outer cells now will contribute to the trophectoderm (TE) lineage, whereas the inner cells will form the inner cell mass (ICM). While the TE represents the first tissue progenitor to be differentiated, the ICM remains pluripotent (see chapter 1.5.1) [Gilbert 2006, Oron and Ivanova 2012].

The pluripotency in the ICM is maintained by transcription factor complexes, mainly involving Oct (Octamer binding transcription factor)-3/4, Nanog and Sox2 (SRY-box 2), that regulate the activity of downsteam genes [Tam and Loebel 2007]. For further details concerning signalling in maintaining pluripotency see chapter 1.5.1. By this time (about E4.0) the early mouse blastocyst reaches the uterus and for implantation needs to hatch from the zona pellucida, the extracellular matrix covering of the zygote avoiding ectopic pregnancy. Following hatching, the blastocyst can interact with the endometrium (uterine

epithelium) and implantation can take place [Gilbert 2006, Rossant and Tam 2009, Oron and Ivanova 2012].

In the following stage of post-implantation development the ICM separates into the primitive endoderm (PE) and the epiblast (EPI, also termed primitive ectoderm) as shown in figure 1.6 [Zwaka and Thomson 2005, Oron and Ivanova 2012].

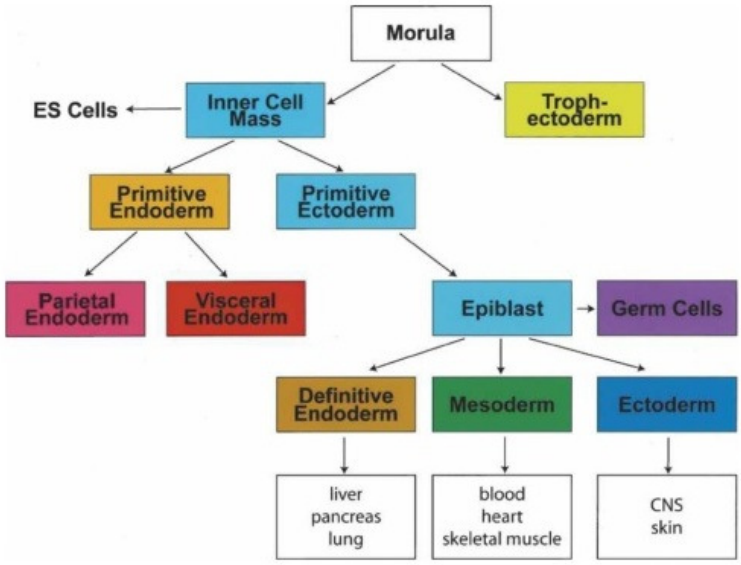

Figure 1.6 *Lineage separation and germ layer differentiation in the mouse development [from Keller 2005].*

The epiblast is the starting point of another determining step in development called gastrulation, in which the three primary germ layers (ectoderm, mesoderm and endoderm) will arise. The formation of the primitive streak is the morphological onset of the gastrulation. The nascent mesoderm arising in the further development can be subdivided into four different regions that develop in the next time after the gastrulation, i.e. the chordamesoderm, the paraxial mesoderm (also called somitic mesoderm), the intermediate mesoderm and the lateral plate mesoderm (see figure 1.7) [Gilbert 2006, Tam and Loebel 2007, Nowotschin and Hadjantonakis 2011].

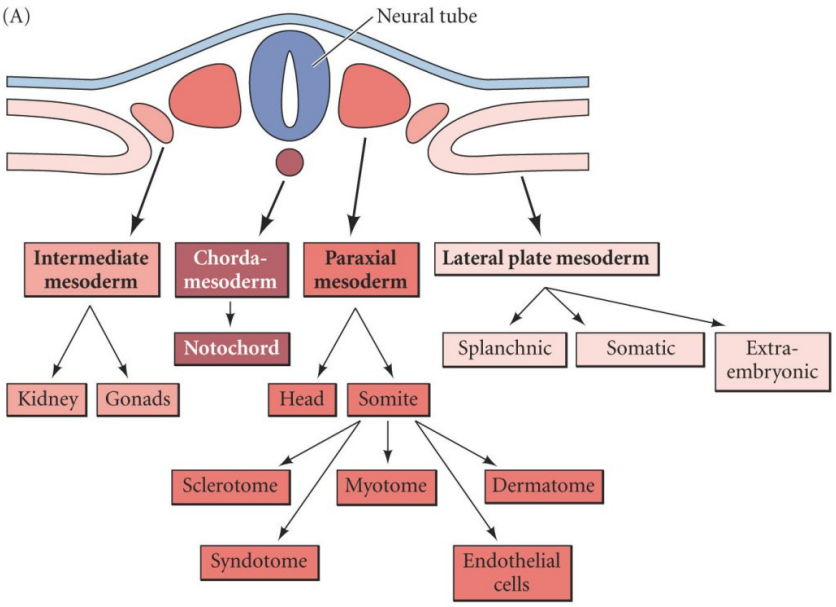

Figure 1.7 *Mesodermal lineage separation [from* ***Gilbert 2006****].*

The lateral plate mesoderm will eventually form the circulatory system, i.e. blood vessels and particularly the heart [Gilbert 2006]. The circulatory system represents the first functional unit in a developing embryo including the heart being the first functional organ. The lateral plate mesoderm subdivides in turn again into different lines (splanchnic, somatic and extraembryonic), from which the anterior splanchnic mesoderm will give rise to the heart (see figure 1.7). The splanchnic lineages from which the heart originates are therefore also termed cardiogenic mesoderm and are located in two clusters lateral from the rostral notochord (see figure 1.8). By this time, the cardiogenic mesoderm already expresses cardiac specific genes like *Nkx2.5* and *Gata4* [Zaffran and Frasch 2002, Gittenberger-de Groot et al. 2005, Gilbert 2006].

Both fields of the bilateral cardiac mesoderm eventually converge contemporary into the midline of the embryo and the former bilateral heart structure will fuse to a single tube (see figure 1.8). The resulting tubular heart subsequently starts beating around the embryonic day 8.5 (E8.5) [Zaffran and Frasch 2002, Gilbert 2006, Wagner and Siddiqui 2007]. The morphogenesis continues via looping and subsequently, the heart chamber formation takes place giving the heart the final shape as seen in the adult organism, including left and right ventricles and atriums etc. [Bruneau 2002, Gilbert 2006].

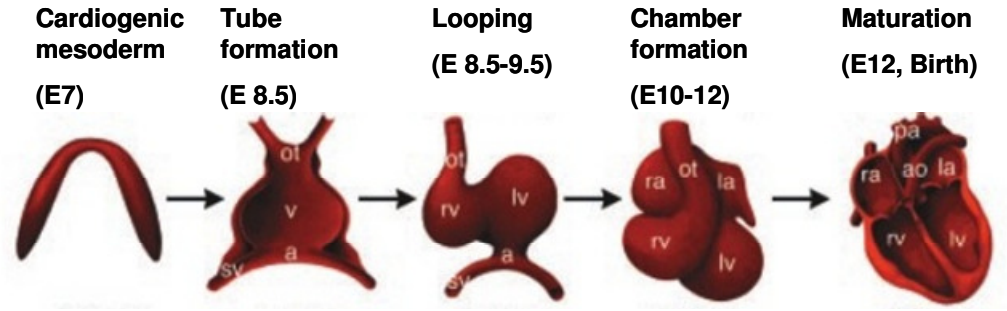

Figure 1.8 *Mouse heart development from cardiac mesoderm to the mature heart [from Bruneau 2002].*

Eventually, the heart has developed out of the cardiac progenitors that form all kind of endocardial and myocardial cells present in a heart, i.e. atrial and ventricular musculature, cushion cells of the valves, Purkinje conduction fibres and the endothelial lining of the heart [Gilbert 2006].

1.5 Embryonic stem cells as a model system

1.5.1 Features of embryonic stem cells

Research on embryonic stem cells (ESC) and their cultivation *in vitro* brought up major advances in biology and experimental medicine. Unlimited self-renewal and multilineage differentiation are classical features of ESC. Therefore, ESC are a suitable model to study early mammalian development and a putative tool for replacement therapy [Keller 2005]. Embryonic stem cell research started in the early 1970s using embryonal carcinoma cells (ECC). ECC lines are generated by isolation from teratocarcinomas and share the capacity of self-renewal and mulitlineage differentiation with other ESC [Yu and Thomson 2008]. A further step in the *in vitro* use of ESC was the establishment in culture of mESC [Evans and Kaufman 1981, Martin 1981]. In the late 1990s, the establishment of human embryonic stem cells (hESC) *in vitro* followed [Thomson et al. 1998]. Two major limitations for the use of hESC in research however are ethical concerns and legal

restrictions [Bundesministerium der Justiz - StZG 2002, Leist et al. 2008]. The use of mESC therefore provides an alternative tool, at least for studies of developmental issues.

Nowadays, mESC cell lines are available commercially. Originally they are derived from the inner cell mass (ICM) of pre-implantation embryos (blastocysts) of the mouse (see figure 1.6). The stage of pre-implantation in which they are commonly isolated is around the embryonic day 3.5. The blastocysts, after isolation from the murine uterus are cultured *in vitro* on mouse embryonic fibroblasts (MEF). Subsequently, through enzymatic dissociation and expansion mESC are generated out of the cells from the ICM and are separated from the throphoblast cells [Evans and Kaufman 1981, Wobus and Boheler 2005].

Cells derived from that stage are considered pluripotent, i.e. they retain the potential to differentiate into cells of all three primary germ layers (namely endoderm, mesoderm and ectoderm) and the primordial germ cells (PGC), the founder cells of male and female gametes (see figure 1.9). Subsequently, they can further differentiate into all cells of the mouse organism [Wobus and Boheler 2005].

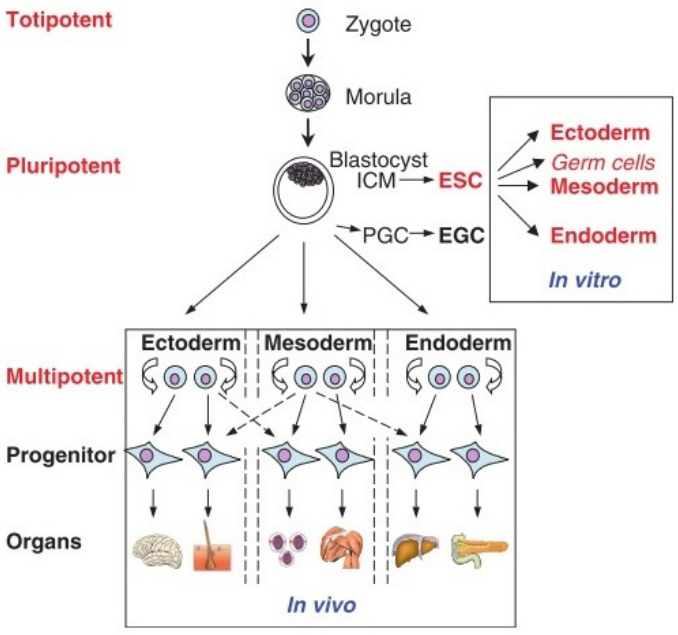

Figure 1.9 *Stem cell hierarchy and differentiation [from Wobus and Boheler 2005].*

Their pluripotent stage can be used *in vitro* for differentiation into cells of all three germ layers as well. However, to retain the pluripotency in culture, mESC need special conditions. A coculture of mESC on a feeder layer of MEF is sufficient to provide all factors maintaining their pluripotency [Keller 2005]. It was found that leukemia inhibitory factor (LIF), a feeder-cell-derived molecule, is one of the pivotal factors maintaining pluripotency. Additionally, it was demonstrated that with recombinant LIF in the presence of a proper fetal calf serum (FCS) the maintenance of pluripotent cells was possible without a feeder layer [Williams et al. 1988, Stewart et al. 1992].

LIF maintains pluripotency of mESC mainly by activating different signalling pathways (see figure 1.10). Prior to all, LIF binds to the LIF receptor (LIFR) which then triggers several signalling pathways. The pathways comprise the JAK/STAT (Janus kinase/signal transducer and activator of transcription 3), the PI3K (phosphoinositide 3-kinase) and the SFK (Src family kinases) pathway. Additionally, the canonical Wnt pathway and bone morphogenetic protein 4 (BMP4) signalling via the Smad pathway are involved. The Ras/RAF/MEK/ERK cascade, also triggered by LIF would result in differentiation instead, showing a double function of LIF, but it is inhibited by the other pathways [Ying et al. 2003, Annerén 2008, Pera and Tam 2010, Hirai et al. 2011].

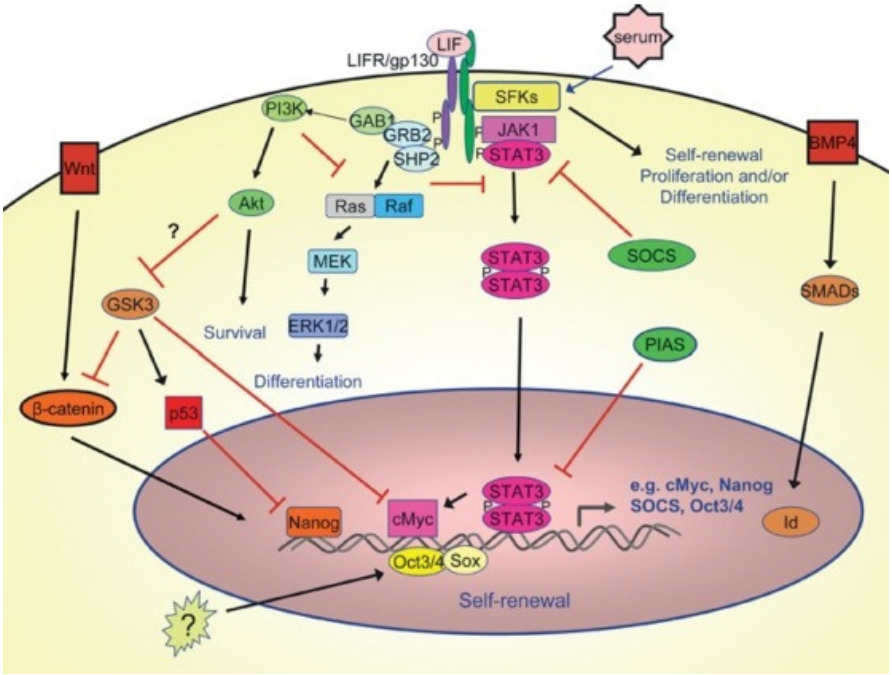

Figure 1.10 *Pluripotency maintained by LIF, BMP and Wnt signalling [from Annerén 2008].*

Eventually, these pathways trigger the expression of transcription factors, which together with epigenetic modifiers, chromatin remodelers and miRNAs form a regulatory system to maintain pluripotency of stem cells. Oct-3/4, Sox2, Nanog and cMyc are among the key players of transcription factors. They co-occupy at promoter regions and thus repress genes involved in early lineage differentiation and activate genes responsible for self-renewal. Furthermore, they positively regulate each others expression to maintain the system keeping mESC in a pluripotent state [Chambers et al. 2003, Masui et al. 2007, Pera and Tam 2010, Smith and Dalton 2011].

1.5.2 *In vitro* differentiation of mouse embryonic stem cells

Mouse embryonic stem cells are able to differentiate *in vitro* spontaneously into a variety cell types [Doetschman et al. 1985]. Under appropriate conditions mESC differentiation starting from ICM cells allows the generation of cells of the three germ layers plus their derivatives (see figure 1.9). Conditions necessary to start the spontaneous differentiation are the aggregation of mESC to form embryoid bodies (EBs) using for example the hanging drop method in the absence of LIF or feeder layer cells providing it. Efficiency and direction in which differentiation is driven depends on the used serum [Keller 2005, Wobus and Boheler 2005].

In vitro differentiation of mESC by EBs can recapitulate in parts the embryonic development of mice. Figure 1.11 shows how EB differentiation resembles to the various developmental steps. Like maintenance of pluripotency and self-renewal, differentiation of mESC *in vitro* is mediated by a complex network of signalling, interplay of transcription factors and others, which is found as well *in vivo* [Niwa 2010].

The process of gastrulation, resulting in the three germ layers, can be recapitulated as well. The signal pathways of BMP, Wnt and activin/Nodal are core components inducing endodermal, ectodermal and mesodermal lineages during gastrulation-like processes and primitive streak-like cell populations were found *in vitro*. From the emerging mesoderm,

among others, hematopoietic, vascular and cardiac lineages can be generated in a defined temporal pattern [Murry and Keller 2008, Tanaka et al. 2011].

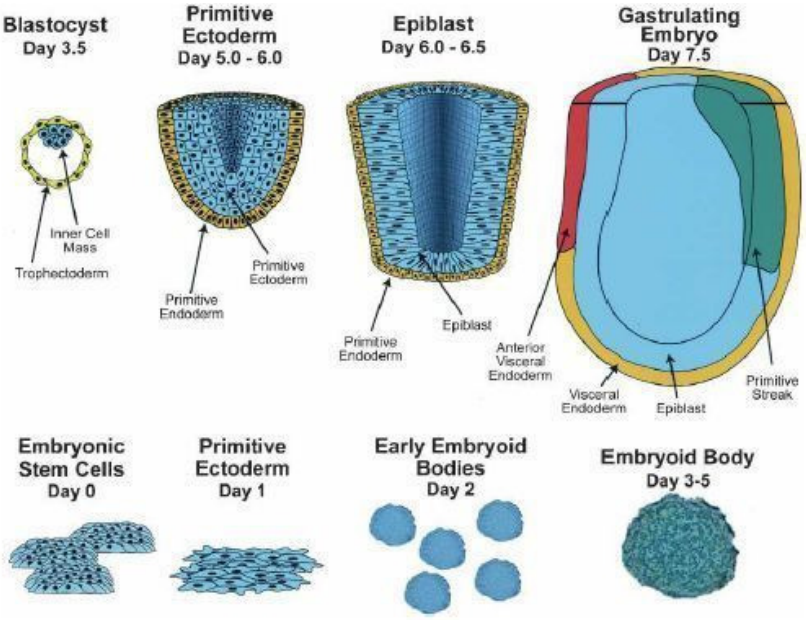

Figure 1.11 *Differentiation of mESC in EBs compared to the in vivo development of a mouse embryo. Day 0 refers to the initiation of spontaneous differentiation, when hanging drops are done and LIF has been removed [from Keller 2005].*

A temporal pattern of activation and inhibition of signalling and factors is typical for developmental processes and it can be recapitulated *in vitro*. However, a spatial expression pattern is needed *in vivo* as well for the shaping of the embryo. It has been shown that even spatial gene expression patterns and spatial self-organization take place in differentiating EBs *in vitro*. Thus, early EBs shortly after differentiation begin consist of an outer layer of cells resembling the primitive endoderm, while the inner cells resemble the primitive ectoderm forming the epiblast (see figure 1.11). Lateron, gastrulation-like processes, such as the formation of a primitive streak-like structure including cell migration, involution and epithelial-to-mesenchymal transition (EMT) were observed in EBs of mESC. These resulted in an anteroposterior polarity and a bilateral symmetry in the EB. Pivotal for mimicking also these processes is an implantation-like process, i.e. the attachment of EBs on the surface of a tissue culture plate after a few days. However, only early stages were found resembling the *in vivo*

situation, as the following organogenesis due to complexity exceeds the possibility of mimicking the development in an EB [ten Berge et al. 2008, Fuchs et al. 2011]. Another crucial feature of embryonic development is programmed cell death, especially apoptosis. It contributes to patterning and normal development of the organism [Fuchs and Steller 2011]. Interestingly, apoptosis related to differentiation processes is also seen in EBs [Karbanová and Mokrý 2002].

Particularly the embryonic development of the heart can be studied by differentiation of mESC into cardiomyocytes. In fact, derivation of cardiomyocytes from mESC is the most successful event in directed lineage differentiation [van Laake et al. 2005] and has been investigated in the present study after exposure to x-rays and carbon ions. A variety of specialized cardiac cell types, for example atrial-like, ventricular-like and Purkinje-like cells can be derived *in vitro* [Boheler et al. 2002, Baharvand et al. 2006] and a spontaneous contraction activity of cardiomyocytes was shown in EBs [Doetschman et al. 1985]. Several days after differentiation begins beating foci emerge in the EBs and their number might increase over the differentiation period. Their electrophysiological properties can be measured and are comparable with those of the *in vivo* situation. The beating activity can last up to several weeks. However, *in vitro* generated cardiomyocytes can be kept in culture beyond that [Boheler et al. 2002, Banach et al. 2003].

1.6 Embryonic stem cell test

The *in vitro* differentiation of mESC into spontaneously contracting cardiomyocytes (see chapter 1.5.2) is also the base of the embryonic stem cell test (EST). The EST is a model to assess embryotoxictiy of drugs and other compounds *in vitro*, using mechanisms like cytotoxicity and differentiation [Seiler and Spielmann 2011]. In the present study, the basics of this assay were used to investigate the embryotoxic effect of ionising radiation.
Embryotoxicity testing commonly is accompanied with the sacrifice of pregnant animals as a model, such as the rat limb bud micromass assay or the postimplantation rat whole embryo culture assay [Scholz et al. 1999]. The EST instead uses established cell lines and pregnant animals as a source for embryonic tissue are not needed to be sacrificed here

[Seiler and Spielmann 2011]. Its protocol has been validated in a study by the European Centre for the Validation of Alternative Methods (ECVAM) and published as a standard operating procedure for embryotoxicity testing [Balls 2002, Scholz and Spielmann INVITTOX no. 113 2002].

The EST uses two commercially available cell lines, namely the murine embryonic stem cell line ES-D3 and the murine fibroblast line Balb/c 3T3. For cytotoxicity testing of compounds, both lines are treated with chemicals before applying the 3-(4,5-dimethylthiazol-2yl)-2,5-diphenyl tetrazolium bromide (MTT) test. To asses the influence of a compound on the differentiation, ES-D3 cells are differentiated into spontaneously contracting cardiomyocytes using the hanging drop method to create EBs (see figure 1.13, for a detailed description of the assay see Scholz and Spielmann INVITTOX no. 113 2002). The compound to be tested is applied over the whole differentiation period and the yield of spontaneously contracting EBs in controls is compared to the yield after treatment with different concentrations [Scholz et al. 1999, Seiler and Spielmann 2011].

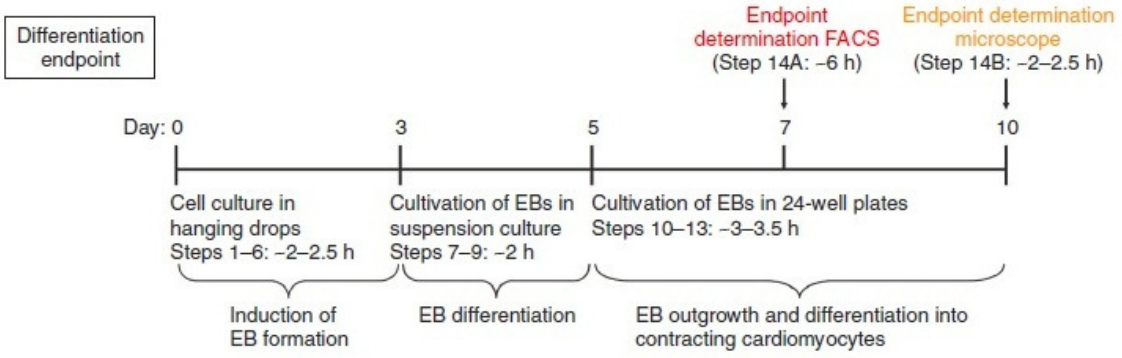

Figure 1.13 *Experimental scheme of the differentiation endpoint of the embryonic stem cell test [from Seiler and Spielmann 2011].*

2. Materials and methods

2. 1 Pluripotent ES-D3 cells and culture conditions

2.1.1 Mouse embryonic stem cell line ES-D3

In this work the pluripotent mouse embryonic stem cell line ES-D3 [Doetschmann et al. 1985] was used. These cells were derived from the inner cell mass of eight blastocysts of day 4 of embryonic development. The blastocysts were isolated from pregnant 129/Sv mice. ES-D3 cells were purchased from American Type Cell Culture (ATCC). Cells were purchased cryo-preserved and defined to be in passage 0, as no further details on the culture age were provided by ATCC. Cells were thawed and subsequently cultured as needed (see below).

2.1.2 Gelatine-treatment of tissue culture flasks and dishes

All tissue culture flasks used for ES-D3 cultivation and all 24-well tissue culture plates used for differentiation of EBs (see 2.2.1) were pre-treated with a 0.1% (w/v) gelatine solution. Gelatine granulate was dissolved in pre-warmed $PBS^{-/-}$ while stirring with a magnetic stirrer. Once gelatine was dissolved, the solution was sterilized by autoclaving and stored at 4°C. To treat the tissue culture flasks or dishes, sterile gelatine solution was filled inside to cover the whole surface (0.2 ml/cm^2). The solution in the flask or dish was then incubated (37°C, 5% CO_2 and 95% humidity) for at least 1h. Following the incubation the gelatine solution was removed and the flasks or dishes prepared as required.

2.1.3 Culture conditions and cultivation

ES-D3 cells were incubated at 37°C, 5% CO_2 and 95% humidity. Due to their fast and colony-like growth they were passaged every second or third day to avoid confluence. For the passage, medium was removed from the tissue culture flask and cells were washed with phosphate buffered saline without calcium and magnesium ($PBS^{-/-}$). Trypsin-Ethylenediaminetetraacetic solution (TE solution) was added (1 ml per 25 cm^2) and incubated at room temperature to detach cells from the surface and to dissociate the colonies. The process was checked under the microscope and supported by smooth tapping. As soon as the cells were detached, the activity of the TE solution was stopped by adding complete medium (see appendix C.3). A single cell suspension was prepared by repeated pipetting. A sample of the cell suspension was diluted 1:10 in $PBS^{-/-}$ and counted with an electrical cell counter to determine the cell number. To completely remove the TE solution, cell suspension was centrifuged at 800 rounds per minute (rpm) for 8 minutes. The supernatant was poured off and cells were resuspended in complete medium to reach $1*10^6$ cells/ml. For further cultivation, $1*10^6$ cells were seeded in a prepared tissue culture flask (gelatine-treated, 6 ml complete medium, preconditioned in incubator for 30 minutes) of 25 cm^2 (T25). LIF was added in a concentration of 1000 U/ml medium to maintain the pluripotency of ES-D3 cultures (see chapter 1.5.1). This very scheme was applied on Mondays and Wednesdays. On Fridays, due to the additional day in culture, only $0.75*10^6$ cells were seeded in a T25 tissue culture flask and 10 ml of complete medium with LIF to avoid nutritional limitations of the cultures.

2.1.4 Heat inactivation of foetal calf serum

The foetal calf serum (FCS) added to the cell culture medium was heat-inactivated before. A 500 ml bottle of FCS was defrosted and aliquots were done in 15 ml or 50 ml tubes. These tubes then were incubated at 56°C for 30 minutes in a water bath and immediately after chilled in an ice bath. Tubes with heat-inactivated FCS were stored at -18°C until needed.

2.1.5 Cryopreservation and thawing

For cryopreservation cells were trypsinized as described in 2.1.3, centrifuged and carefully resuspended in cryo medium (see appendix C.3) to reach a concentration of $2.5*10^6$ cells/ml. The cryo vials were then filled with 1.2 ml of cell suspension so that each contained $3*10^6$ cells and were placed in a cell freezing container filled with isopropanol to ensure a freezing rate of 1°C/min while kept at -80°C. After one to three days cryo vials were moved to a liquid nitrogen container for long-term preservation.
To thaw cells, a cryo vial was taken and the screw cap was slightly opened to allow degassing. Cells in the vial were then defrosted at 37°C in a water bath. Cell suspension was transferred in a 15 ml tube containing 9 ml pre-warmed complete medium and centrifuged at 800 rpm for 8 minutes. The supernatant was poured off and the pellet resuspended in 1 ml complete medium. This suspension was transferred in a prepared tissue culture flask (T25, gelatine-treated, 6 ml complete medium including LIF, preconditioned in incubator for 30 minutes). and incubated under normal culture conditions (see 2.1.3). One day later, the medium was replaced by 7 ml fresh complete medium including LIF. Cells were passaged the following day as described in 2.1.3.

2.2 Differentiation of ES-D3 cells to spontaneously contracting cardiomyocytes

2.2.1 Differentiation protocol

For the differentiation into spontaneously contracting cardiomyocytes, only ES-D3 cells up to a passage number of 20 were used in analogy to the embryonic stem cell test [Scholz and Spielmann INVITTOX no. 113 2002]. A scheme of the procedure is shown in figure 2.1. To initiate the spontaneous differentiation, LIF was removed from the culture medium and the hanging drop method was applied [e.g. Seiler and Spielmann 2011]. The start of the differentiation process was defined as day 0. Briefly, cells were trypsinized (see 2.1.3), resuspended in complete medium to adjust a cell titre of $3.75*10^4$ cells/ml and transferred to a sterile multipipette tray. Regularly, the multipipette

tray was smoothly shaken to avoid cells to sink down and thereby generating a titre gradient. From that cell suspension 40 drops (20 µl each) were put inside the lid of a bacterial Petri dish using a multichannel pipette. Thus, each drop contained about 750 cells. The Petri dish was filled with 5 ml sterile $PBS^{-/-}$ to prevent evaporation of the small volumes. After seeding 40 drops, the lids were flipped around carefully without moving the drop's positions and put on the dish. The dishes containing were then incubated (37°C, 5% CO_2 and 95% humidity) for 3 days. Thus, due to gravity the cells gathered in the tip of the drop forming EBs. On day 3 of differentiation, the lids of the dishes were carefully flipped around and the EBs of three lids were transferred to Petri dish containing 15 ml complete medium and cultured for two more days in suspension to allow further growth. On day 5 of differentiation, when visible by the naked eye, single EBs were picked and transferred in a cavity of gelatine-treated 24-well tissue culture plates (one per well). For the transfer, pipette tips were used, where the end was cut off to decrease shear forces. In the tissue culture plates EBs attached, flattened and grew extending into the periphery. While differentiating EBs gave rise to several cell types, among them spontaneously contracting cardiomyocytes.

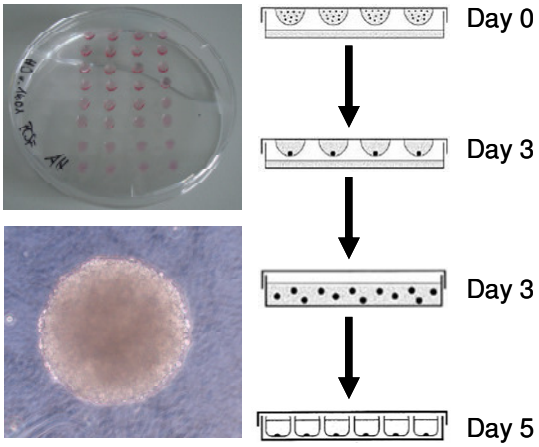

Figure 2.1 *Scheme of ES-D3 differentiation. The formation of the EBs is achieved by aggregation in the hanging drops (days 0 to 3, upper left picture). Subsequently the spherical EBs are grown in suspension culture (days 3 to 5, lower left picture) and plated in a 24-well tissue culture plate (day 5).*

2.2.2 Determination of the fraction of beating embryoid bodies

Spontaneously beating cardiomyocytes can be easily detected about ten days after initiation of the differentiation (five days after transfer in 24-well tissue culture plates) due to their visible contractions. The number of beating EBs showing one or more beating areas was determined by light microscopy (10x magnification). At least 48 EBs per dose and time-point were examined. For high doses with an expected low occurrence of beating cardiomyocytes up to 96 EBs were examined. Analysis was done in regular intervals between day 10 and day 30 of differentiation. The cumulative fraction of beating EBs, i.e. EBs were counted as positive if they had been beating at least once, was determined over the time-course.

2.2.3 Serum test to obtain high numbers of spontaneously contracting cardiomyocytes

The protocol described in 2.2.1 was applied to test three different sera for their potential to induce the differentiation into high numbers of spontaneously contracting cardiomyocytes and thus in a high fraction of beating EBs. The 3 sera used were A, B and C (see appendix C.4). Before differentiation protocols with the mentioned sera were applied, pluripotent ES-D3 cultures were kept for at least three passages before initiating the differentiation in the serum of choice to allow adaption to changed conditions. Then, cells were differentiated and the efficiency of the tested serum was calculated by determining the fraction of contracting EBs as described in 2.2.2. For each serum at least one differentiation was performed including at least two 24-well tissue culture plates (48 EBs).

2.3 Radiation experiments

2.3.1 Sample preparation

Pluripotent ES-D3 cultures were irradiated either one or two days after seeding (see 2.3.4) in gelatine-treated 12.5 cm^2 tissue culture flasks (T12.5). The cell number seeded was $0.5*10^6$ per T12.5, if cells were irradiated one day after seeding. For irradiations two days after seeding, $0.4*10^6$ cells were seeded to ensure that cells were in the exponential phase at the time of exposure. In both cases, cells were kept in 3.5 ml complete medium including LIF. Irradiations were done both with x-rays or accelerated carbon ions at room temperature (details are given in chapters 2.3.2 and 2.3.3). Controls were sham-irradiated.

2.3.2 Exposure to x-rays

Exposure of ES-D3 cells to x-rays was performed with an Isovolt DS1 x-ray tube of 250 kV accelerator voltage and 16 mA cathode current. While running, the wolfram anode of the tube emitted x-rays. In front of the exit window of the x-rays, a filter consisting of 7 mm beryllium, 1 mm aluminium and 1 mm copper was mounted to absorb long-wave x-rays to harden the spectrum. The applied dose was measured using a dosimeter (SN4). The distance between the exit window and the sample was about 20 cm which resulted in a dose-rate of 2 Gy/min. The T12.5 flasks containing the cells were positioned horizontally below the exit window and exposed to doses of 1 to 10 Gy of x-rays. Following irradiation the samples were transferred to the laboratory for further processing.

2.3.3 Exposure to carbon ions

The exposure of ES-D3 cells to high-energy carbon ions was performed at the SIS18 (*Schwerionensynchrotron*) at GSI in Darmstadt. Shortly before irradiation, the flasks were entirely filled with complete medium and placed in vertical positions on a belt

conveyer in front of the beam exit window. The bottom of the flask with the cells on it faced that exit window. A laser-system was used for positioning. Cells were irradiated with carbon ions (25 mm-extended Bragg peak, energy-range: 106-147 MeV/u with a mean LET of 75 keV/µm at the sample position) using the intensity controlled raster scanning technique [Haberer et al. 1993] and a 30 mm poly(methyl methacrylate) bole. Doses ranged from 0.5 to 3 Gy of carbon ions. Irradiations of a set of several doses in average took about 1h. Following exposure the samples were transferred to the laboratory for further processing as required.

2.4 Experimental processing scheme following radiation exposure

Two main experimental schemes for processing were applied after irradiation of ES-D3 that are referred to as 0h experiments (0h) and 72h experiments (72h).

2.4.1 Experiments at 0h

For the 0h experiments, cells were processed directly after exposure to assess the direct damage induced by radiation. They were harvested as described in 2.1.3. The cell suspension then was used for different experiments as required.

2.4.2 Experiments at 72h

For the 72h experiments, to asses delayed damage or effects of radiation cells were processed one day after exposure. After exposure to x-rays the tissue culture flasks were transported to the laboratory and placed in an incubator. In contrast, following exposure to carbon ions, where flaks were entirely filled, medium was removed completely to restore the proper LIF concentration. Then, 3.5 ml complete medium including LIF were added. Tissue culture flaks were then put in the incubator for further 24h. Cells were

harvested as described in 2.1.3 one day after exposure and the suspension was used for different experiments as required.

2.5 Differentiation of ES-D3 and analysis of beating embryoid bodies after radiation exposure

2.5.1 Experiments at 0h

ES-D3 cells were processed immediately after exposure as described in 2.4.1 and differentiation was performed subsequently (2.2.1). Analysis of beating EBs and calculation of their cumulative fractions was done as described in 2.2.2. The scheme is shown in figure 2.2.

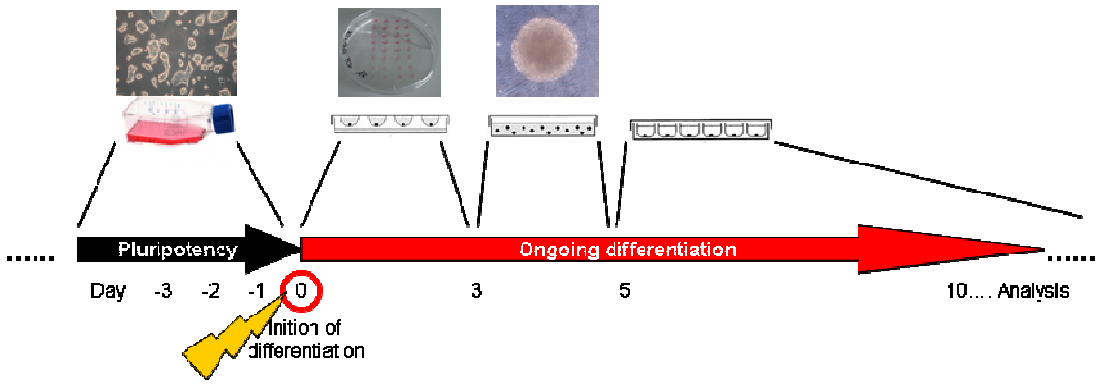

Figure 2.2 *Scheme for differentiation and analysis of beating embryoid bodies after exposure in 0h experiments. The yellow flash and the red circle indicate the time of radiation exposure. Initiation of differentiation is defined as day 0. Beforehand, cells were grown in culture conditions for the maintenance of pluripotency (black arrow, days -3 to 0). After that, differentiation via hanging drops, EB formation and plating of EBs took place (red arrow, day 0 and following). Microscopic analysis of beating EBs started at day 10.*

2.5.2 Experiments at 72h

ES-D3 cells were processed after exposure as described in 2.4.2. At 24h post-irradiation cells were passaged. Differentiation was done 72h after radiation exposure as described (2.2.1). Analysis of beating EBs and calculation of their cumulative fractions was done as described in 2.2.2. The scheme is shown in figure 2.3.

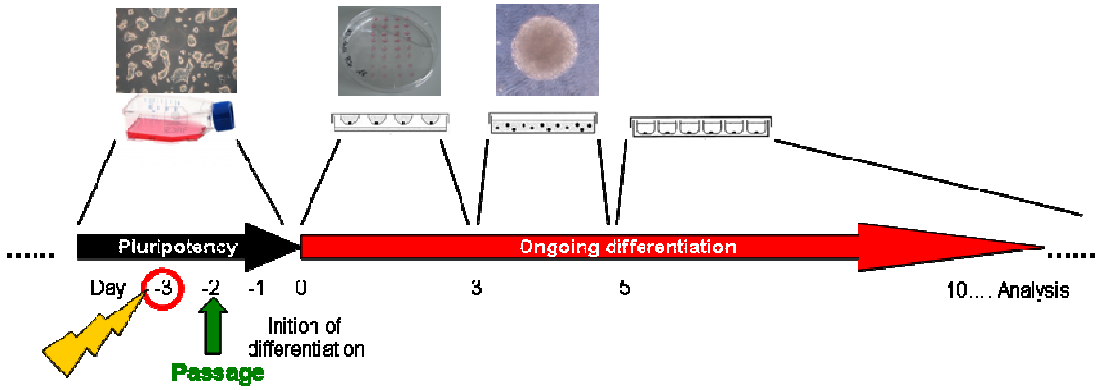

Figure 2.3 *Scheme for differentiation and analysis of beating embryoid bodies after exposure in 72h experiments. The yellow flash and the red circle indicate the time of radiation exposure. The green arrow indicates the passage which is performed one day after exposure. Initiation of differentiation is defined as day 0. Beforehand, cells were grown in culture conditions for the maintenance of pluripotency (black arrow, days -3 to 0). After that, differentiation via hanging drops, EB formation and plating of EBs took place (red arrow, day 0 and following). Microscopic analysis of beating EBs started at day 10.*

2.6 Measurements of cell death after radiation exposure

Apoptosis was measured in two systems, i.e. in pluripotent cultures reseeded directly or one day after exposure and in differentiating EBs for 0h and 72h experiments.

2.6.1 Reseeded pluripotent cultures

Cell death after exposure was measured in pluripotent ES-D3 cultures. For analysis, cells were reseeded in T12.5 tissue culture flasks immediately after exposure (0h experiments,

2.4.1) or one day after exposure (72h experiments, 2.4.2). For each sample and control, three T12.5 were seeded with each $0.5*10^6$ cells. Cells were harvested for analysis one, two and three days after.

Cells were harvested and counted as described above (see 2.1.3). The $PBS^{-/-}$ used to wash the cells and the cell suspension were transferred in the 15 ml tube and centrifuged for 10 minutes at 1200 rpm. Then, the supernatant was poured off and the pellet resuspended in 1 ml $PBS^{-/-}$. To fix cells, 333 µl of 3.7% paraformaldehyde (PFA) solution was added and samples were stored at 4°C until further processing. Cell nuclei were stained by adding 116 µl of 10 µg/ml Hoechst 33 342 solution (final concentration of 0.8 µg/ml). The cells were incubated in the staining solution for at least 15 minutes at room temperature. Then, a few micro litres were dropped on a glass slide (76 x 26 mm), covered with a cover slip (24 x 46 mm) and analysed under a fluorescence microscope using a DAPI filter and a 40x magnification. The fraction of apoptotic nuclei was determined based on morphological criteria, i.e. mainly condensation and fragmentation of cell nuclei. For each dose and time point at least 1000 cells were evaluated.

2.6.2 Differentiating embryoid bodies

Cell death was also measured in EBs derived from exposed cells. For that, samples were taken on day 1, 3 and 5 of differentiation corresponding to days 1, 3 and 5 after exposure (0h experiments) and to days 4, 6 and 8 after exposure (72h experiments), respectively.

To obtain a sufficient number of cells, on day 1 and 3 of differentiation, 3 dish lids containing hanging drops were flushed and EBs were collected in 10 ml $PBS^{-/-}$. On day 5 of differentiation, one dish of EBs in suspension culture was used. By rotating the dish, EBs were collected in the centre and taken with a pipette in 1 ml medium. The EBs were transferred into a 15 ml tube containing 10 ml of $PBS^{-/-}$. In both cases, the tubes with the EBs were centrifuged for 8 minutes at 800 rpm. The supernatant was removed and 1 ml of TE solution was added. EBs in the TE solution were incubated at 37°C in a water bath for 5 minutes. Afterwards, EBs were resuspended by repeated strong pipetting to enhance the dissociation process. The dissociation was controlled under a light microscope. Once, single cells predominated, 3 ml of complete medium were added to inhibit the activity of

the trypsin in the TE solution. Then, cells were centrifuged at 800 rpm for 8 minutes and the supernatant was poured off. The pellet was resuspended in 1 ml of $PBS^{-/-}$ and 333 µl of 3.7% PFA solution was added to fix the cells. Samples were stored for 1h at room temperature. Thereafter, cell nuclei were stained and analysed as described in 2.6.1.

2.6.3 Caspase-3 activity assay

Additionally to the morphological analysis of apoptotic cells, caspase-3 activity was measured in a few samples of a 0h experiment by means of the *FITC Active Caspase-3 Apoptosis Kit*. Cells were reseeded after exposure as described in 2.6.1 and harvested one, two and three days after exposure (see 2.1.3). The $PBS^{-/-}$ used to wash the cells and the cell suspension were transferred in the 15 ml tube and cells were processed according to the manufacturer's protocol. Generally, $1*10^6$ were transfered to a separate 15 ml tube and centrifuged at 300 g for 5 minutes. The supernatant was poured off and cells were washed twice with ice-cold $PBS^{-/-}$ and centrifuged each at 300 g for 5 minutes. Subsequently, cells were resuspended in 500 µl *Cytofix/Cytoperm Fixation and Permeabilization Solution* and incubated on ice for 20 minutes. Then, they were washed twice with *Perm/Wash Buffer* (1x diluted) and centrifuged each at 500 g for 5 minutes. The cell pellet was resuspended in an antibody staining solution (per sample 100 µl *Perm/Wash Buffer* and 20 µl *FITC Rabbit Anti- Active Caspase-3*) and incubated for 30 minutes at room temperature in the dark. Subsequently, cells were centrifuged at 500 g for 5 minutes and washed in 1 ml of *Perm/Wash Buffer* followed by another centrifugation step. The pellet was then resuspended in 500 µl Perm/Wash Buffer containing 1 µg/ml DAPI to allow simultaneously the detection of cell nuclei in the flow cytometer.

As a first gating step the cell cycle distribution measured with DAPI stained cells was used. A following gating step was performed on the FSC/SSC plot that displays the size distribution of the cell population. These gating steps excluded putative debris and clumps. For the remaining population the FITC intensity was analysed. For that, the control of each time point was analysed first and its FITC-intensity was set to a background containing 5% FITC positive cells, i.e. active caspase-3 positive cells. The

very same gating parameter was then applied for all measurements and results were normalized to control.

2.7 Size measurements of embryoid bodies after radiation exposure

To gain information on the growth of EBs after radiation exposure their diameter was measured on day 5 of differentiation, right after plating in the cavities of the 24-well tissue culture plates. Measurements were performed by a scale in the ocular of a light microscope.

2.8 Clonogenic survival assay

The determination of the clonogenic survival after irradiation is a central assay in radiation biology. The clonogenic survival describes the capability of a single cell to grow to a colony of at least 50 cells within a certain time [Franken et al. 2006]. To reach a sufficient statistical value, a total of about 100 colonies per sample were aimed at and each sample was plated three times. In the case of ES-D3, a defined cell number was plated in T25. After seven days of incubation (37°C, 5% CO_2 and 95% humidity), cells were fixed and stained with 3x *Loeffler's Methyleneblue* solution. Colonies with more than 50 cells were counted as survivors. The plating efficiency (PE) of control cells (i.e. the ratio between seeded cells and formed colonies) is an important parameter for this assay. The PE was calculated for each experiment and set to 1. The surviving fractions of the exposed samples were then calculated as the ratio between counted colonies and seeded cells and normalised to the control value.

2.9 Isolation and immunocytochemical staining of cardiomyocytes

Cells samples isolated from EBs were stained with for the protein cardiac troponin I to proof the formation of cardiomyocytes. On day 21 of differentiation, EBs containing contracting areas were scraped with a cell scraper and transferred in a 15 ml tube with 5 ml $PBS^{-/-}$. The sample was then centrifuged at 800 rpm for 2 minutes and the pellet was transferred in a reaction tube. EBs were washed three times with $PBS^{-/-}$ and centrifuged shortly to spin them down. The $PBS^{-/-}$ was removed and 500 µl of TE solution were added. Samples were incubated for 6 minutes at 37°C in a water bath to dissociate the EBs. Then, the suspension was resuspended several times with a pipette to remove the remaining clumps. Afterwards, 1 ml of complete medium was added to inactivate the TE solution. The cell suspension was transferred to gelatine-treated chamber slides with each two chambers (400 µl/chamber). Additionally, 1.6 ml of complete medium per chamber were added and slides were shaken carefully to distribute the cells. Samples were then incubated (37°C, 5% CO_2 and 95% humidity) for 20h to 24h before further processing.
To fix and stain the cells, medium was completely removed, cells were washed with $PBS^{-/-}$ and afterwards 1 ml of a 2% PFA solution was added. Samples were incubated for 15 minutes at room temperature. Then, the PFA solution was removed, cells were washed with $PBS^{-/-}$ and 1 ml of 0.5% Triton solution was added. The samples were incubated for 10 minutes at room temperature. After removing the solution, they were washed twice with $PBS^{-/-}$ for 3 minutes. This was followed by blocking the samples for 20 minutes with 0.4% BSA solution. Meanwhile, primary antibody solution was prepared by diluting the antibody stock (rabbit, cardiac troponin I) to 2.5 µg/ml in 0.4% BSA solution. After removal of the BSA solution, 300 µl of primary antibody solution were added per chamber. Two chambers were used as control, i.e. one was only filled with BSA as autofluorescence control and one with the secondary antibody to assess unspecific immunostaining. Incubation was done for 2h at room temperature in a humidified chamber. Subsequently, the primary antibody solution was removed and samples washed three times with $PBS^{-/-}$ for 5 minutes. Following the washing steps, in each chamber 300 µl of secondary antibody solution (sheep, anti-rabbit, TexasRed-labeled, 5 µg/ml in 0.4%

BSA solution) were added and incubated at room temperature for 45 minutes in a humidified chamber. Afterwards, samples were washed with $PBS^{-/-}$ for 5 minutes. Staining of the cell nuclei was performed by adding 0.1 µg/ml DAPI solution. After 15 minutes samples were washed with $PBS^{-/-}$ and subsequently with deionised water (each 5 minutes). Samples were dried at room temperature and the walls of the chamber slides were removed. A few drops of *VectaShield Antifade* were added on the slides and they were covered with cover slips (24 x 46 mm). Analysis was done with a fluorescence microscope using DAPI and TexasRed filters and 40x and 100x magnifications. Images were taken with a monochrome CCD camera and analysed using the ISIS software.

2.10 Alkaline phosphatase staining

A high activity of alkaline phosphatase is typical marker for the pluripotency of embryonic stem cells [Wobus et al. 1984]. Therefore, ES-D3 cells were tested for alkaline phosphatase activity in regular intervals to proof whether they were still pluripotent. The assays were performed with the *Alkaline Phosphatase Kit* (Sigma Aldrich) according to the manufacturer's protocol with minor changes. All steps were performed at room temperature. Cells for the assay were grown in T25. Per T25 the following reaction volume was prepared before the start of the staining procedure. Staining solution was produced by mixing 133 µl *Sodium Nitrite Solution* and 133 µl *FRV-Alkaline Solution* and incubating it for 2 minutes. After that 6 ml of deionised water and 133 µl *Naphthol-AS-BI* were added. The fixative solution was prepared by mixing 2.5 ml *Citrate Solution*, 6.5 ml Acetone and 0.8 ml of 37% formaldehyde.

Following the preparations, medium was removed and cells were washed carefully with $PBS^{-/-}$. The fixative solution was added and incubated for 30 seconds. Cells were then washed for 45 seconds with deionised water. Right after, the staining solution was added and incubated for 15 minutes avoiding direct exposure to a light source. Cells were washed with tap water and the sample was air-dried. The staining was evaluated using a light microscope.

2.11 Western blot analysis

Western blot analysis was performed along the differentiation period of ES-D3 to proof the development of cardiomyocytes in EBs. Therefore, samples were taken at different time points both from EBs and from the pluripotent culture, i.e. day 0 of differentiation. At day 0 a total of $6*10^6$ cells were collected from the cell suspension prepared to produce hanging drops (see **2.2.1**). At days 10, 15, 21 and 30 of differentiation 48, 46, 24 and 13 EBs, respectively, were collected by scrapping. Collected samples were washed twice with $PBS^{-/-}$ and disrupted in RIPA buffer. The samples were incubated on ice for 15 minutes, subjected to mechanical disruption by ultrasound sonication for 10 periods of 15 seconds on medium intensity, with pauses of 15 seconds in between. The cell lysate was cleared by centrifugation at 13000 rpm for 10 minutes at 4ºC. The protein content in the supernatant was quantified by the Bradford method [Bradford 1976 from thesis Winter]. Of each sample, 100 µg of protein including molecular weight ladder were loaded into 12% SDS-PAGE gels (see appendix) and subjected to electrophoresis (120V, 90 minutes) using SDS runnig buffer (see appendix). The electrophoresed proteins were transferred into PVDF membranes using 1x Transfer buffer (see appendix) at a voltage of 100V for 35 minutes. Following the transfer, membranes containing the protein bands were blocked for 1h at room temperature in TBST (see appendix) containing 5% milk with gentle agiation. The membranes were blotted with antibodies specific for cardiac troponin I and alpha tubulin (both 1 µg/ml in TBST, overnight, 4°C) and horseradish peroxidase (HRP)-linked anti-rabbit secondary antibody (1:5000 in TBST, 1h, room temperature). The immunoreactive bands were visualized by chemiluminescence using ECL-Plus and Amersham HyperflimTM ECL film. The films were developed in a developer.

2.12 Cell proliferation in embryoid bodies

To measure proliferation of cells in the EBs, the *Click-iT EdU Flow Cytometry Assay Kit* and the *Click-iT EdU Imaging Kit* were used according to the manufacturer's protocol with minor changes. EdU (5-ethynyl-2'-deoxyuridine) is an analogue to the nucleoside thymidine and is incorporated into the DNA during synthesis. For the EdU-pulse

labelling, 10 µM of *EdU* were added to control EBs and to EBs from the progeny of a 3 Gy x-rays exposed sample on day 5 of differentiation in suspension culture. The EBs were incubated for 2h under normal conditions. Sample collection and single cell suspension was obtained from EBs as described in 2.6.2 and the cell suspensions of the control and the exposed sample were separated in two to subject them to the different analyses.

Firstly, for flow cytometry analysis (*Click-iT EdU Flow Cytometry Assay Kit*), $1*10^6$ cells of the suspension were centrifuged at 975 rpm for 3 minutes. The cells were washed in 3 ml 1% BSA solution in $PBS^{-/-}$ and centrifuged. The supernatant was poured off, the pellet resuspended in the residual volume, 200 µl of *Click-iT fixative* were added and incubated light-protected at room temperature for 15 minutes. Cells were subsequently washed in 3 ml 1% BSA solution in $PBS^{-/-}$ and centrifuged. The pellet was resuspended in 200 µl 1x *Click-iT saponin-based permeabilization and wash reagent* and incubated as mentioned above for 15 minutes. Meanwhile, for each sample 0.5 ml of the *Click-iT reaction cocktail* using the *Alexa Fluor 488 azide* dye were prepared as described in the manufacturer's protocol, added to the samples and incubated light-protected at room temperature for 30 minutes. Then, cells were washed with 3 ml 1x *Click-iT saponin-based permeabilization and wash reagent* and centrifuged. The pellet was resuspended in 500 µl 1x *Click-iT saponin-based permeabilization and wash reagent* including 1 µg/ml DAPI and incubated in the same conditions for another 15 minutes. The samples were analysed by flow cytometry. Several gating steps were performed as described in 2.6.3 and the fluorescence intensity of *Alexa Fluor 488* (FITC channel) was analysed first in the control and its level of EdU-positive cells, i.e. cycling cells was set arbitrarily to 10% to allow comparison with the exposed sample. Then, the fluorescence intensitiy of the exposed samples was normalized to the control.

Secondly, for the microscopic analysis (*Click-iT EdU Imaging Kit*), the cell suspensions from both samples were fixed and dropped on glass slides (76 x 26 mm) as commonly done for chromosome spreads [Ritter et al. 1996]. Staining was done as described for flow cytometry analysis adjusting the conditions and the volumes for a sample fixed on a glass slide. As dye, *Alexa Fluor 594 azide* was used here instead. Following the staining procedure, both control and exposed sample were analysed with a fluorescence

microscope using a TexasRed filter. At least 1000 cells were analysed in each sample and the percentage of EdU-positive cells was determined.

2.13 Gene expression

For the gene expression studies the quantitative reverse transcription polymerase chain reaction (qRT-PCR) method was used. The method requires isolation of RNA from samples and the subsequent reverse transcription reaction to yield cDNA that is then subjected to quantitative analysis of gene expression.

On day 0 (undifferentiated cells), samples were harvested from non-exposed ES-D3 cultures as described in 2.1.3. For all other time points, both controls and EBs derived from cells exposed to 3 Gy of carbon ions or x-rays were harvested. On day 4, each two dishes of EBs in suspension cultures were collected and on day 6, each 36 randomly chosen EBs were scraped and harvested. For the following time points (day 10, 15, 21, 25 and 30), with increasing differentiation time less EBs were harvested (12, 10, 7, 6 and 4 EBs) to avoid interference of the RNA isolation efficiency due to excessive sample material. The selection for harvesting beating or non-beating EBs reflected the fraction of beating EBs counted for the respective day. All samples were washed twice with ice-cold $PBS^{-/-}$ and transferred in a 1.5 ml reaction tube.

For RNA extraction, the *MasterPure RNA Purification Kit* was used according to the manufacturer's protocol with minor changes. The supernatant was removed carefully from the washed and centrifuged samples. EB samples from day 10 of differentiation on were additionally pre-treated with a pestle on ice during the subsequent cell lysis step. The following RNA isolation procedure was performed according to the manufacturer's protocol. The purified RNA pellets of the samples in the end of the procedure were resuspended in 20 µl *TE Buffer* including 1 µl of *RiboGuard RNase Inhibitor* and stored at -80°C until they were used for RNA concentration measurement and cDNA synthesis.

RNA concentration was measured by diluting the sample 1:50 in ultrapure water in a photometer. For the reverse transcription reaction, the *High Capacity RNA-to-cDNA Kit* was used to synthesise cDNA. Briefly, 2 µl of each cDNA sample were reversed transcribed as recommended in the manufacturer's protocol.

For qRT-PCR analysis the reagent *Fast SYBR Green Master Mix* was applied and each 2 µl of cDNA of the samples were subjected to the reactions. Quantification was done by using standard curves for each analysed gene and each measure point was performed in triplets. For details about the primers (see appendix C.7). The reactions were performed in a thermocycler with integrated fluorescence reading unit applying the following program: initial denaturation (95°C, 20 seconds), 40 cycles of denaturation (95°C, 3 seconds) followed each by primer annealing and extension (60°C, 30 seconds), denaturation (95°C, 15 seconds) and final elongation (60°C, 60 seconds). As a final step, a melting curve was performed by increasing the temperature stepwise (0.3°C/min) to 95°C. The relative quantity of the analysed genes was each normalised to the relative quantity of the geometric mean of two house keeping genes (*Gapdh* and *Eef2*). Furthermore, for pluripotency-associated marker genes (*Sox2*, *Nanog* and *Oct-3/4*) the relative quantity of expression was normalised to an undifferentiated control sample. For cardiac marker genes (*Gata4*, *cAct*, *cTropT2*, *Myh7*, and *Hcn4*, see chapter 4.5.5), the relative quantity of expression was normalised to a control sample of day 10 of differentiation.

2.14 Mathematical modelling

To justify the hypothesis that the effects concerning the beating fraction of EBs after radiation exposure are mainly due to the cell number, a mathematical model containing a simple cell number-based feature was developed (see equation 2.2)

$$P_{beat}(N) = 1 - e^{-((k/N_0)\exp((t/\tau)-(D/D_0)))^{\nu}} \quad (2.2)$$

where $P_{beat}(N)$ is the probability that a spontaneous beating activity occurs, k the initial number of cells, N_0 the threshold necessary for beating activity, time t the day of differentiation, τ the growth rate, D the dose, D_0 the dose necessary to obtain a survival rate of 1/e and ν a parameter determining the slope.

The model reflects the contribution to the overall cell number due to cell killing

$$N_S = ke^{-D/D_0}$$

and counteracting cell growth

$$N(t) = N_S e^{t/\tau}$$

Combining those in a probabilistic approach for a spontaneous contraction in an EB results in

$$P = 1 - e^{-(N(t)/N_0)^{\nu}}$$

which is equation 2.2. To find the needed parameters, a non-linear fitting to the mean value of all control data was done using the OriginPro 8G software. The used control data were derived from the four figures displaying the developmental kinetics of spontaneously contracting cardiomyocytes as shown in **3.3.2**. The initial cell number k used for calculations was 750 and the population doubling time t_d to calculate τ was assumed as for pluripotent ES-D3 with 17h. For that purpose, the above mentioned equation without the radiation influence term (D/D_0) was applied. The parameters were found to be $N_0 = 97$ and $\nu = 0.041$. Subsequently, using the calculated parameters, the measured data were modelled using equation 2.2 for exposed data sets. For controls, equation 2.2 was used without the radiation influence term (D/D_0).

2.15 Error analysis and significance tests

For the error calculation the standard error of the mean (SEM), the standard deviation (SD), the Poisson distribution or the Bernoulli distribution were used as indicated. For

significance testing, the Fisher's exact test or the t test were used to compare experimental results.

3. Results

The main purpose of this work was to get deeper insight on how radiation exposure might affect the early embryonic development. Therefore, pluripotent ES-D3 cell cultures (resembling the early blastocyst stage) and their differentiation ability (resembling the early embryonic development) were examined after irradiation. Differentiation into beating cardiomyocytes was the central endpoint of the studies. Carbon ions as used for cancer therapy and x-rays as a reference radiation were applied. In a first approach, stem cells were differentiated immediately after radiation exposure (0h experiments). Possible delayed effects were assessed by maintaining them after exposure for three days in pluripotent culture conditions before differentiation (72h experiments).

For pluripotent cultures clonogenic cell death was assessed by performing survival curves (3.2.1). Apoptosis after exposure was mainly measured by counting DAPI stained apoptotic cell nuclei. Additionally, measuring points of apoptosis were confirmed by a caspase-3 activity assay (3.2.2). The radiation influence on the differentiation potential was monitored analysing the occurrence of spontaneously contracting cardiomyocytes (3.3.1 and 3.3.2). The existence of cardiomyocytes in the EBs was proven by means of Western Blot technique and immunocytochemistry (3.1.3). For assessing radiation damage in differentiating cells, EBs were dissociated and screened for apoptotic nuclei (3.3.6). Furthermore, the cell growth in the EBs used for the assays was assessed by measuring the diameter of EBs (3.3.3) and their proliferation (3.3.4). To verify the influence of the cell number and cell killing on the final outcome different initial cell numbers were seeded to produce EBs (3.3.5) and a mathematical model was applied (3.3.7). Complementary, gene expression studies of pluripotency-related and cardiac markers were carried out to screen putative radiation-induced changes (3.3.8).

3.1 Preparatory experiments

The pluripotency stage of the used ES-D3 cultures was examined. Additionally, sera were tested for the efficiency of differentiation into cardiomyocytes and in contracting EBs the presence of cardiomyocytes was proven.

3.1.1 Pluripotency of ES-D3

ES-D3 cells were stained in regular intervals for the alkaline phosphatase activity to investigate whether cells used for experiments were still pluripotent. Cultures were examined at an early passage number (one passage after thawing), i.e. passage number 6 and at a later passage number (11 to 15), i.e. when radiation experiments were performed. Staining was analysed with light microscopy. The analysis showed that all colonies in the passages expressed the alkaline phosphatase activity. Figure 3.1 demonstrates the result of such a staining. The ES-D3 colonies displayed the red/purple colour indicating the pluripotent state. Few cells surrounding them do not. Those cells were typically present in the cultures and did not show alkaline phosphatase activity, indicating a progenitor or differentiated state. However, the majority of cells remained positive for alkaline phosphatase activity.

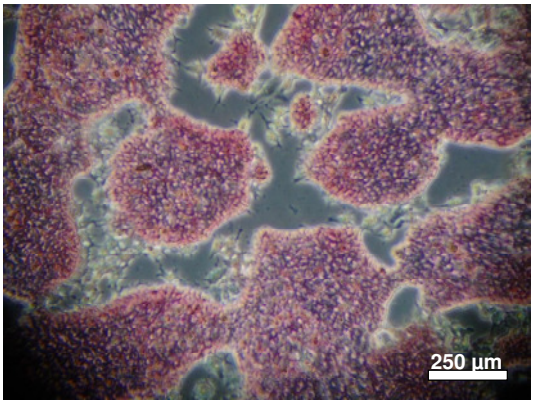

Figure 3.1 *ES-D3 cells stained for alkaline phosphatase activity (red/purple stain) in passage number 6. The ES-D3 colonies display the red/purple stain.*

Further tests to analyse the cells' potency state were performed in the context of that work. Flow cytometry was used to analyse the immunocytochemically stained plruripotency markers Sox2 and Oct-3/4. These data showed that both markers were expressed in the cultures indicating the pluripotent stage of the ES-D3 cultures. Results are shown elsewhere [Luft et al. 2013a, in press].

3.1.2 Serum testing to obtain a high efficiency of differentiation into spontaneously contracting cardiomyocytes

Before the performance of the radiation experiments, three different sera (A, B and C, for details see appendix C.4) were tested for their potential to obtain a high fraction of beating EBs. A sufficient number of contracting EBs is important to obtain statistically relevant data. For the present study, a benchmark of at least 60% in controls was chosen for the experiments. Interestingly, all three tested sera induced a similar and sufficient proportion of beating EBs, i.e. 80% ± 10% on day 10 of differentiation [Helm et al. 2011]. Therefore, the serum commonly used in the laboratory (serum A) was chosen for all further experiments and to maintain the ES-D3 cultures.

3.1.3 Expression of cardiac troponin I in beating embryoid bodies

The formation of cardiomyocytes can be monitored under a light microscope as they contract spontaneously. To further prove the existence of cardiomyocytes, spontaneously beating EBs were tested for expression of cardiac-specific markers. The analyses described below were performed at a few selected time points in some differentiation experiments to verify the existence of cardiomyocytes.

First, eight beating EBs at day 10 of differentiation were dissociated and the cardiomyocytes were immunocytochemically stained by fluorescence-labelling with antibodies against cardiac troponin I as shown in figure 3.2. The fraction of cardiomyocytes positive for cardiac troponin I among all cells counted was always below 5%.

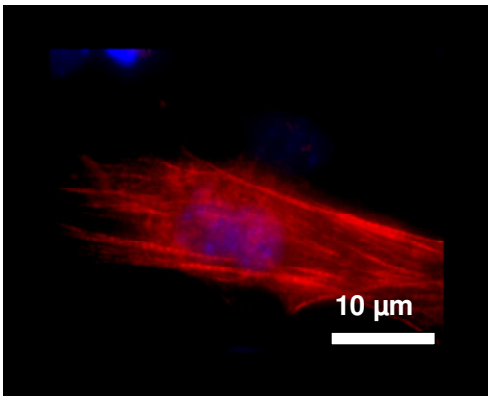

Figure 3.2 *Differentiated cardiomyocyte from a contracting embryoid body. The EB was dissociated, cells were reseeded and cardiac troponin I as a marker for cardiomyocytes detected by immunocytochemistry and fluorescence-labelling under a fluorescence microscope (100x magnification).*

Additionally, analysis of protein expression of cardiac troponin I by Western Blot technique was performed for EBs along the differentiation period (figure 3.3). On days 10, 15, 21 and 30 the protein was detected regularly. As shown in the figure, cardiac troponin I could not be detected on day 0 in the pluripotent cultures, although the double amount of proteins was loaded on the gel to detect also small traces. This is due to the fact that differentiation had not yet begun and the sample consists of pluripotent embryonic stem cells that did not express structural proteins of cardiomyocytes. Those, however, were present from day 10 on.

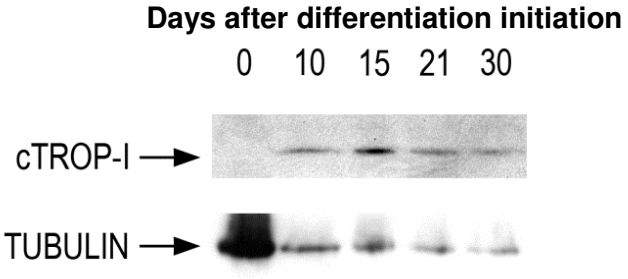

Figure 3.3 *Expression of the cardiomyocyte marker cardiac troponin I (cTROP-I) along the differentiation period of the embryoid bodies (0 to 30 days). Contracting EBs were taken as samples, lysed and analyzed by Western Blot technique using chemiluminscence. Tubulin was used as a loading control. The gel was loaded with 50 µg (days 10, 15, 21 and 30) and 10 µg (day 0) of protein sample.*

3.2 Effects of radiation on pluripotent ES-D3 cultures

3.2.1 Cell survival

Survival curves up to doses of 5 Gy are shown in figure 3.4. Cells were plated immediately after exposure (0h) or three days after exposure including a passage in between (72h). In both cases, carbon ions are more effective in cell inactivation than x-rays. The RBE of carbon ions is about 3 for 0h as well as for 72h. The cell survival for both radiation qualities is at 72h by a factor of 2 higher than at 0h comparing iso-effective doses.

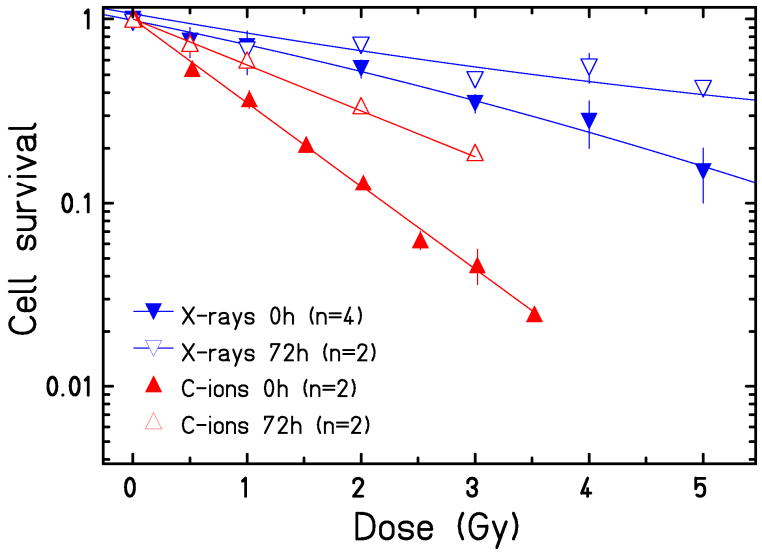

Figure 3.4 *Survival curves for carbon ions and x-rays plated immediately after irradiation (0h) and 3 days after exposure (72h). Data show mean values of different independent experiments and the error bars express the standard deviation. For curve fittings a linear fit was used.*

3.2.2 Cell death

Cell death in proliferating pluripotent cultures reseeded directly after irradiation was measured at one, two and three days after exposure. Additionally, to estimate a putative influence of radiation-induced cell death on the differentiations performed three days

after exposure (72h experiments), apoptosis on day 2, 3 and 4 was measured from cells reseeded on day 1 after irradiation.
To evaluate the relevance of effects, firstly the mean cell death rate of all control samples from all experiments (n=10) was calculated. Values for days 1 and 2 after reseeding were used. The mean value was found to be 2.3% (± 0.3%, standard error of the mean). On day 3 after reseeding the rate of cell death was elevated in all experiments to around 9%. This is most likely due to starvation. Therefore, values measured at day 3 after reseeding were not pooled with the control background. Moreover, the influence of starvation on the cell death on this day exacerbates the distinction of radiation-induced cell death.

In figure 3.5 the number of dead cells in percent is shown one, two and three days after exposure to 0.5 and 3 Gy of carbon ions. On day 1 after irradiation only the 3 Gy exposed sample shows a significant increase in apoptosis (approximately 17%, $p < 0.05$, t test) compared to the control (around 2%). On the second day an increase was measured also for 0.5 Gy, while the sample exposed to 3 Gy is still significantly ($p < 0.05$, t test) elevated compared to both other samples. The control remains on its level from before. On the third day, all samples are on a higher apoptosis level when compared to before. Starvation of the cultures might be the reason here, however, the 3 Gy exposed sample still is higher than the other two.

Figure 3.6 shows the cell death rates one, two and three days after exposure to different doses of x-rays. Apoptosis on day 1 after exposure to 6 and 10 Gy is higher than the control level in (about 7 and 18% respectively, $p < 0.01$, Fisher's exact test); 1 and 3 Gy do not differ from the control, which is about 3%. At two days after exposure, the control remains at the same level (approximately 4%). The irradiated samples instead have a higher level of cell death when compared to the control. The increase in cell death is dose-dependent at day 2. The sample irradiated with 10 Gy shows a steep rise of the cell death rate up to about 38%. On day 3 after exposure, all samples including the control have increased cell death levels around 15%, again probably due to nutrition limitations of the cultures. The dose-effect is no longer measurable.

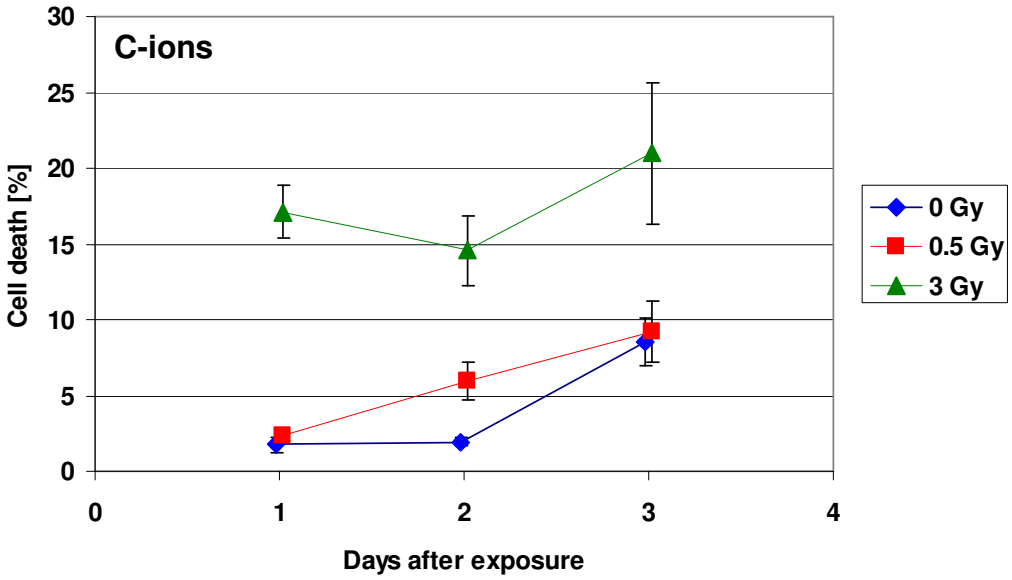

Figure 3.5 *Cell death measured in cells immediately reseeded after exposure to carbon ions. After DAPI staining the fraction of apoptotic cell nuclei was counted. Data show the mean value of two independent experiments where the error bars express the standard error of the mean.*

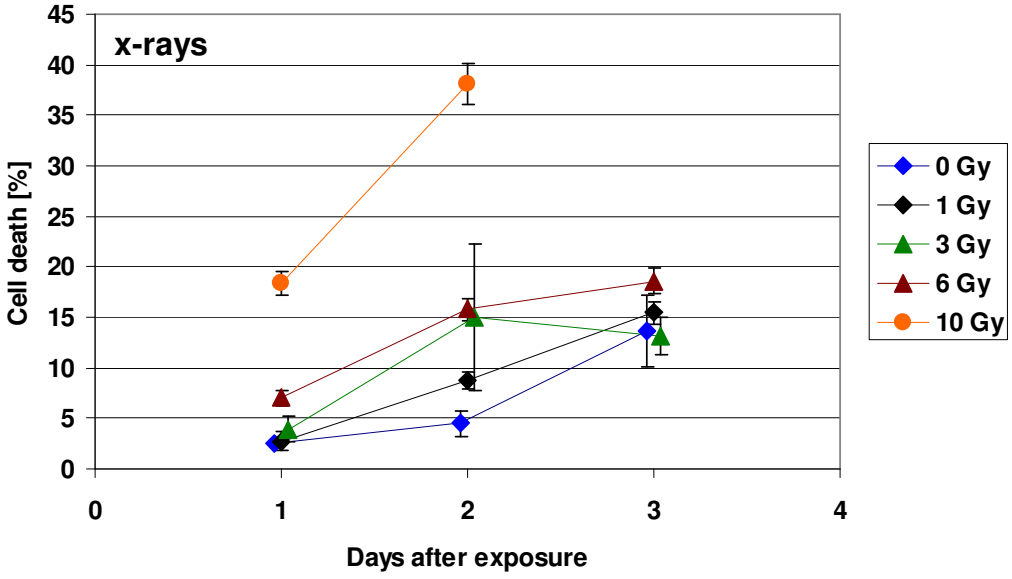

Figure 3.6 *Cell death measured in cells immediately reseeded after exposure to x-rays. After DAPI staining the fraction of apoptotic cell nuclei was counted. Data show mean values of different independent experiments. Error bars express the standard error of the mean or Poisson distribution (details are given in table A.1).*

Conclusively, data points from day 3 after reseeding (equals to day 3 after exposure) indicate a bias by the culture conditions. At day 1 after exposure to both x-rays and carbon ions, only the high doses show an increased level of apoptosis compared to the control. Low doses do not or only slightly exceed the background level of cell death estimated with 2.3% (± 0.3%). Two days after exposure to both radiation qualities instead, all irradiated samples have a dose-dependent higher level of cell death compared to the control.
At two days after exposure carbons ions are more effectively inducing apoptosis than x-rays. Apoptosis levels in samples exposed to carbon ions are about twice as high as in those exposed to x-rays. Thus, comparing 3 Gy of carbon and 6 Gy of x-rays on day 1 after exposure, carbon ions induce apoptosis earlier, however, 6 Gy data are obtained from one experiment only.

The percentages of cell death two, three and four days after exposure to carbon ions and a subsequent passage are shown in figure 3.7. On day 2 and 3 after exposure, the cell death rates of the lower doses 0.5 and 1 Gy are only slightly increased compared to the control. Cells irradiated with 2 and 3 Gy of carbon ions instead display a significant dose-dependent increase in apoptotic cell death ($p < 0.05$, t test, except for 2 Gy on day 3). On day 4 after exposure, the percentages of cell death in the 0.5 Gy sample and the control are both higher than compared to day 2 and 3. The levels of the higher doses instead are decreased if compared to day 2 and 3 and are now close to all others. No dose-dependence is observable here as apoptosis may be influenced by the culture conditions when cells remain for three days without passage or medium change.

The cell death data after exposure to x-rays and a subsequent passage, as presented in figure 3.8 show only a slight increase for the 3 Gy irradiated sample two days after exposure. While the percentage of cell death of the control remains on a similar level three days after exposure, the irradiated sample rises steeply. On day 4 after exposure, both control and irradiated sample show an elevated level of cell death compared to their very levels before, but the difference between them is within the uncertainty of the error

bars. The apoptotic frequency is also here biased by the culture conditions as mentioned above.

Figures 3.7 and 3.8 reveal that reseeding one day after exposure partly attenuates the cell killing effect of radiation in the cultures. On day 2 after exposure (first day after reseeding) to carbon ions doses up to 1 Gy do not differ significantly from control levels as the case in measurements without delayed reseeding (0.5 Gy, see figure 3.5). At day 2, also the apoptosis level following 3 Gy carbon ions exposure is lower than without the passage but it increases again to it the following day. Data for 3 Gy x-rays (figure 3.8) also show attenuation of the cell death on day 2 due to delayed reseeding and a subsequent increase one day later. But the apoptosis rate remains lower than in the experiments without delayed reseeding. Taken together, apoptosis, when cells are reseeded one day after the exposure is attenuated temporary but increases again, pointing to a delayed but persistent of cell death through the passage.

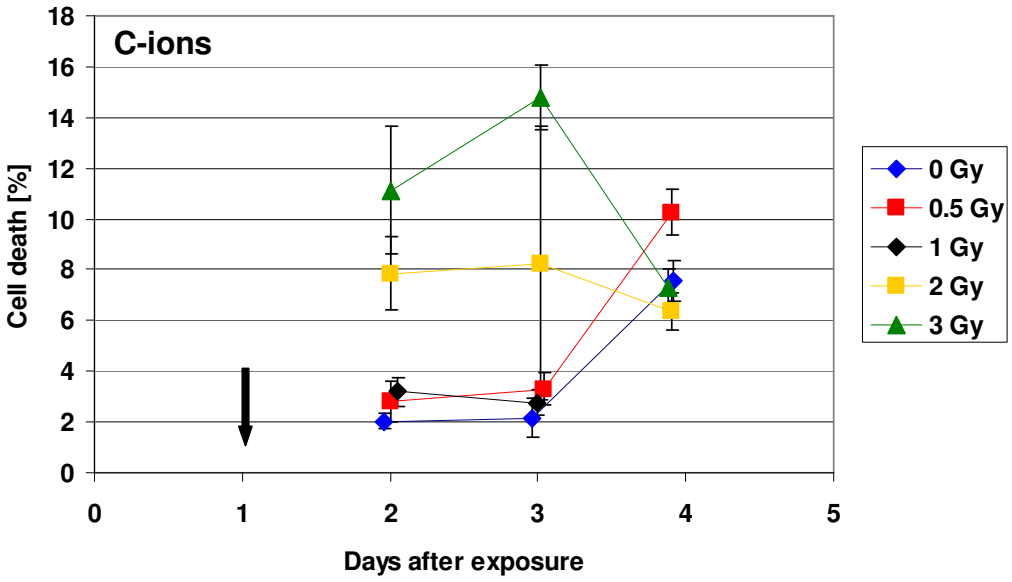

Figure 3.7 *Cell death after exposure to carbon ions. Cells were passaged one day after exposure (black arrow). After DAPI staining the fraction of apoptotic cell nuclei was counted. Data show mean values of different independent experiments. Error bars express the standard error of the mean or Poisson distribution (details are given in table A.2).*

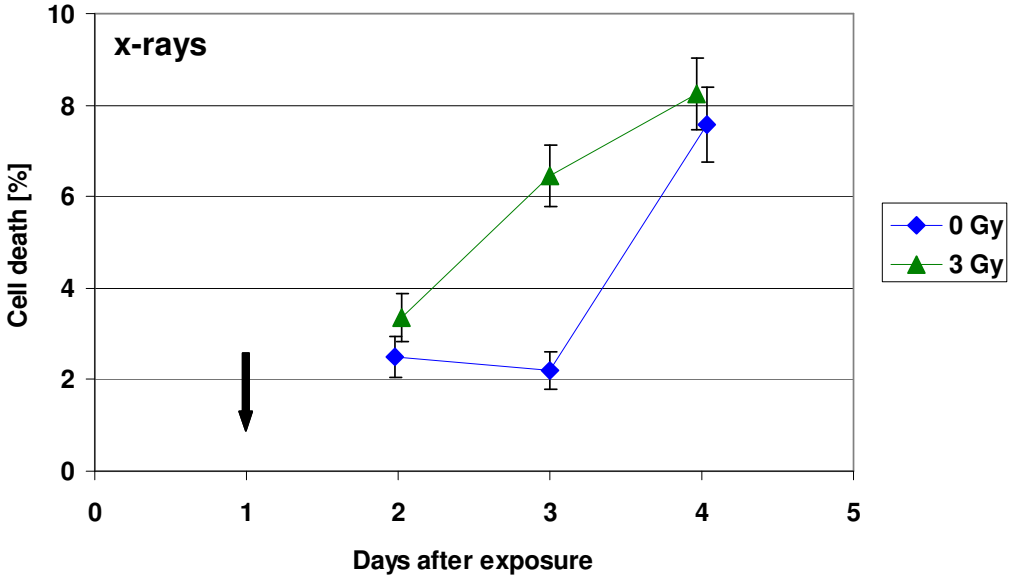

Figure 3.8 *Cell death after exposure to x-rays. Cells were passaged one day after exposure (black arrow). After DAPI staining the fraction of apoptotic cell nuclei was counted. Data were gained from one experiment where the error bars show the Poisson distribution.*

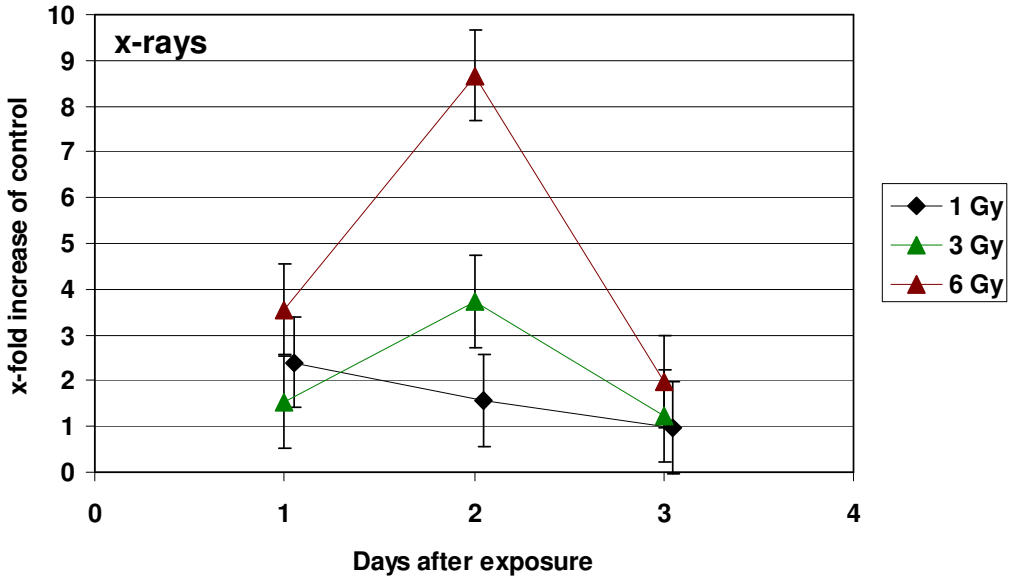

Figure 3.9 *Cell death measured after exposure to x-rays. Cells were reseeded immediately following exposure. X-fold increase of caspase-3 activity normalized to control (1-fold) is displayed. The values were obtained from one experiment. The error was estimated with ± 1-fold according to experimental experience with this assay.*

Apoptosis was analysed in a few samples by the caspase-3 activity assay, to proof the data acquired by morphological analysis apoptotic nuclei. Results of the caspase-3 assay after irradiation with x-rays (cells reseeded immediately after exposure) are shown in figure 3.9. On day 1 after exposure there are only slight increases for samples irradiated with 1 (about 1.5-fold) and 3 Gy (about 2.5-fold), but the 6 Gy sample (about 3.5-fold) differs more from the control. Dose-dependent increases in apoptosis become pronounced two days after exposure. The cell death rate in 6 Gy and 3 Gy samples was elevated about 9-fold and 4-fold, respectively. The 1 Gy sample is only slightly but not significantly increased as can be inferred from its error bars. At three days after exposure no differences to the control are detectable anymore.
These results are comparable to the data of figure 3.6, where cell death was assessed by counting apoptotic nuclei. For both assays one day after exposure only the samples irradiated with 6 Gy exhibit an increase clearly different from controls while all other samples show no or only slight rises in cell death. In both cases, significant and dose-dependent effects are only seen two days after exposure. Furthermore, three days after exposure with both assays no or only slight differences are measurable anymore between control and irradiated samples. The analysis with the caspase-3 activity assay hence verifies the data acquired by counting apoptotic nuclei.

3.3 Differentiation of pluripotent ES-D3 cells after irradiation

Proliferating pluripotent ES-D3 cells were exposed to radiation followed by a differentiation into spontaneously contracting cardiomyocytes. Differentiation was performed by creating EBs.

3.3.1 Fraction of beating embryoid bodies on day 10 of differentiation

The appearance of spontaneously contracting cardiomyocytes in the EBs was examined to measure the influence of radiation on the cardiac development. The assay is based on the *Embryonic Stem Cell Test*. In accordance, the effects were measured 10 days after the

initiation of differentiation. As mentioned above, differentiation was performed by two methods, i.e. with differentiation begin either directly (0h) or 72h after exposure.

Figure 3.10 shows the fraction of spontaneously beating EBs 10 days after initiation of the differentiation for different doses. Control levels were set to 1. For cells differentiated directly after exposure (0h), dose-dependent inhibition occurs for both radiation qualities. Carbon ions are about twice as effective as x-rays when comparing iso-effective doses (see table 4.1). The fraction of beating EBs is lower (about 2.5%) for 3 Gy carbon ions and 6 Gy x-rays. In contrast, for 72 h experiments, x-rays do not affect the differentiation into beating cardiomyocytes. While carbon ions still inhibit the development of beating EBs, even at the lowest dose examined (0.5 Gy). The effect of the differentiation potential still is dose-dependent, although less pronounced than for 0h. Interestingly, the dose-effect curve for carbon ions at 72h is similar to the one for x-rays at 0h.

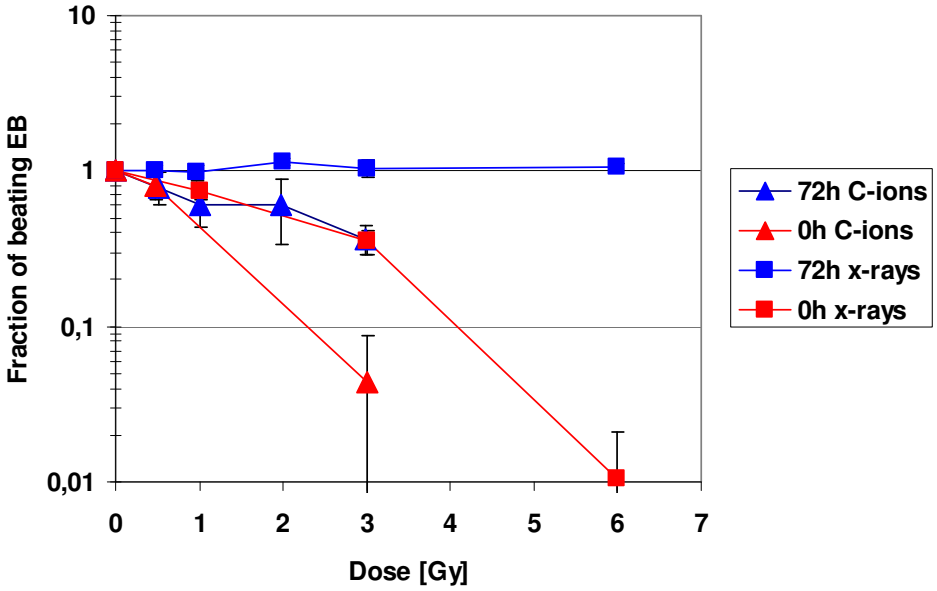

Figure 3.10 *Dose-effect curves of carbon ions and x-rays on the development of spontaneously contracting cardiomyocytes. The fraction of beating EBs was determined on day 10 of differentiation and plotted semi-logarithmically against the dose. Control levels were set to 1. Differentiation was initiated directly after exposure (0h) or 72h after exposure. Data show mean values of different independent experiments. Error bars express the standard error of the mean or Bernoulli distribution (details are given in table A.3).*

3.3.2 Developmental kinetics of beating embryoid bodies during the differentiation period

To examine whether ionising radiation affect the developmental processes the emergence of spontaneously contracting cardiomyocytes in EBs was measured between day 10 and day 30 of differentiation. Data were plotted as the cumulative fraction of beating EBs, i.e. EBs were counted as positive if they had been beating at least once. Commonly, contraction can be monitored for several days after differentiation begin, however, some of the EBs can stop contraction activity earlier. This stop of the spontaneous beating was not taken into account here. Data were acquired here again for both differentiation methods performed, immediately after irradiation (0h) and with a delay of 72h after irradiation of pluripotent ES-D3 cells.

Data obtained for cells differentiated immediately after exposure to carbon ions is shown in figure 3.11. The control shows a high level of beating EBs (96%) on day 10. The progeny of irradiated cells display a pronounced dose-dependent delay in development of contracting cardiomyocytes with 77% for 0.5 Gy and 4% ($p < 0.01$, t test) for 3 Gy on day 10. Over time, their fractions of beating EBs increase continuously. On day 21 the samples irradiated with 0.5 Gy reach 92% and thus almost the control level, considering the error bars. The 3 Gy irradiated sample still exhibits a significantly lower level of beating EBs than the control. Data points on days 25 and 30 were obtained from only one experiment. This might be the reason for the decrease in the curve of 0.5 Gy on day 25.

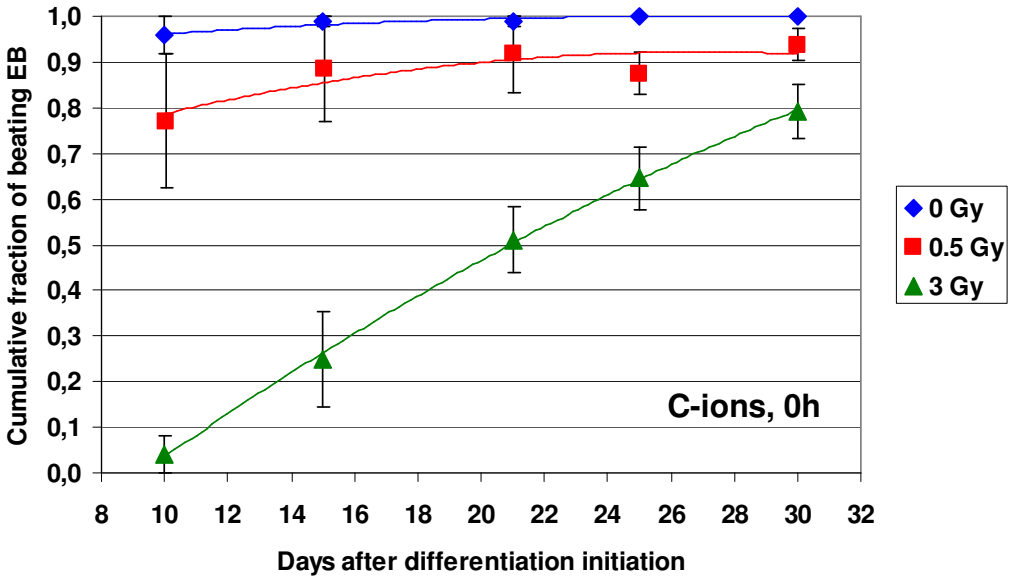

Figure 3.11 *Cumulative fraction of beating embryoid bodies differentiated 0h after exposure to carbon ions. Data show mean values of different independent experiments. Error bars express the standard error of the mean or Bernoulli distribution (details are given in table A.4). To guide the eye, polynomial fits are superimposed on the obtained values.*

Figure 3.12 depicts the results for x-rays of differentiations started immediately after exposure (0h). Here again, the cumulative fraction of beating EBs for the control is high from the beginning and remains at the same level (99%) throughout the differentiation period. A dose-dependent significant decrease (according to the t test) in the formation of beating EBs is seen for all three applied doses (1, 3 and 6 Gy) on day 10 with 73, 35 and 1%, respectively. The cumulative fractions for all irradiated samples rise throughout the differentiation period. At day 25, the data for 1 Gy are slightly lower, probably due to the fact that this point is obtained from one experiment only. Nevertheless, for 1 Gy the cumulative fraction of beating EBs (i.e. around 90%) approaches the control level. Similarly, the fractions to of 3 and 6 Gy develop. Taken together, the previous dose-dependency vanishes at the last two time-points of the differentiation for the irradiated samples, but all reach the control level.

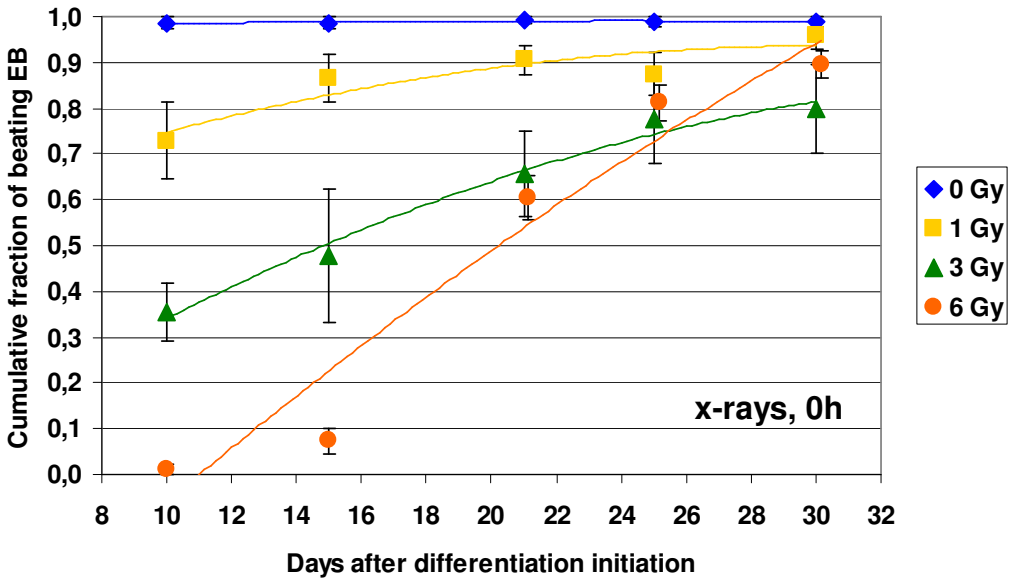

Figure 3.12 *Cumulative fraction of beating embryoid bodies differentiated 0h after exposure to x-rays. Data show mean values of different independent experiments. Error bars express the standard error of the mean or Bernoulli distribution (details are given in table A.5). To guide the eye, polynomial fits are superimposed on the obtained values.*

The emergence of spontaneous contraction in EBs from cells differentiated 72h after exposure to carbon ions is shown in figure 3.13. The beating fraction in the control on day 10 was 87%, while a lower cumulative fraction of beating EBs is seen in all irradiated samples. However, the effect has no clear dose-dependence, as data for 1 and 2 Gy suggest (see table A.6). Throughout the differentiation period all fractions rise. Control and 0.5 Gy irradiated samples finally reach 100% levels. As the fractions increase over time, differences between doses vanish and reach the control level. The 3 Gy exposed sample has a significantly ($p < 0.01$, t test) reduced fraction of beating EBs until the last data point (day 30, 89%).

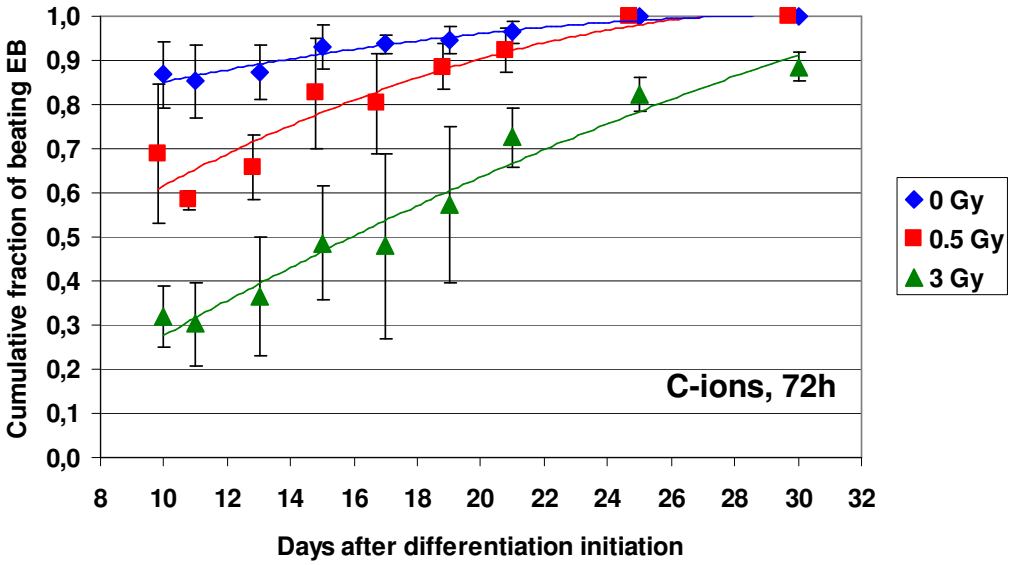

Figure 3.13 *Cumulative fraction of beating embryoid bodies differentiated 72h after exposure to carbon ions. Data show mean values of different independent experiments. Error bars express the standard error of the mean or Bernoulli distribution. For reasons of clarity data sets for 1 and 2 Gy are not plotted (complete set of data and further details are given in table A.6). To guide the eye, polynomial fits are superimposed on the obtained values.*

Figure 3.14 depicts the results of differentiation experiments started 72h after exposure to x-rays. Taking into account the error bars the differences between the control and all samples are low during the time interval investigated. The inhibition of differentiation into beating cardiomyocytes was not dose-dependent here. Even the sample exposed to 6 Gy (85%) does not exhibit any inhibition compared to the control. The cumulative fraction of beating EBs increases for all doses during the differentiation period, confirming observations from other experiments (figures 3.11 to 3.13). Decreases for the control and the 3 Gy curve are due to different numbers of experiments used for calculations (two and three, respectively). Interestingly, the 2 Gy exposed sample is slightly higher than the other samples until day 21. Data points for samples exposed to 1 Gy of x-rays are consistent with the other data sets and lie within the same range. For clarity, data for 1 Gy irradiated samples are not presented in the plot (see table A.7).

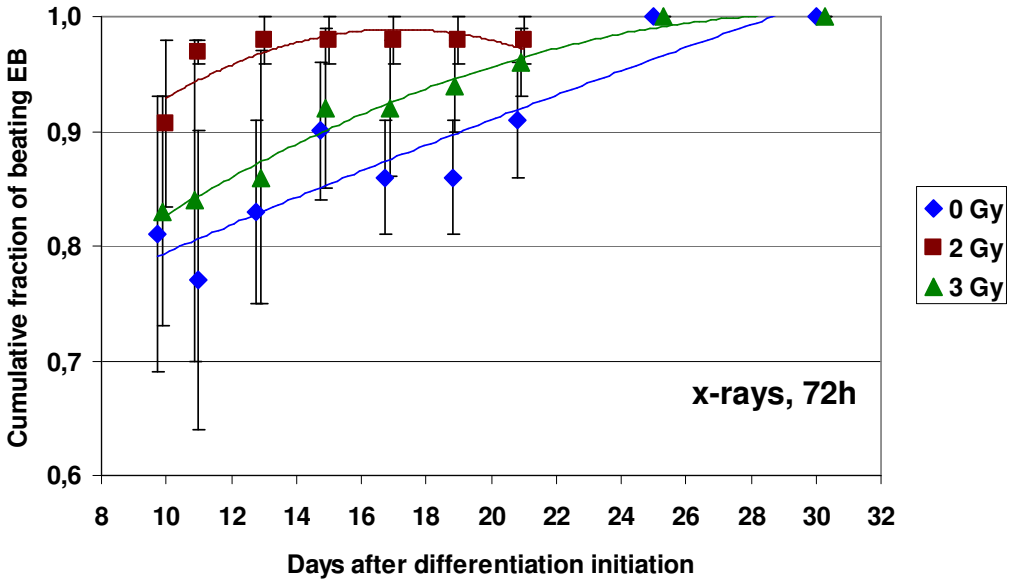

Figure 3.14 *Cumulative fraction of beating embryoid bodies differentiated 72h after exposure to x-rays. Data show mean values of different independent experiments. Note the different y-axis scaling. Error bars express the standard error of the mean or Bernoulli distribution. For reasons of clarity data sets for 0.5, 1 and 6 Gy are not plotted (complete set of data and further details are given in table A.7). To guide the eye, polynomial fits are superimposed on the obtained values.*

Data from chapter 3.3.1 showed that carbon ions were about twice as effective as x-rays in inhibiting differentiation into beating cardiomyocytes on day 10 of differentiation. The developmental kinetics of beating cardiomyocytes for 0h experiments (figures 3.11 and 3.12) showed a similar behaviour for iso-effective doses (i.e. 0.5 Gy and 3 Gy carbon ions versus 1 Gy and 6 Gy x-rays, respectively), confirming the RBE of about 2. Fractions of beating EBs for all doses of both radiation qualities reached the control level within the time interval investigated (up to day 30). Fractions of iso-effective doses reached similar levels. For 72h experiments (3.3.1), an inhibition of the development of beating cardiomyocytes was observed only after carbon ion exposure but not after x-ray exposure. Hence, an RBE estimation cannot be done. However, data from 3.3.1 revealed a similarity between the curves for 0h x-rays and 72h carbon ion. This similarity was also seen in the developmental kinetics when comparing the data obtained for 3 Gy, carbon ions or x-rays (figures 3.12 and 3.13). For 72h x-rays, the developmental kinetics did not

significantly differ from the control kinetic. Only the data points of 2 Gy exposed samples instead were slightly higher than all other samples (see chapter 4.5.1).

The RBE values for carbon ions in 0h experiments of developmental inhibition of contracting cardiomyocytes (3.3.1) and the cell inactivation (3.2.1) were close to each other (2 and 3, respectively). Additionally, developmental kinetics of beating cardiomyocytes between iso-effective doses in 0h experiments were similar. That indicates an influence of the initial cell number when EBs aggregate on the beating fraction obtained from them. The initial cell number might be altered by cell killing effects of radiation in the nascent EB. Vice versa, the similarity of kinetics between 72h carbon ions and 0h x-rays were not found in the cell survival experiments.

3.3.3 Size of embryoid bodies from exposed cells

The diameter of EBs was measured on day 5 of differentiation to assess the putative influence of radiation exposure on cell growth and the differentiation to contracting cardiomyocytes. For diameter measurements, day 5 was chosen for two reasons. First, on that day single EBs were transferred in the cavities of 24-well tissue culture dishes. Second, by that time, right before the attachment, they still show a regular spheroid size that later changes to irregular structures that are difficult to measure. EBs used here were the very same ones used for determining the beating fraction on day 10 of differentiation (see above) for cells differentiated 0h or 72h after exposure to x-rays or carbon ions.

Figure 3.15 relates the size of EBs to the fraction of beating EBs after exposure to both carbon ions and x-rays. Differentiation was started immediately after exposure (0h). For comparison, the fractions of beating EBs after exposure are replotted from figure 3.10. With an increasing dose, the diameter of the EBs decreases. The twice higher effectiveness of carbon ions also appears in the diameter reduction. Controls in both cases are around 450 µm. The lowest dose each (0.5 Gy carbon ions and 1 Gy x-rays) results in a moderate decline of size to about 400 µm (carbon ions) and 430 µm (x-rays), respectively. The size reduction is not significant according to the t test. For 3 Gy carbon

ions and 6 Gy x-rays, the diameter of the EBs is about 250 µm. The error bars here are clearly separated from the ones of the control, underlining the significance ($p < 0.01$, t test). Hence, the reductions in size for low doses are moderate whereas response to the higher doses is rather strong. This corresponds to the moderate and strong reductions in the fraction of beating EBs for low and high doses, respectively.

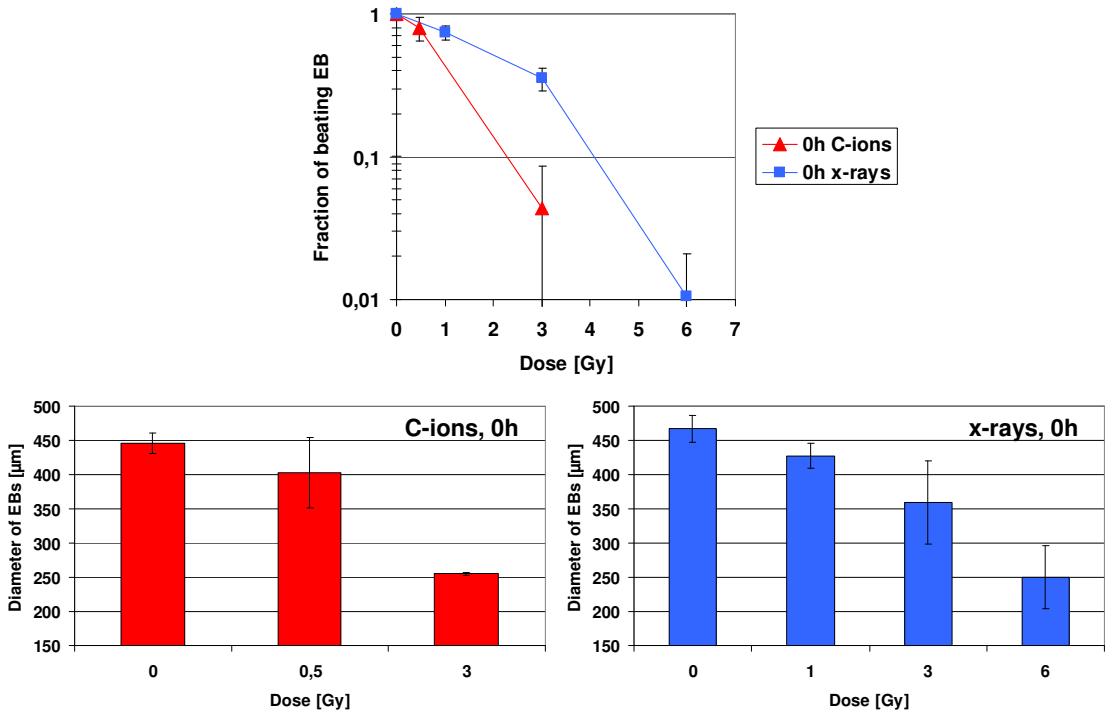

Figure 3.15 *Size of embryoid bodies and fraction of beating embryoid bodies after exposure to carbon ions and x-rays (differentiation initiation at 0h). The diameter of the bodies was measured on day 5 of differentiation immediately after seeding in 24-well tissue culture plates. Beating fractions were determined five days later (day 10 of differentiation). Data show mean values of different independent experiments. Error bars express the standard error of the mean or Bernoulli distribution (details are given in table A.8).*

Similarly the size of EBs and its relation to the fraction of beating EBs after exposure to both carbon ions and x-rays was examined for cells differentiated 72h after exposure (figure 3.16). The fractions of beating EBs after exposure is replotted from figure 3.10. For carbon ions, the size of the EBs is smaller for 0.5 Gy (about 400 µm) than for controls (about 500 µm). The size of EBs for 3 Gy irradiated samples is reduced to about

300 µm. Significantly different from the control, however, are only the 2 Gy exposed sample ($p < 0.05$, t test) and the 3 Gy exposed sample ($p < 0.01$, t test). Interestingly, the differences between the various irradiated samples are less pronounced, resembling the reduction of the fraction of beating EBs (figure 3.16, upper panel). The control value of EB-size in the x-ray experiments is in the same level of the controls value for carbon ion experiments (about 500 µm). The samples exposed to 3 Gy x-rays show a strong decrease ($p < 0.01$, t test) in size of the EBs, however, there is no data for any other dose concerning the EB diameter. The samples exposed to x-rays instead do not differ from controls concerning the fraction of beating EBs.

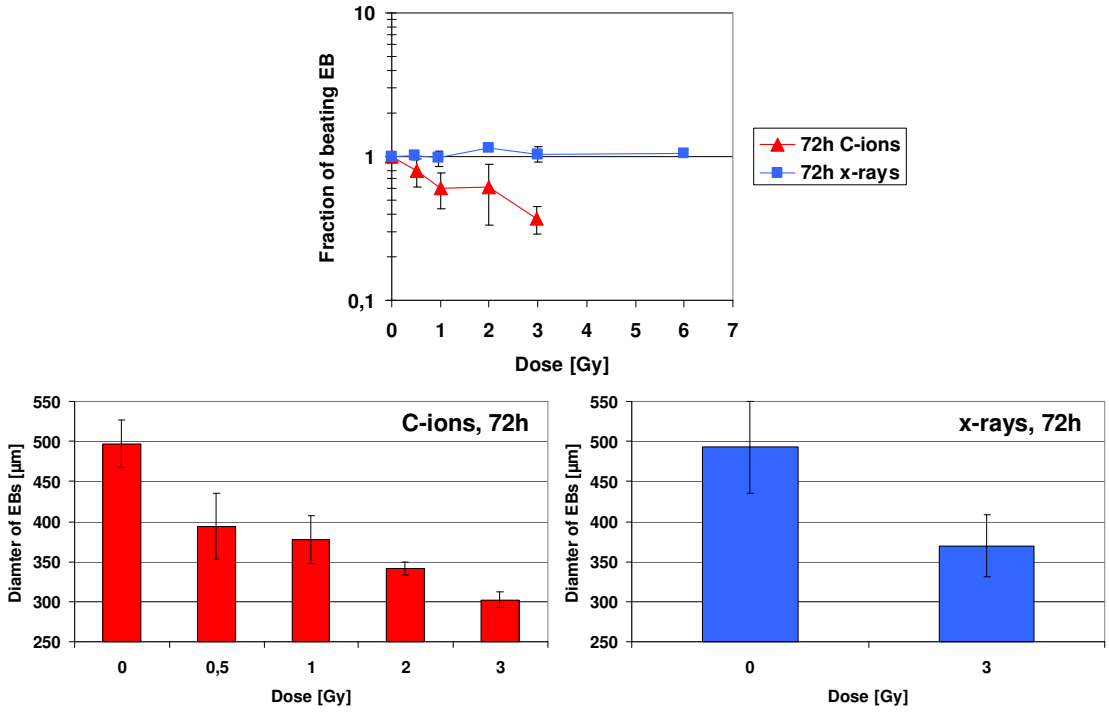

Figure 3.16 *Size and beating fraction of embryoid bodies after exposure to carbon ions and x-rays (differentiation initiation at 72h). The diameter of the bodies was measured on day 5 of differentiation right after seeding in 24-well tissue culture plates. Beating fractions were determined five days later (day 10 of differentiation). Data show mean values of different independent experiments. Error bars express the standard error of the mean or Bernoulli distribution (details are given in table A.9).*

Altogether, the data from both 0h and 72h experiments suggest a dependence of the fraction of beating EBs on the EB size and thereby also a dependence on the cell number. The 3 Gy x-rays exposed sample in the 72h experiment, however, is an exception as size was reduced but no influence on the development of EBs was found.

3.3.4 Cell proliferation in embryoid bodies differentiated from exposed cells

Cell proliferation was measured in EBs on day 5 of differentiation of a 0h experiment to investigate whether 3 Gy of x-rays still affect the number of cycling cells after a time span of five days. The cell proliferation was measured by quantifying EdU-positive cells with flow cytometry or by fluorescence microscopy. Flow cytometer analysis revealed an increase in cell proliferation in EBs differentiated from cells exposed to 3 Gy x-rays. The increase was 1.7-fold (± 0.2, error estimation based on experimental experience with this assay) when compared to the control. No difference between control and exposed sample was found when EdU-positive cells were analysed by fluorescence microscopy (49% ± 2% error calculated with Poisson distribution). Both data sets were derived from the same experiment. Flow cytometer data were gained through processing the raw data by several gating steps and finally an arbitrary threshold was chosen to compare control and exposed sample. This data processing, however, can impair the significance of the data. Therefore, results obtained by scoring EdU-positive cells with a microscope may be considered more robust in that case .In conclusion, the data suggest that differences in the proliferation rate between control and the exposed sample are unlikely. This indicates that the cells might have overcome damaging radiation effects on day 5 of differentiation.

3.3.5 Effect of the initial cell number on the emergence of spontaneously contracting cardiomyocytes

To disentangle the influence of initial cell number and radiation on the cardiomyocyte development, EBs were produced from 500, 750 and 800 cells, respectively, 72h after exposure to 2 Gy of carbon ions (figure 3.17). The standard protocol as used in all other

experiments is 750 cells. The controls do not show a dependence on the used initial cell numbers. On day 10 they exhibit high fractions of beating EBs (around 85%) that increase during the differentiation time observed (until day 21 after differentiation initiation). A similar fraction of beating EB was found after irradiation with 2 Gy and 850 cells seeded. EBs generated from 750 and 500 exposed cells instead have a lower fraction of beating EBs (53 and 42%, respectively). The fraction of beating EBs declines with a lower cell number. Their fractions, however, increase over the time-course observed. The fraction of the initial cell number of 750 cells exposed to 2 Gy carbon ions finally reaches the levels of the other, the 500 cell sample instead does not reach it during that period.

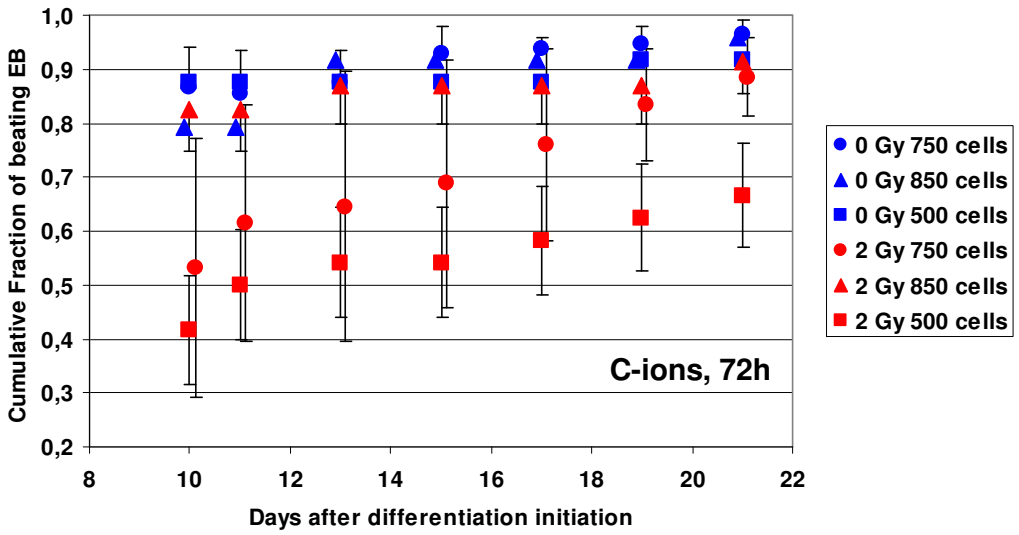

Figure 3.17 *Relationship between initial cell number and fraction of beating embryoid bodies after exposure to carbon ions (differentiation initiation at 72h). Samples with 750 (standard protocol) initially seeded cells are replotted from figure 3.13. Data sets for 500 and 850 initially seeded cells are derived from one experiment. Error bars express the standard error of the mean or Bernoulli distribution. For reasons of clarity only two curves of the data sets with higher fractions are presented with error bars depicting the outermost error in this group (details are given in table A.10).*

Taken together, the results here indicate that in control samples a different initial cell number in the EBs alone (500, 750 and 850 cells of control) has no influence on the fraction of beating EBs. When the reduced initial cell number is combined with radiation (2 Gy of carbon ions), differences emerge.

3.3.6 Cell death in embryoid bodies

The number of cells undergoing apoptosis in the EBs after radiation exposure was measured at day 1, 3 and 5 of differentiation. Both differentiation protocols, 0h and 72h were applied. The background level for cell death in control EBs was found to be 12% ± 1% (n=7), 38% ± 6% (n=7) and 32% ± 6% (n=5) on days 1, 3 and 5 of differentiation (0h and 72h experiments), respectively. Hence, apoptosis rate for controls is higher in EBs than in pluripotent cultures (see chapter 3.2.2).

Figure 3.18 demonstrates that cell death in EBs, differentiated immediately after exposure (0h) to carbon ions is only affected by radiation on day 1 of differentiation. The level of apoptosis is around 10%, whereas it is significantly higher in the 3 Gy exposed sample (i.e. around 27%, $p < 0.01$, t test). The cell death level of the sample exposed to 0.5 Gy slightly increases on day 1. On days 3 and 5 of differentiation no dose-dependent effect was detected. In general, the cell death rate on day 3 of development rises but decreases on day 5.

For doses up to 3 Gy x-rays, cell death in EBs differentiated immediately after exposure (0h) does not show any dose-effect, as demonstrated in figure 3.19. Apoptosis rates for 1 and 3 Gy irradiated samples rise from day 1 to day 5 of differentiation (i.e. one, three and five days after exposure, respectively), but are close to the control levels (roughly 13% to 39%). In contrast, the sample exposed to 6 Gy exhibits an increased rate of cell death (about 36%) only on day 1 of differentiation when compared to control, 1 and 3 Gy exposed samples. Highest numbers of cell death were found for the sample exposed to 10 Gy as it has a significant increase at both time points (around 48% and 76%, respectively) each compared to the control. It rises further on day 3 and remains higher than the

control. Data for the 10 Gy sample could not be assessed as EBs had disaggregated after few days of differentiating.

In summary, apoptosis levels in EBs differentiated directly after exposure to carbon ions were dose-dependently elevated only one day after exposure. For x-rays, only doses higher than 3 Gy exceeded the cell death level of the control on day 1. An exception is the 10 Gy exposed sample that also exhibited an increased level of cell death three days after irradiation. When comparing 0.5 Gy of carbon ions on day 1 to 1 and 3 Gy of x-rays, carbon ions were more effective in inducing apoptosis. Doses of 3 Gy carbon ions and 6 Gy x-rays had an iso-effect for other endpoints, however, here they did not.

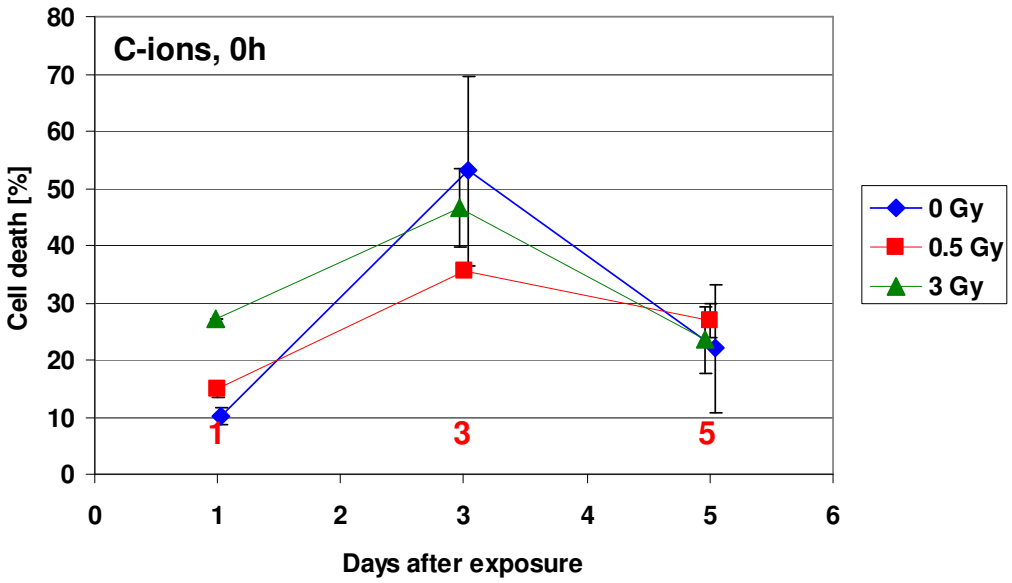

Figure 3.18 *Cell death in embryoid bodies after exposure to carbon ions, 0h experiments. EBs were dissociated to single cell suspension. After DAPI staining the fraction of apoptotic cell nuclei was counted. The red numbers indicate the days of differentiation. Data show the mean value of two independent experiments where the error bars express the standard error of the mean.*

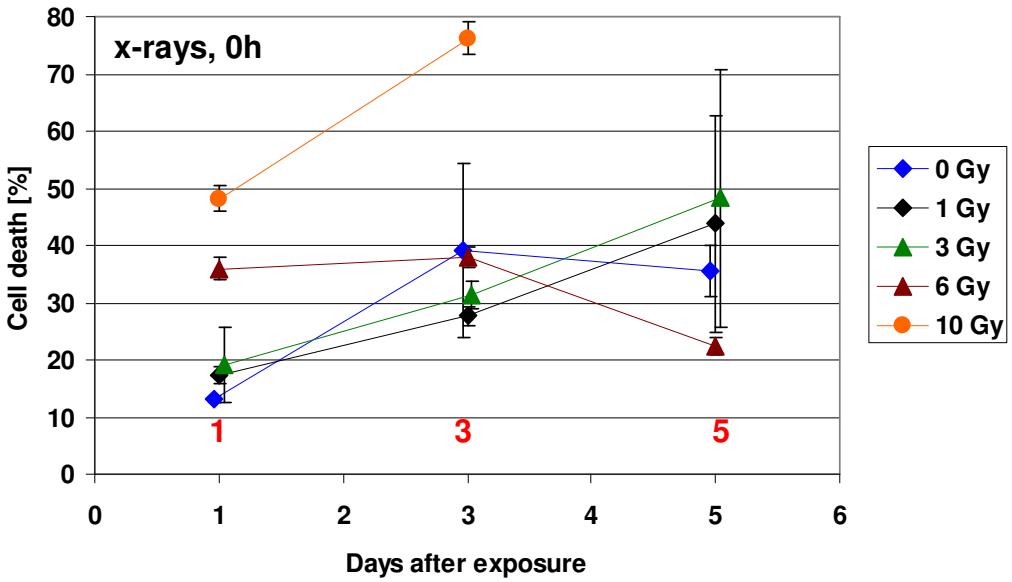

Figure 3.19 *Cell death in embryoid bodies after exposure to x-rays, 0h experiments. EBs were dissociated to single cell suspension. After DAPI staining the fraction of apoptotic cell nuclei was counted. The red numbers indicate the days of differentiation. Data show mean values of different independent experiments. Error bars express the standard error of the mean or Poisson distribution (details are given in table A.11).*

Cell death in EBs where differentiation began at 72h after exposure to carbon ions is not affected by radiation in a dose-dependent manner (figure 3.20): on day 1 of differentiation (four days after exposure) the apoptosis rates are around 13% in all samples. On differentiation day 3 the cell death rate rises to about 38% for all samples and remains on that level on day 5 of differentiation for most samples, except for 0.5 Gy (about 25%), which decreases at that time point.

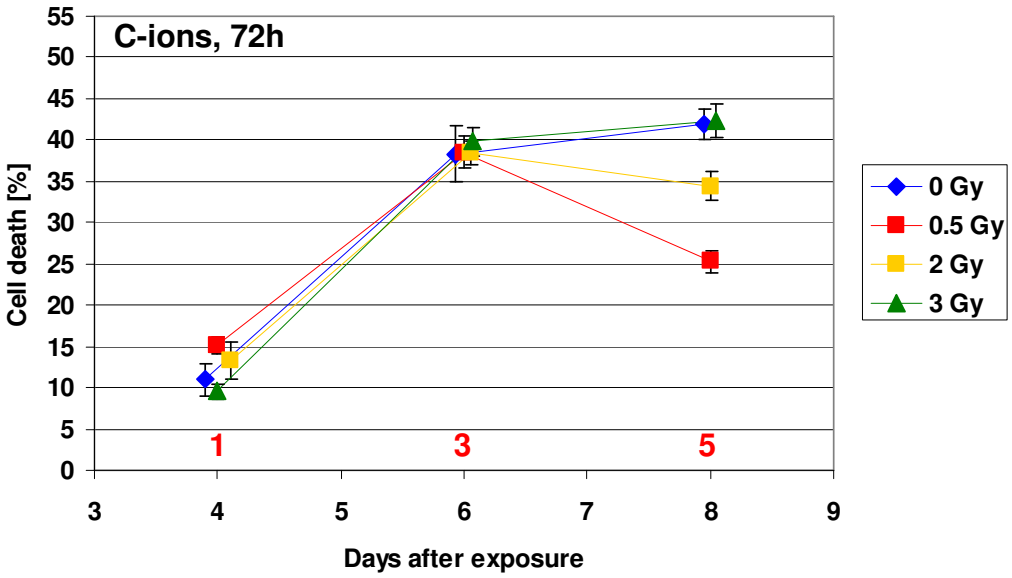

Figure 3.20 *Cell death in embryoid bodies after exposure to carbon ions, 72h experiments. EBs were dissociated to single cell suspension. After DAPI staining the fraction of apoptotic cell nuclei was counted. The red numbers indicate the days of differentiation. Data show mean values of different independent experiments. Error bars express the standard error of the mean or Poisson distribution (details are given in table A.12).*

The cell death rates in EBs where differentiation was started 72h after irradiation with 3 Gy x-rays are displayed in figure 3.21. The differences between control (about 15%) and the exposed sample (about 18%) are small on day 1 of differentiation. However, the differences increase slightly over time and the cell death rate of the exposed sample remains higher. Cell death rates in general rise on day 3 of differentiation (43% control and 49% exposed sample) and remain on that level on differentiation day 5 (42% control and 50% exposed sample).

Data obtained so far indicate that radiation-induced apoptosis in EBs differentiated 72h after exposure to carbon ions and x-rays is minimal.

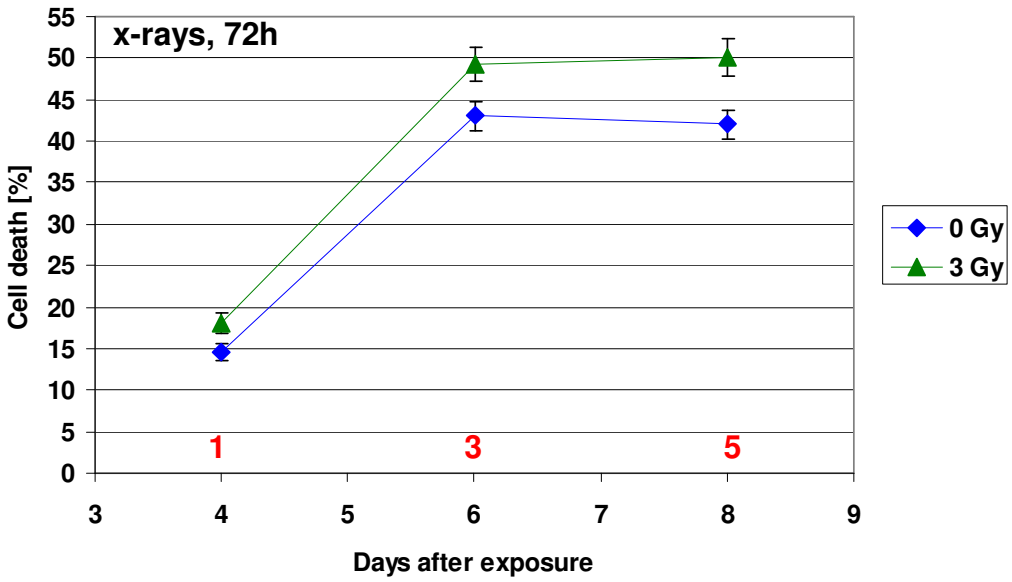

Figure 3.21 *Cell death in embryoid bodies after exposure to x-rays, 72h experiments. EBs were dissociated to single cell suspension. After DAPI staining the fraction of apoptotic cell nuclei was counted. The red numbers indicate the days of differentiation. Data are from one experiment where the error bars express Poisson distribution.*

Comparing the apoptosis rates after radiation exposure in pluripotent ES-D3 cultures and in EBs, points out that radiation induced cell death was measurable in ES-D3 up to day 3 after exposure, particularly when a passage was done one day after irradiation. In EBs however, a radiation induced increase in the apoptosis was only seen one day after exposure in 0h experiments. After the passage and a subsequent differentiation (72h experiments) radiation-induced apoptosis was not distinguishable. Hence, cell death induction by radiation was lower in EBs generated from irradiated ES-D3 than in exposed pluripotent ES-D3 cultures, probably due to the higher background level of apoptosis in the controls per se (see chapter 4.5.4). This higher background of apoptosis in later EB stages (38% and 32%, respectively) hampered the measurement of radiation-induced apoptosis in that system.

3.3.7 Mathematical modelling of the fraction of beating embryoid bodies

To gain further information about the contribution of the initial cell number seeded for EB formation on the fraction of beating EBs and its developmental kinetics over the differentiation time-course, a mathematical model was applied. The model reflects the contribution of the initial cell number influenced by radiation-induced cell inactivation and connects it with the probability of the EBs to show contraction. The data as presented in 3.3.2 were thus modelled.

The modelled data for the differentiation 0h after exposure to carbon ions (figure 3.22) are exemplarily shown compared to the measured fraction of beating EBs on day 10 of differentiation. The reproduced data are not in agreement with the measured data. While the fraction of beating EBs for the measured data was inhibited dose-dependently, the reproduced data do not show any inhibition at all. Additionally, for the other experiments, i.e. 0h x-rays, 72h carbon ions an x-rays the modelled data were not in agreement with the measured data neither. No inhibition for any dose was found (graphs not shown). The model thus was not able to reproduce the experimentally obtained data. Hence, no conclusion on whether the initial cell number reduced by radiation plays a pivotal role can be drawn from it.

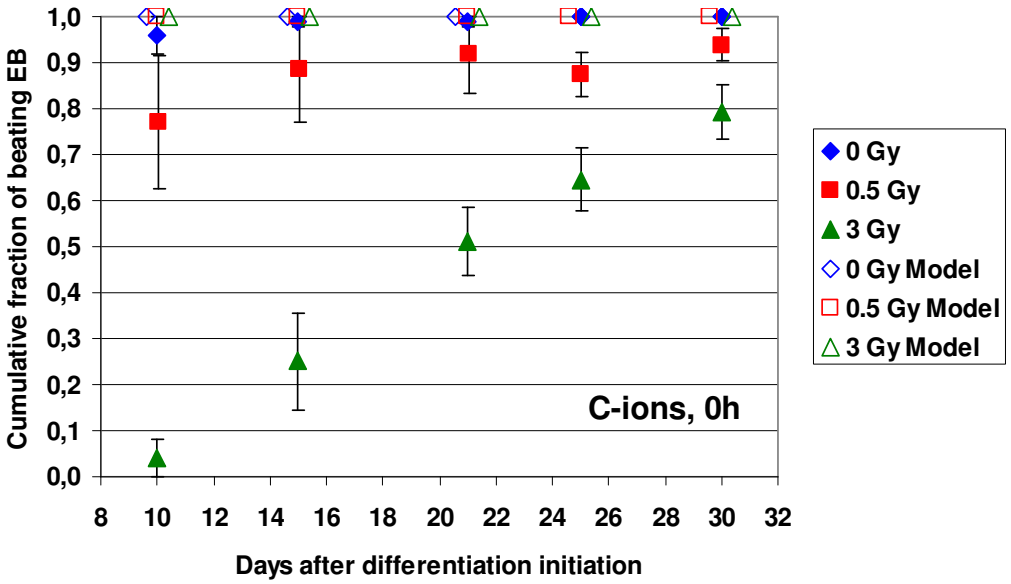

Figure 3.22 *Measured and modelled data for the cumulative fraction of beating embryoid bodies differentiated 0h after exposure to carbon ions. Measured data are redrawn from figure 3.11.*

3.3.8 Expression of pluripotency and cardiac marker genes in embryoid bodies derived from exposed cells

Putative effects of 3 Gy carbon ions or x-rays on the transcript expression of genes related to pluripotency and cardiomyocytes were studied by qRT-PCR.

Figure 3.23 displays the expression of pluripotency-associated marker genes, i.e. *Nanog*, *Sox2* and *Oct-3/4*. For controls, the expression levels of *Nanog* and *Sox2* both are highest on day 0 (undifferentiated state) and decrease constantly over the differentiation time-course. A decrease was found as well for the samples exposed to x-rays. However, the *Sox2* expression decreases slower in x-ray irradiated samples than in the controls. The levels of the samples exposed to carbon ions for *Sox2* and *Nanog* instead do not decrease but remain at the same level with minor fluctuations. A different expression pattern was found for *Oct-3/4*. In controls and irradiated samples an increase in the expression was measured when compared to the control of day 0, followed by a decline. That decline in expression levels is more pronounced for the control than after exposure. The least

change in expression was found for samples irradiated with carbon ion. The rise in the expression levels in the early differentiation period found in all samples may be related with another function of *Oct-3/4* during the incipient differentiation as discussed in chapter 4.2. A pronounced difference between high- and low-LET was found for all three investigated genes.

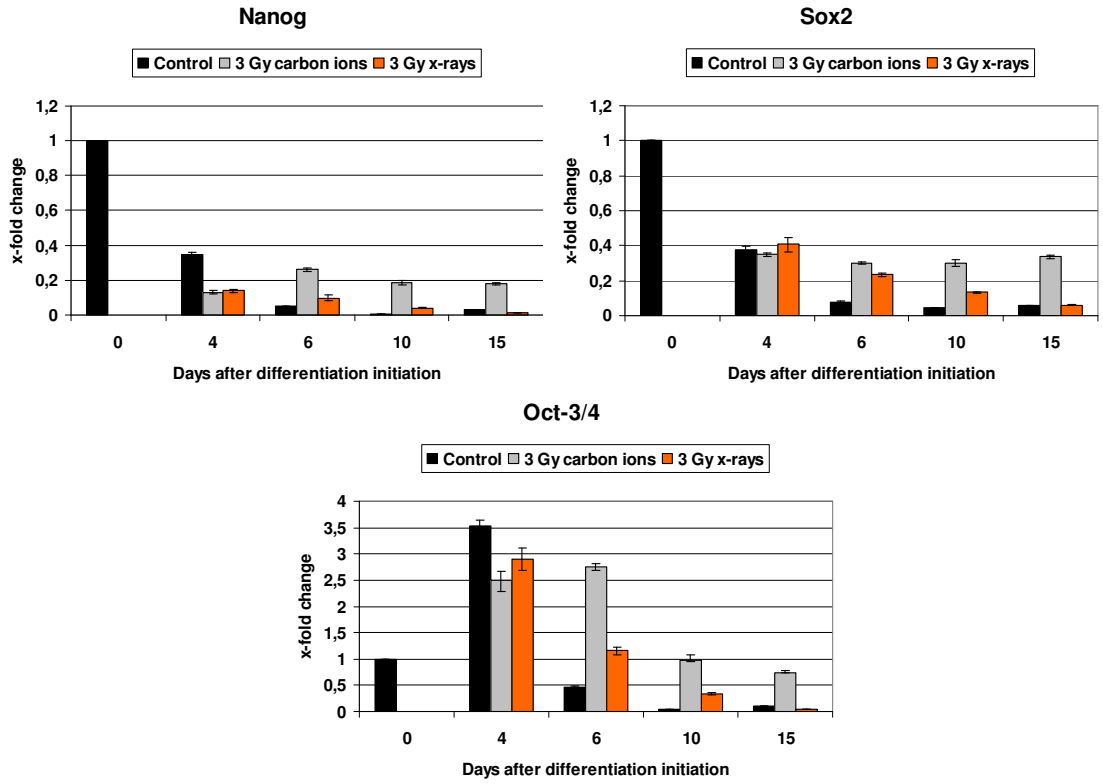

Figure 3.23 *Expression of pluripotency marker genes in embryoid bodies differentiated 0h after exposure to carbon ions and x-rays. Expression is normalized to undifferentiated control cells (day 0 after differentiation initiation). Data are obtained from three technical replicates of one experiment and error bars represent their standard error of the mean.*

The ongoing differentiation may serve as an explanation for the decrease in the expression of the pluripotency-associated genes over the observed time-course. The differences between control and the various exposed samples (higher RBE for carbon ions) were found as well for the inhibition of differentiation into beating cardiomyocytes. The initial fractions of beating EBs and the resulting delayed increase of the fractions

were found to be more affected by carbon ions (3.3.1 and 3.3.2, respectively). Therefore, a relation between the delayed cardiac differentiation and the delayed decrease of the pluripotency-associated gene expression is likely.

Complementing the pluripotency gene studies over the time-course of differentiation, the gene expression of cardiac differentiation markers was studied using the same samples (figure 3.24). Generally, expression levels of all investigated genes are low in the beginning and increase up to day 10, demonstrating the onset of cardiac differentiation. Concerning the gene expression of the transcription factor *Gata4*, the control and the sample from EBs exposed to x-rays increase over time and from day 10 on remain at a certain level with minor fluctuations. The EBs derived from cells exposed to carbon ions instead show a slower increase in the expression and reach the levels of the other samples not before day 21. The peak in the expression on day 25, due to the fact that the results are from one experiment, may be considered an outlier. For *Hcn4*, the ion channel protein, expression in the control increase after day 10. That was found as well for samples exposed to carbon ions and x-rays, although slower. While the expression in control and x-rays exposed samples apart from minor fluctuations rise, it declined in samples irradiated with carbon following day 21 of differentiation. Generally, a delay through exposure was found also for *Hcn4*. Concerning the three structural and functional markers *Myh7*, *cAct* and *cTropT2* analysed, the gene expression levels in the controls decrease after day 10 of differentiation. The exposed samples show a delayed rise in expression compared to the control, i.e. *Myh7* and *cTropT2* reach the peak value of the control later. For *cAct*, there is a delay for exposed samples, too, but the control level is not reached. The high expression for carbon ions on day 30 is probably an outlier.
Thus, the data indicate that the delayed increase of the cardiac marker gene expression consequentially follows the delay in the decrease of pluripotency-associated genes and reflects the developmental kinetics of cardiomyocyte emergence.

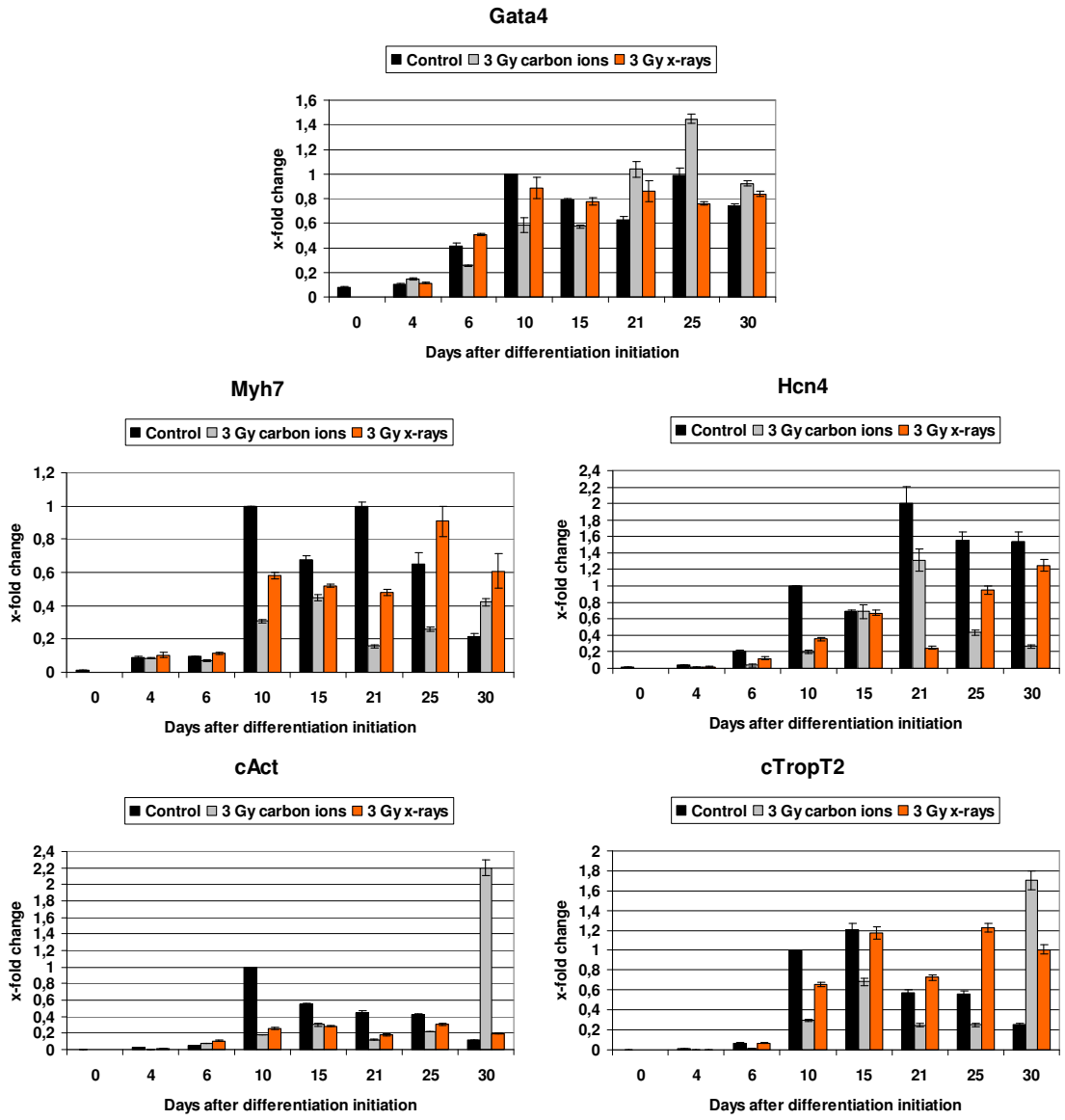

Figure 3.24 *Expression of cardiac marker genes in embryoid bodies differentiated 0h after exposure to carbon ions and x-rays. Expression is normalized to the control on day 10 after differentiation initiation. Data are obtained from three technical replicates of one experiment and error bars represent their standard error of the mean.*

4. Discussion

4.1 Risk of an unanticipated radiation exposure of the early embryo

The influence of ionising radiation exposure during the early embryonic development (pre-implantation stage) is insufficiently understood, however, it is of interest for public health to gain information on that topic. To date, that information is mainly derived from experimental *in vitro* data or animal studies. Most studies focus on low-LET radiation. They point out a high radiation sensitivity of the embryo throughout the whole prenatal period *in utero* (for a summary see ICRP 2003). The data further suggest lethality as the dominating effect of radiation exposure in the pre-implantation period starting from doses of about 0.1 Gy of low-LET radiation. Malformations following an exposure in the pre-implantation stage have been also observed, but seem to depend on a genetic predisposition of the mouse strain [Streffer 2006]. Experiments with neutrons provide the only data for high-LET radiation and suggest a higher RBE when compared to x-rays [e.g. Pampfer and Streffer 1988]. Most of these data however are derived from experiments when embryos were exposed in the zygote stage [e.g. Weissenborn and Streffer 1988]. With ongoing development, even within the pre-implantation stage, the probability of a lethal effect declines rapidly. Thus, an LD_{50} (dose leading to lethality in 50% of the cases) from the zygote stage to the blastocyst stage, both still pre-implantational, was estimated to be 1 Gy. The lethality according to the report is mainly due to cytogenetic damage and chromosomal aberrations that develop in the rapidly dividing cells, although DNA repair seems to be efficient [European Commission 2002, ICRP 2003].

Humans are exposed to a natural background level of ionising radiation, which can penetrate tissues deeply. That background level is about 2 mSv per year. Additionally, exposure comes from radiation sources such as diagnostic applications, security scans at

airports and flights. X-ray diagnostics for example contribute with another 1.8 mSv per year and per capita [Bundesamt fuer Strahlenschutz 2001, Bundesamt fuer Strahlenschutz 2009]. The likelihood of foetal radiation exposure additionally to the natural background hence is high. About 50% of all pregnancies in North America for example are unplanned [Pennsylvania Patient Safety Advisory 2008]. Thus, especially in the pre-implantation phase, the pregnancy might still be unknown to many expectant mothers and an unanticipated radiation exposure of the embryo through diagnostic or therapeutic means is of concern in that context. A computed tomography (CT) scan on the abdomen for example can result in a foetal radiation dose of 30 mGy (about 10 mSv). To compare, the natural foetal background dose is about 1 mGy and the Radiation Safety Committee of the United States Centers for Disease Control and Prevention recommends not to exceed a cumulative foetal dose of 5 mGy [Ratnapalan et al. 2003, Pennsylvania Patient Safety Advisory 2008]. Furthermore, an unanticipated exposure can result from therapeutic application of radiation, as radiotherapy is an effective treatment for cancer patients. Approximately 50% of all patients with localized malignant tumours are treated with ionising radiation [Durante and Loeffler 2010].

The accident of Fukushima in March 2011 has shown recently that an accidental exposure of a large collective of people is a realistic scenario that can lead to an exposure with different qualities of ionising radiation [Doerr and Meineke 2011, Thielen 2012]. The same danger can emanate from nuclear attacks, for example through the explosion of a large radiologic dispersal device (“dirty bomb”) in a scenario of nuclear terrorism [Wolbarst et al. 2010, Williams and McBride 2011]. Given the exposure of a large collective of individuals, for instance in a densely populated city, it is likely that pregnant women are among them.

Nontheless, data for high-LET radiation are rather rare but of great importance for radiation protection as well. About half of the 2 mSv natural background radiation comes from the inhalation of radon which produces high-LET alpha particles in its decay chain [Bundesamt fuer Strahlenschutz 2009, Newhauser and Durante 2011]. Taking flights, especially intercontinental ones with higher altitude, cosmic radiation partly comprised of high-LET particles contributes more to the exposure of a body than on earth [Singh et al.

2011a]. In nuclear disasters, for example from dirty bombs high-LET radiation may be emitted [Durante 2003]. Additionally, high-LET charged particles are increasingly used for therapeutic applications, such as proton or carbon ion radiotherapy or radiosurgery [Schardt et al. 2010, Bert et al. 2012]. Apart from the accuracy, which is one of the advantages of particle therapy, the creation of secondary particles, mainly neutrons due to fragmentation is a concern and its severity remains to be elucidated [Newhauser and Durante 2011]. However, Muenter et al. [2010] showed that particle therapy with carbon ions may be used to treat pregnant women for cancer keeping the *in utero* dose as low as the natural background. These facts point out the necessity for data on the effects of high-LET radiation on the early embryonic development. To contribute to a better understanding of the risk during early embryonic development, the present study used the *in vitro* differentiation of mESC as a model.

4.2 Pluripotency of the ES-D3 cultures

The ES-D3 cell line, used in the present work as a model for embryonic development, was shown to have pluripotency potential by the formation of teratomas after injection in mice and by the creation of chimeras after injection in blastocysts [Doetschman et al. 1985, Pease and Willimas 1990]. The term pluripotency describes the potential to differentiate into cells of all three primary germ layers (endoderm, mesoderm and ectoderm) and is related with unlimited self-renewal and proliferation of the cells. However, with ongoing differentiation they loose potency and finally remain as differentiated cells [Wobus and Boheler 2005]. The undifferentiated pluripotent stage of the ES-D3 used in the radiation experiments is an important prerequisite. Therefore, the used ES-D3 cultures were tested in regular periods while in culture for the expression of pluripotency markers.

First, the activity of alkaline phosphatase was investigated (3.1.1). The expression of alkaline phosphatase was found in pre-implantation development in embryos and is a feature of pluripotent stem cells, although not being exclusively expressed by stem cells and early progenitors [Wobus et al. 1984, Hahnel et al. 1990]. The assay revealed that all

colonies in the cultures showed the red/purple staining indicating active alkaline phosphatase and thus pluripotency. This is in line with data from Toumadje et al. [2003] showing that all colonies of ES-D3 were positive for alkaline phosphatase. As depicted in figure 3.1, around the colonies, unstained cells with a different morphology from the cells inside the colonies were regularly found. The different shape and also the bigger size of these cells indicate that they may represent differentiated cells.

Next, transcription factors that are crucial for pluripotency maintenance were investigated. These factors, together with others, interact with each other controlling and maintaining their expression levels and the pluripotency of the cell [Masui et al. 2007]. They are regulated by diverse signalling pathways, where LIF, which is present in the ES-D3 cultures also in this work is a main player regulating this network [for an overview see Annerén 2008]. Some of the key players in pluripotency maintenance are Oct-3/4, Sox2 and Nanog [Mullen et al. 2007, Wobus and Loeser 2011]. In this work, pluripotency of ES-D3 therefore was investigated by measuring gene expression with qRT-PCR as shown in 3.3.8. *Oct-3/4*, *Sox2* and *Nanog* were expressed in the ES-D3 cultures right before they were differentiated (day 0, figure 3.23). The highest expression of *Sox2* and *Nanog* was found on day 0, i.e. in pluripotent cultures. *Sox2* and *Nanog* are down-regulated when differentiating into mesoderm [Thomson et al. 2011], which is consistent with data shown in figure 3.23. *Oct-3/4* expression pattern is an exception, as it first (day 4 of differentiation) rose and then decreased. However, it has been reported that an increase in the expression of *Oct-3/4* is accompanied with a differentiation into endoderm and mesoderm [Niwa 2001]. The differentiation into mesodermal lineages and subsequently cardiac lineages is especially the case for the EST-like assay used in this work. In summary, alkaline phosphatase activity and the expression of *Oct-3/4*, *Sox2* and *Nanog*, all four being markers for pluripotent mESC [Pera and Tam 2010] indicated that the ES-D3 cells used for the experiments here were pluripotent.

4.3 Influence of radiation on the pluripotency

The influence of the radiation on the expression of pluripotency-associated genes was first measured on day 4 following differentiation initiation. As mentioned above, the decrease in expression of these genes was found. Samples exposed to 3 Gy x-rays and 3 Gy carbon ions had a delayed decrease of *Oct-3/4*, *Nanog* and *Sox2*. EBs derived from the progeny of cells irradiated with 3 Gy x-rays all decreased the expression levels of *Oct-3/4*, *Sox2* and *Nanog*, but slower than the control EBs. The EBs derived from the progeny exposed to 3 Gy carbon ions instead maintained their expression levels (*Nanog* and *Sox2*) or their level declined even slower (*Oct-3/4*) than in x-rays exposed samples. Given the same dose, high-LET radiation was more effective. Most likely, the reason for that is a delayed differentiation that does not result from a radiation-altered expression of pluripotency-associated genes, as discussed below. However, the progeny of irradiated ES-D3 kept their pluripotency potential as shown by the expression of marker genes of all three germ layers when differentiated [Arrizabalaga, unpublished data]. Data on the influence of radiation of the differentiation and the pluripotency potential are rare. Our data are in accordance with data published by Rebuzzini et al. [2012] who found that the survivors of the mESC line R1 irradiated with 5 Gy γ-rays maintained their pluripotent potential and were able to differentiate into the three germ layers. For hESC, exposed to 4 Gy of γ-rays the capability of teratoma formation when injected in mice after irradiation was reported [Wilson et al. 2010], which is considered the definitive proof for pluripotency. Data for high-LET radiation for a comparison with the results found here are not available.

The above-mentioned results were measured in differentiating cells that were derived from exposed pluripotent ES-D3 cells. Effects of radiation on pluripotency-associated gene expression in pluripotent ES-D3 cultures were investigated in the context of the present study, too. Luft et al. [2013b, submitted] could show that up to 17 days after exposure of ES-D3 cultures to carbon ions (up to 2 Gy) or x-rays (up to 3 Gy) no changes in the protein expression of Oct-3/4 and Sox2 occurred. Similarly, Rebuzzini et al. [2012] reported that 96h after radiation exposure the mESC line R1 after exposure to γ-rays still

expressed Oct-3/4 and two other pluripotency markers. Wilson et al. [2010] found for hESC, that survivors after exposure up to 4 Gy γ-rays still expressed Oct-3/4, Sox2 and Nanog. That was found as well for lower doses up to 1 Gy by Sokolov et al. [2010]. Available data are rare also here and no data at all were found up to date to compare with results for high-LET radiation.

In conclusion, neither low-LET nor high-LET radiation in the doses used here could affect the expression in ES-D3 cell cultures, even several days after exposure. Effects of radiation and differences between low- and high-LET were found instead in differentiating EBs. However, these effects may be explained with a dependence on the cell number in the EBs as discussed below, and not primarily due to radiation-induced gene expression changes.

4.4 Differentiation of embryonic stem cells to functional cardiomyocytes

The basic method of the current work is the *in vitro* differentiation of the mESC line ES-D3 into contracting cardiomyocytes, which is a broadly used and promising technique for research. The formation of functional, i.e. spontaneously contracting cardiomyocytes was among the first events to be described from mESC differentiation using EBs. In fact, derivation of cardiomyocytes from mESC is a frequent event in directed lineage differentiation [van Laake et al. 2005]. Wnt/β-catenin, transforming growth factor β (TGFβ), BMP and fibroblast growth factor (FGF) signalling is a crucial event to induce or promote *in vitro* differentiation into cardiomyocytes [van Laake et al. 2005, Murry and Keller 2008]. Nkx2.5 and Gata4 are among the earliest transcription factors expressed [Boheler et al. 2002, Kouskoff et al. 2005]. Other early markers of cardiac differentiation are Flk-1, insulin gene enhancer protein-1 (Isl-1) and Cripto-1 [Wei et al. 2005, Murry and Keller 2008]. The expression of these functional genes resembles the early cardiogenesis in the embryo and leads to *in vitro*-differentiated cardiomyocytes that share various features with their *in vivo* equivalents. Thus, *in vitro*-derived cardiomyocytes express structural and functional cardiac genes, some of which were used as marker to

study the cardiac differentiation in that work (see chapter 3.3.8). They may build organized bundles of myofibrils that are connected to each other in a network of gap junctions. The cardiac *in vitro* differentiation can give rise to a variety of specialized cardiac cell types [Maltsev et al. 1993, Boheler et al. 2002, Baharvand et al. 2006]. Cardiomyocytes generated *in vitro* were shown to have a spontaneous contraction activity [Doetschman et al. 1985]. Several days after differentiation begin beating foci arise within the EBs. Contractions can be seen from several days up to one month but cardiomyocytes can be kept in culture even beyond that. The electrophysiological properties of these cardiomyocytes can be assessed and are comparable with those of the *in vivo* situation [Boheler et al. 2002, Banach et al. 2003].

The EST is a generally accepted *in vitro* assay used to study embryotoxicity of drugs and other chemical compounds and is based on the differentiation of mESC (line ES-D3) into beating cardiomyocytes [Kuske et al. 2012]. *In vivo* studies for that purpose are time-consuming and expensive [Scholz et al. 1999]. The EST, validated by the ECVAM offers an *in vitro* alternative for embryotoxicity testing of chemicals [Balls 2002, Scholz and Spielmann INVITTOX no. 113 2002]. Typical concentration-response curves can be derived of the EST to estimate the ID_{50} value (inhibition of cardiac cell differentiation to 50% of a control). This value, together with cytotoxicity values derived from other accompanying assays, is used to classify chemical compounds or drugs either non-embryotoxic, weakly embryotoxic or strong embryotoxic [Wobus and Loeser 2011, Seiler and Spielmann 2011]. Considering the at least 30000 chemical compounds to be classified for their effects on the human health in the Registration, Evaluation, Authorisation and Restriction of Chemicals (REACH) programme of the European Union, the EST may be useful but has not yet been accepted to completely replace animal testing [European Union 2006, Wobus and Loeser 2011]. However, the EST is under permanent revaluation to apply new aspects such as molecular markers or endpoints considering gene expression and to improve its features for high-throughput applications [e.g. Buesen et al. 2009, Groebe et al. 2010, Theunissen and Piersma 2012, Theunissen et al. 2013].

Despite its promising features to screen embryotoxicity, the EST has up to date never been used to investigate the effects of ionising radiation on the early embryonic development. Especially the early embryonic development is similar between mammals [ICRP 2003]. Therefore the basic principle of the EST, the differentiation of ES-D3 cells into spontaneously contracting cardiomyocytes, was used in the current work to assess information on how radiation during the blastocyst stage affects the early cardiac development in mammals.

A crucial step in establishing the EST-like assay was to improve the efficiency of the cardiac differentiation by testing different sera (chapter 3.1.2). All three tested sera resulted in an efficiency of 80% ± 10% when analysed on day 10 of differentiation. This is in the range of the official requirements for the validated EST (i.e. at least 87.5% in each run for the control) [Seiler and Spielmann 2011]. Hence, it provided enough beating EBs for statistically relevant results.

Following the establishment of the cardiac differentiation of ES-D3 according to the recommended protocol, a validation using the EST-classified teratogen retinoic acid (RA) [Scholz et al. 1999, Wobus and Loeser 2011] was done. RA, a derivative of vitamin A and a central factor in embryonic development was found to influence the cardiac *in vitro* differentiation in a time- and concentration-dependent manner [van Laake et al. 2005, Gilbert 2006]. It has a crucial function in the embryonic development through regional patterning control, especially in the organogenesis of the heart, where it is involved in anteroposterior patterning and looping [Campo-Paysaa et al. 2008]. When not expressed in a temporally and spatially controlled manner, in physiologically high concentration for instance, RA instead acts as a teratogen hampering organogenesis of several organs [Lee et al. 2012]. Application of 5 nM RA throughout the differentiation period (described in Materna et al. 2013) showed an inhibition of cardiac differentiation similar to the one reported for example by Scholz et al. [1999], proving the validity of the assay as performed in the current work.

The formation of spontaneously contracting cardiomyocytes is one crucial endpoint of the assay. However, also other muscle types can develop in the *in vitro* cultures that show spontaneous contraction, such as skeletal myocytes [Dinsmore et al. 1996]. Hence, the formation of cardiomyocytes was, along with the spontaneous contraction proven regularly by Western Blot analysis and immunocytochemistry (see 3.1.3). The Western Blot analysis demonstrated the expression of cardiac troponin I throughout the observed period (days 10 to 30, Figure 3.3) in which contractions are visible. Cardiac troponin I is a regulatory protein controlling the calcium-mediated interaction between actin and myosin and it is only found in myocardium [Sharma et al. 2004]. The expression of it in cardiomyocytes derived from mESC is in accordance with Baharvand et al. [2006]. Cardiac troponin I was additionally detected by immunocytochemistry (Figure 3.2). The analysis of these samples revealed that the fractions of cardiomyocytes among all cells was found to be below 5% each. A percentage of cardiomyocytes differentiated from mESC of 3 to 5% has been reported in literature as well [Boheler et al. 2002]. The gene expression studies of other cardiac markers (discussed in 4.5.5) further confirm the formation of cardiomyocytes in the system used in this work.

Conclusively, the assay as performed in the current work was successfully validated and thus used in subsequent radiation experiments.

4.5 Influence of radiation on the differentiation

4.5.1 Fraction of beating embryoid bodies

As mentioned above, the spontaneous differentiation of ES-D3 into contracting cardiomyocytes was based on the EST. ES-D3 cells were irradiated in pluripotent culture, to mimic the exposure in the very early developmental stadium of the blastocyst. The differentiation assays were then performed at two different time-points, 0h and 72h after exposure of the cells with either carbon ions or x-rays (chapter 2.5). For the 0h experiments ES-D3 were differentiated immediately after exposure to examine the

influence of direct radiation damages, i.e. mainly cell death and cell inactivation but also altered gene expression. For the 72h experiments, exposed ES-D3 cells were allowed to grow further under pluripotent culture conditions. They were passaged 24h after exposure and differentiated 48h later, i.e. 72h after exposure. In the time frame of 72h, cells exposed to 2 Gy of carbon ions for example were found to have doubled around 3.7 times [Luft et al. 2013b, submitted]. In that way, even after a passage, the effects on the differentiation should be observed independent from cell death. The fraction of spontaneously beating EBs (i.e. containing contracting cardiomyocytes) was measured. Additionally, cell death, cell growth through EB size and proliferation in EBs were performed to complement the results.

Consistent with the EST the influence of radiation on the formation of beating EBs was measured on day 10 of differentiation. Here, a clear LET-dependent inhibition was noticed, both for 0h and 72h experiments. High-LET carbon ions were about twice as effective as low-LET x-rays comparing iso-effective doses for the 0h experiments (figure 3.10 and table 4.1). Interestingly, an RBE of about 3 was found for cell killing, also measured directly after radiation exposure (0h, figure 3.4 and table 4.1). This suggests a dependence of the inhibition to beating EBs on the cell inactivation and thus on the initial number of viable cells present in the EBs. For 72h experiments, the fraction of beating EBs there was not affected by x-rays, whereas for carbon ions there was still a dose-dependent inhibition (figure 3.10). In the cell survival data, however, a slight decrease in the survival of cells irradiated with x-rays plated 72h after exposure is still measurable and carbon ions here were still three times as effective as x-rays (72h, figure 3.4 and table 4.1). Probably there might be a threshold necessary to induce an effect, as x-rays 72h after exposure did not inhibit the fraction of beating EBs any more. To further confine that threshold, an experiment using a high dose of 10 Gy x-rays with differentiation directly after exposure was performed. Under these conditions EBs persisted not longer than day 3 of differentiation, i.e. besides a threshold for a measurable effect with this EST-like system, there is a lower limit in which cell killing concurrently hampers the formation of EBs.

Table 4.1 *RBE values of carbon ions in comparison to x-rays for different endpoints. All effects where clear iso-effective doses were found were taken into account. Data originate from figures 3.4, 3.10 and 3.15 (n.a.= not applicable for 72h experiments).*

Effect	Time point of cell processing after exposure	RBE	Iso-effective Doses (C-ions vs. x-rays) [Gy]
Survival	0h	3	all
	72h	3	all
Fraction of beating Ebs on day 10	0h	~2	0.5/1 and 3/6
	72h	n.a.	
Size reduction of embryoid bodies	0h	~2	0.5/1 and 3/6
	72h	n.a.	

Interestingly, for EBs derived from cells exposed to 2 Gy x-rays and differentiated 72h after exposure the fraction of beating EBs was higher than in the control and all other doses, i.e. 0.5, 1, 3 and 6 Gy (figure 3.14). This effect was observed in all experiments (n=2), but only in one out of two the difference was statistically significant when compared to the control (Fisher's exact test). A probable explanation for the elevated fraction of beating EBs is the production of reactive oxygen species (ROS). At the time of irradiation a burst of ROS is produced but is discussed to persist only less than a second. It is though under discussion whether radiation can perturb the balance of the natural ROS production leading to a long-term elevated level of ROS in the scale of days [Spitz et al. 2004, Buonanno et al. 2011]. On the other hand ROS were shown to enhance the differentiation into cardiomyocytes at a certain concentration [Sauer et al. 1999, Buggisch et al. 2007]. The conditions of an exposure to 2 Gy of x-rays and a subsequent differentiation 72h later might provide a ROS level necessary for the induction of an enhanced cardiomyogenesis. To prove this hypothesis, further experiments are necessary.

4.5.2 Initial cell number in embryoid bodies

For the formation of beating EBs on day 10 of differentiation, the initial cell number at the time of the EB production and its reduction due to radiation exposure seems to be important. Furthermore, a threshold seems to exist for that effect. In agreement with this hypotheses are the data derived from the differentiation of EBs with different initial cell numbers irradiated with 2 Gy carbon ions and differentiated 72h after exposure (figure 3.17). They clearly point at a threshold for cell inactivation after radiation necessary for an effect. The control with the reduced number of 500 cells showed no lower fraction of beating EBs on day 10 when compared to the control with 750 cells, i.e. the cell number of the standard protocol commonly used for all other experiments. When irradiated instead, both 750 cell EBs and 500 cell EBs exhibited a decreased beating fraction. The effect was more pronounced for 500 initially seeded cells. EBs made from 850 exposed cells did not show a decrease different from the normal condition control. The data indicate the threshold to be below 500 cells. That the cell number used to create the EB can influence the differentiation and its outcome has been reported in literature. Mansergh et al. [2009] found that for mESC a variation of the initial cell number changes the gene expression on day 4 of differentiation. Kurusowa [2007] states the rapid loss of any synchrony in differentiation for heterogeneously sized EBs. The direct influence on the cardiac differentiation for varying initial cell number in EBs was found as well and 500 cells were shown insufficient to induce an effective cardiomyogenesis with mESC [Preda et al. 2013]. Ng et al. [2005] found that in hESC, the number of cells affected the hematopoietic differentiation, which is closely related to the cardiac differentiation [Gilbert 2006]. In the resulting EBs an efficient blood formation required more than 500 cells. In the present study 500 cells were found to be able to induce an efficient cardiac differentiation. Taking into account inter-laboratory differences, the different species (mESC versus hESC) and all uncertainties, data from literature confirm a threshold close to 500 cells for an effective differentiation to cardiomyocytes.

4.5.3 Correlation of size and fraction of beating embryoid bodies

The size of the EBs was measured on day 5 of differentiation directly after they were selected and transferred into the cavities of 24-well tissue culture plates. It was found that with an increasing dose of both carbon ions and x-rays, both for 0h and 72h differentiation experiments, the size of the EB was reduced. Carbon ions also here were found to be about twice as effective as x-rays (see table 4.1). Preda et al. [2013] also reported a direct correlation between the initial number of mESC in EBs and the size on day 4 of differentiation. This demonstrates again that the cell number in the EBs was altered by radiation induced cell killing in this work. Mansergh et al. [2009] found that EBs seeded with cell numbers from 500 to 1000 cells reach a size plateau at day 4 of differentiation. A direct correlation between the reduced size of the EBs and the resulting decline in the beating fraction was found in the present study (figures 3.15 and 3.16). This indicates that for the inhibition of the beating EB fraction, the threshold is around or below 500 cells, as in the case of the work no plateau but a decrease was found that was correlated with the effect and the dose. If size and initial cell number are related, and if the initial cell number influences the differentiation, consequently the size affects differentiation as well. This is further supported by the same RBE (about 2) of carbon ions for inhibiting the fraction of beating EBs and for reducing their size (see table 4.1). That size affects differentiation was already reported by Messana et al. [2008] who found implications of the EB size on chondrogenesis of differentiating ES-D3. Preda et al. [2013] and Choi et al. [2010] showed the dependence of cardiac differentiation on the size in mESC. Yet, in the 72h differentiation experiment, a significantly reduced EB size was found after exposure to 3 Gy x-rays but no decline in the fraction of beating EBs (figure 3.16). However, this measurement is derived from one experiment only and might therefore be considered an outlier. Deductively, so far the results instead indicate a correlation of EB size and initial cell number with the resulting effect.

4.5.4 Cell proliferation and apoptosis

Measurements of proliferation and apoptosis of differentiating cells in the EBs were performed to further elucidate the role of the cell number in the differentiation assays. Proliferation was analysed by two different methods, i.e. by measuring EdU-positive cells with flow cytometry or analysis by fluorescence microscopy. EBs derived from a control and from a 3 Gy x-rays irradiated sample, differentiated immediately after exposure (0h), were analysed on day 5 of differentiation by both techniques (see chapter 3.3.3). No comparison with high-LET radiation is available here. Neither flow cytometry nor microscopic analysis showed a significant difference between the samples indicating that low-LET radiation damage did not persist until day 5 of differentiation. The data rather suggest that a crucial point for a radiation-induced effect is the initial cell number.
Embryonic stem cell cultures contain a high fraction of S-phase cells (i.e. proliferating cells) and have a short G1-phase, progenitors and differentiating cells with ongoing lineage selection lower that fraction [White and Dalton 2005]. Further studies, especially kinetics in terms of EdU-uptake are needed to estimate the fraction of cells that is not yet differentiating in control or exposed samples. This may contribute to obtain further information on the delay in differentiation as discussed below.

The influence of radiation on the cell death was investigated by analysing the morphology of the cell nuclei and a few data points were confirmed by the caspase-3 activity assay. High-LET carbon ions were found to be generally more efficient in inducing apoptosis in pluripotent ES-D3 cultures than x-rays (figures 3.5 to 3.8). For cells reseeded directly after exposure (figures 3.5 and 3.6), only high doses (i.e. 3 Gy carbon ions, 6 and 10 Gy x-rays) elevated the apoptosis level already one day after exposure, while for the lower doses, cell death levels increased not before two days after exposure. This is in accordance with data from Rebuzzini et al. [2012] that showed an earlier onset in apoptosis for the mESC line R1 for 5 Gy γ-rays than for 2 Gy γ-rays. In general, data from the current work revealed a rise in apoptosis with dose for both high- and low-LET radiation when cells were reseeded directly after irradiation. A trend towards increasing cell death at higher doses of low LET γ-rays is reported also by Wilson et al. [2010] for

hESC. Cell death data for high LET radiation are not available in literature up to date. To investigate the influence of the passage (performed for the 72h differentiation experiments) on the persistence of cell death in pluripotent ES-D3, cells were reseeded also for apoptosis measurements (Figures 3.7 and 3.8). Due to the passage, the low doses applied here (i.e. 0.5 and 1 Gy carbon ions) showed apoptosis levels only slightly increased compared to control, whereas the higher doses still exhibited relatively high levels two and three days after exposure. Although being passaged, and thereby likely undergoing enhanced selection, ES-D3 cultures retained elevated cell death levels. This underlines the pronounced role of apoptosis, which is reported for mESC cultures. To avoid passing DNA damage to the progeny, mESC are discussed to facilitate a massive induction of cell death when compared to somatic cells [Hong and Stambrook 2004, Tichy 2011]. That might explain why an elevated level of apoptosis for high doses persists even after a passage. It is therefore remarkable that when measured in differentiating EBs, apoptosis was found to be affected by radiation only on day 1 after exposure in the 0h experiments (figures 3.18 and 3.19). Carbon ions here again were more effective than x-rays, concordantly with all other endpoints. However, for all later data points no cell death rate different from control was detected. The only exception, in which elevated cell death rates in EBs were detected beyond day 1 after exposure was the sample irradiated with 10 Gy x-rays (0h experiment, figure 3.19). However, these cells were not capable of forming stable EBs as they disaggregated after day 3 of differentiation, most likely due to the exacerbated damage. Radiation-induced cell death in the early EBs is consistent with the data discussed above. They confirm that radiation reduces the initial number used for EB formation due to cell killing and thus can affect the differentiation into beating cardiomyocytes. Interestingly, for 72h experiments, no significant persistent increase of apoptosis levels was found after exposure to both radiation qualities (figures 3.20 and 3.21). However the passage did not remove apoptotic cells from the culture and differentiation was still affected in the case of carbon ions. The slight increase of cell death for x-rays (figure 3.21) must be valuated carefully due to its poor statistics, especially as no influence on the differentiation was found here. The discrepancy in the persistence of radiation-induced apoptosis between pluripotent ES-D3 cultures and differentiating EBs has to be evaluated also in the context of the two

different cultures conditions, i.e. mainly with or without LIF and the EB as a 3D structure. Additionally, the reason that radiation-induced cell death was detectable only on day 1 after exposure might be explained with a high background level of apoptosis in the EBs probably impeding the distinction of the radiation-induced fraction. Two hypotheses can be discussed in the context of a high background level of apoptosis.

Firstly, a limitation of nutrient and oxygen supply due to a gradient influencing the viability of the cells in the center of the EB might occur. However, EBs are thought to be loosely packed [Mansergh et al. 2009] and therefore should not suffer this phenomenon. Furthermore, Gassmann et al. [1996] showed that under norm-oxic (20%) culture conditions, the EBs' core regions were sufficiently oxygenated. Another supply constriction could result from the limited volume of medium in the hanging drop, in which the EBs stay until day 3 of differentiation. However, subsequently they are transferred in suspension culture and in most cases apoptosis levels remained similar on days 3 and 5 of differentiation. Increased background apoptosis due to limitations is therefore unlikely.

Secondly, apoptosis is known to play a crucial role in the embryonic development [Miura 2011]. It was shown that in EBs from ES-D3, inner cells undergo apoptosis and thereby contribute to the process of cavitation, resembling the embryonic yolk sac formation. Apoptosis is therefore pivotal in EBs for advanced morphogenesis [Karbanová and Mokrý 2002]. Hence, the high background level of cell death in EBs is very likely due to the mentioned developmental processes.

In summary, data for proliferation and apoptosis in EBs suggest that radiation mainly affects the initial cell number in the first days of the differentiation. Hence, they indicate that radiation is primarily influencing differentiation by reducing the cell number in the EBs.

4.5.5 Time-course of cardiac differentiation

The fractions of beating EBs on day 10 of differentiation were shown to be decreased by radiation in a dose-dependant manner, most likely due to cell killing in the early EB as

discussed above. However, cardiac differentiation continued over time resulting in a delayed emergence of spontaneously contracting EBs (figures 3.11 to 3.14). Over the differentiation time-course all cumulative fractions of beating EBs approached the control levels. The cumulative fractions of the controls themselves increased in the time-course and reached 100% at the end in most cases. This is in line with findings of others that reported a rise in the number of spontaneously beating foci with time so that finally all EBs were contracting [Boheler et al. 2002]. The RBE of carbon ions for inhibiting the development of beating EBs on day 10 was about 2. Iso-effective doses of carbon ions and x-rays also showed a similar behaviour in developmental kinetics of beating cardiomyocytes pointing to the hypothesis that the origin of the lower fraction of beating EBs for both samples is the same, i.e. the reduction in cell number due to radiation.

Over the observed time-course of differentiation the expression of cardiac marker genes was measured on the basis of one experiment with EBs differentiated immediately (0h) after exposure to 3 Gy of carbon ions or 3 of Gy x-rays (figure 3.24). The cardiac markers used comprised proteins related to function in embryonic cardiomyocytes. Thus, cardiac α-actin (cAct) is the main actin isoform in the heart and the major component in the myofibrils in the cardiac muscle where it is involved in contraction [Kumar et al. 1997, Rai et al. 2008]. β-myosin heavy chain (β-Myh, also termed Myh7) is one of the isoforms of the myosin heavy chains that mediate muscle contraction in the mammalian heart. Myh7 is the predominating isoform in cardiomyocytes of a developing heart [Tardiff et al. 2000, Quiat et al. 2011]. Cardiac troponin T (cTropT2) is a cytoskeletal regulatory protein involved in cardiomyocyte contraction by controlling the calcium mediated interaction between actin and myosin [Sharma et al. 2004, Mobley et al. 2010]. The hyperpolarisation-activated, cyclic nucleotide-gated channel (Hcn4) is a part of the pacemaker current I_f and is mostly expressed in cardiomyocytes of the pacemaker regions, i.e. the sinoatrial node [Stieber et al. 2003, Chen et al. 2010]. It is essential for heart impulse generation and conduction [Baruscotti et al. 2011]. Finally, Gata4 is an early cardiac marker as it is expressed from the first cardiac lineages on and it remains expressed over the time of cardiomyocyte specification up to adulthood. In all stages, it

plays an important role as key regulator for gene expression and cellular activity and has a pivotal contribution to heart lineage differentiation [Molkentin 2000, Zhou et al. 2012]. Generally, an increase in the gene expression of cardiac markers was found until day 10. For the control sample, later on the expression levels of *cAct*, *Myh7* and *cTropT2* tended to decrease. As the cumulative fraction of beating EBs also for controls increased with continued differentiation (discussed above), the reason is most likely not a loss of cardiomyocytes with time, but the continued growth of other cell types in the expanding EBs. Differentiated cardiomyocytes in the contractile focis of EBs can cease beating or slow down beating rate over time but remain viable in culture [Boheler et al. 2002]. As the three mentioned markers are not only structural proteins but also involved in the contractile function, another reason for their expressional decline could be the ceased contraction, that beating clusters typically showed after several days in culture. However, these transcripts remained expressed over the differentiation time-course which is in accordance with literature [Rohwedel et al. 2001, Boheler et al. 2002, Wei et al. 2005]. *Hcn4* expression after day 10 tended to increase in the control, indicating a specification of embryonic cardiomyocytes as it is a marker for pacemaker activity. Its function and abundance in mESC derived cardiomyocytes was reported [Boheler et al. 2002, Wei et al. 2005]. The reason for the decline in the later differentiation days of the carbon ion exposed sample remains to be elucidated and needs to be confirmed by further experiments. *Gata4* in the control sample maintained the level of gene expression which is in accordance with its multiple functions not only in development but also in differentiation and cardiomyocyte function. An early and continued expression over differentiation is reported in literature [Boheler et al. 2002, Wei et al. 2005]. Generally, for exposed samples a delayed pattern of expression was found when compared to the controls. This delay is more pronounced for the sample exposed to carbon ions than for the one exposed to for x-rays that tends to reach levels similar to the control more often and earlier for the different genes. Given the findings discussed above, where a delay in the differentiation into beating cardiomyocytes was found, the delay in the gene expression correlates with that. Hence, data from the gene expression study can be interpreted in two ways. Firstly, one can hypothesise that radiation perturbed the gene expression pattern per se and that the initial lowered fractions of beating EBs and the

subsequent delayed increase over time-course is due to the altered expression of genes involved in cardiac development. Radiation indeed was shown to alter the gene expression [e.g. Ding et al. 2005] in somatic cells. However, another assumption is more likely. The data obtained in the current work point to the cell number hypothesis. If there is indeed a threshold of the cell number initially needed in an EB for an efficient cardiac differentiation, this can explain the delayed expression of cardiac genes. The EBs then might need more time to gain a sufficient number of cells to start an efficient cardiac differentiation. The resulting delay when compared to unexposed EBs is then seen in the expression of genes related to cardiac differentiation. The delayed increase of differentiation-associated genes is consistent with the analysis of pluripotency-associated genes expression as discussed above, where a delay in their decline was found. However, data obtained in the current work or gene expression in general have to be valued carefully as they are derived from one experiment only.

A mathematical model was developed in order to justify the cell number hypothesis. The model reflects the contribution of the cell number, the counteracting cell killing and the probability that EBs start beating. The modelled data were not in agreement with the experimentally obtained data. Thus, the model does not support the cell number hypothesis. However, at the same time it did not indicate a disproof of that hypothesis.
The discrepancy between modelled and measured data might be explained with some weak points of the model. Firstly, the data used for the growth rate τ in the equation are derived from pluripotent ES-D3. As mentioned above, mESC have short G1 phases and cultures contain a high percentage of S-phase cells. Their population doubling time is short. With beginning and ongoing differentiation the percentage of pluripotent cells in the EBs decreases continuously and hence the cell cycle distribution changes [White and Dalton 2005], accompanied by a change in the population doubling time. The dynamic changes of it are difficult to estimate and are not reflected in the current model. Being a simplified model, the doubling time of pluripotent ES-D3 was chosen as an approximation. Furthermore, the fitting to find the proper parameters for the model was performed using mean values of the controls. Controls, however, as the model is based on the influence of cell number reduced by cell killing represent extreme values in that

context, as they have a high fraction of beating EBs already from day 10 on that increases only slightly with time. This affects the robustness of the parameters that were subsequently used to reproduce all curves with the model.

4.6 Future perspectives

The hypothesis inferred from these results, whereby the cell number reduction may be the determining effect for the delay in cardiac differentiation has to be confirmed in further experiments. The results point to that hypothesis, however, another effect of radiation cannot be excluded. The aspect of a threshold for the cell number in EBs to induce an effect as suggested by the data presented needs to be confined to disentangle the cell number influence from other radiation-mediated influences.

Furthermore, given the broad spectrum of cells, which can be derived from the *in vitro* differentiation of mESC [Keller 2005], other aspects of the influence of radiation on the embryonic development can be studied. However, mESC lines, such as ES-D3 and R1 tend to accumulate chromosomal aberrations, both numerical and structural, during *in vitro* culture that might influence their differentiation capacity [Luft diploma thesis 2011, Rebuzzini et al. 2012 Luft et al. 2013b submitted]. Indeed, for the validated EST, cells should be used only until an accumulated passage number of 25 as cultures older than that lead to inconsistent differentiation [Seiler and Spielmann 2011]. Data from our lab suggest that hESC instead are genetically more stable with continued differentiation [Luft, unpublished data]. Furthermore, derived from the same species, hESC are more relevant for radiation risk studies on development than mESC are. *In vitro* differentiation of hESC into cardiomyocytes is established [Wobus and Loeser 2011] and its potential for radiation risk assessment exceeds embryonic development. Cardiomyocytes differentiated from hESC may serve as a model to study adverse cardiac effects of radiation, a further topic of interest in radiation therapy. Data published by Azimzadeh et al. [2011] suggest that the heart reacts with fast structural and functional changes to ionising radiation that might be transformed in long-term damage. Radiation-induced cardiovascular damage and subsequent adverse effects, mostly in patients that received

radiotherapy have been reported and remain a concern especially for conventional radiotherapy, whereas particle therapy might be an alternative to minimise cardiac side-effects [Adams et al. 2003, Wittig et al. 2011]. Furthermore, particle therapy is discussed as a tool for radiosurgery also in the heart [Bert et al. 2012]. It is therefore necessary to improve the risk estimation of radiation therapy on the heart and functional cardiomyocytes derived from hESC may provide a useful tool in that context.
However, ethical objections and restrictive legislation limit the application of *in vitro* differentiation of hESC [Bundesministerium der Justiz - StZG 2002, Leist et al. 2008]. Furthermore, differentiation of hESC into cardiomyocytes is more complex due to the requirement of growth factors and hence more expensive than for mESC [Wobus and Loeser 2011]. Additional limitation is imposed on by the low efficiency of cardiac differentiation below 1% when compared to mESC [Murry and Keller 2008], although effort is done to improve the efficiency [e.g. Fonoudi et al. 2013]. Hence, the *in vitro* differentiation of mESC remains an alternative for risk assessment studies in the mentioned fields.

4.7 Conclusions

The question the current work is based upon is whether radiation affects the early cardiac development and whether high-LET carbon ions differ in inducing a putative effect when compared to low-LET x-rays. Using the EST-like assay, it was found that radiation inhibited the formation of spontaneously contracting cardiomyocytes in EBs and that high-LET radiation was more effective. A first clue that the radiation influence might be related to cell inactivation and consequently to a reduced initial cell number in the EBs was provided by the data from the survival curves. Those are in accordance concerning the RBE of carbon ions for the inhibition of the beating EB fraction and the attenuation of same when cells were differentiated 72h after exposure. The elevated radiation-induced apoptosis in ES-D3 until the moment of differentiation and the reduced size of the EBs, correlated with the dose-effect curves underpin the cell number hypothesis. Furthermore, the differentiation assay with various initial cell numbers strengthens that hypothesis and additionally suggests a threshold to which the cell number has to be reduced to measure

an effect. The delay in the cardiac differentiation, as seen over the differentiation period both in the cumulative fractions of beating EBs and in the gene expression of cardiac markers further supports the hypothesis of the initial cell number. Furthermore for all endpoints, high LET carbon ions were shown to be more effective than x-rays.

EBs resemble the early embryo and their *in vitro* differentiation thus the early embryonic development. Hence, the assumption of the dependence of the cardiac *in vitro* differentiation on a certain cell number necessary might be valid for the early embryonic development in general. Data on the influence of ionising radiation on the early development (pre-implantation stage) point to lethality as the dominating effect. This is mainly assumed from experiments where mice zygotes or blastomeres were exposed [ICRP 2003]. The cells used in this work resemble the blastocyst stage, i.e. the latest stage of the pre-implantation phase and thus the results obtained in the current work contribute to a better understanding of radiation effects on the pre-implantation embryo.

The data indicate that cells of the blastocyst are damaged by radiation and that the consequence is a delayed development rather than lethality. In that early stage, damaged cells probably are eliminated from the pool to allow correct development and undamaged cells or cells with repaired damage might compensate the cell loss [ICRP 2003, Rebuzzini et al. 2012]. Indeed, ESC are discussed to possess efficient DNA repair mechanisms and the induction of apoptosis following DNA damage is significantly higher than in differentiated cells [Denissova et al. 2012, Nagaria et al. 2012]. The hypothesis of a minimum number of cells needed for normal development and the time required to compensate cell loss thus might explain a developmental delay of the pre-implantation embryo.

Apart from the appropriate blastocyst development, a timely regulated expression of embryonic growth factors and cytokines, controlled by a complex network of different factors is prerequisite for an efficient implantation [Singh et al. 2011b]. In the menstrual cycle, however, there is only a limited implantation time span of a few days, to which the blastocyst is restricted for an interaction with the endometrium of the uterus [Teklenburg et al. 2010]. A radiation-induced delay in development may perturb that intricate signalling and thus prevent the embryo from a proper implantation in the narrow time frame, leading to a pregnancy loss. In that context, high-LET radiation, as it is more

efficient in cell killing would comprise a higher risk for the blastocyst-stage embryo than low-LET radiation does.

Appendix

A Tables

Table A.1 *Additional information to figure 3.6. Cell death measured in cells immediately reseeded after exposure to x-rays.*

Dose [Gy]	Days after Expsoure	Mean Value [%]	Error [%]	Error Type	Number of Experiments
0	1	2,58	0,16	SEM	3
1		2,73	0,94	SEM	2
3		3,91	1,28	SEM	2
6		7,00	0,82	Poisson	1
10		18,36	1,21	Poisson	1
0	2	4,49	1,27	SEM	3
1		8,68	0,84	SEM	2
3		15,03	7,25	SEM	2
6		15,77	1,15	Poisson	1
10		38,11	2,05	Poisson	1
0	3	13,65	3,56	SEM	3
1		15,44	1,11	SEM	2
3		13,13	1,87	SEM	2
6		18,62	1,27	Poisson	1

Table A.2 *Additional information to figure 3.7. Cell death after exposure to carbon ions.*

Dose [Gy]	Days after Expsoure	Mean Value [%]	Error [%]	Error Type	Number of Experiments
0	2	2,04	0,29	SEM	3
0.5		2,80	0,82	SEM	3
1		3,18	0,56	SEM	2
2		7,86	1,45	SEM	3
3		11,13	2,49	SEM	3
0	3	2,14	0,77	SEM	3
0.5		3,30	0,62	SEM	3
1		2,74	0,50	Poisson	1
2		8,26	5,41	SEM	2
3		14,76	1,27	SEM	2
0	4	7,57	0,82	Poisson	1
0.5		10,27	0,88	Poisson	1
2		6,34	0,75	Poisson	1
3		7,29	0,76	Poisson	1

Table A.3 *Additional information to figure 3.10. Dose-effect curves of carbon ions and x-rays on the development of spontaneously contracting cardiomyocytes.*

Dose [Gy]	Radiation	Plating after exposure [h]	Fraction of beating EB	Error	Error Type	Number of Experiments
1	x-rays	0	0,74	0,08	SEM	2
3			0,35	0,06	SEM	2
6			0,01	0,01	Bernoulli	1
0.5		72	1,02	0,06	SEM	3
1			0,98	0,12	SEM	2
2			1,15	0,05	SEM	3
3			1,04	0,13	SEM	3
6			1,06	0,06	Bernoulli	1
0.5	carbon ions	0	0,80	0,15	SEM	2
3			0,04	0,04	SEM	2
0.5		72	0,79	0,18	SEM	3
1			0,60	0,17	SEM	2
2			0,61	0,28	SEM	2
3			0,37	0,08	SEM	3

Table A.4 *Additional information to figure 3.11. Cumulative fraction of beating embryoid bodies differentiated 0h after exposure to carbon ions.*

Dose [Gy]	Days of Different.	Fraction of beating EB	Error	Error Type	Number of Experiments
0	10	0,96	0,04	SEM	2
0.5		0,77	0,15	SEM	2
3		0,04	0,04	SEM	2
0	15	0,99	0,01	SEM	2
0.5		0,89	0,11	SEM	2
3		0,25	0,10	SEM	2
0	21	0,99	0,01	SEM	2
0.5		0,92	0,08	SEM	2
3		0,51	0,07	SEM	2
0	25	1,00	0,00	Bernoulli	1
0.5		0,88	0,05	Bernoulli	1
3		0,65	0,07	Bernoulli	1
0	30	1,00	0,00	Bernoulli	1
0.5		0,94	0,03	Bernoulli	1
3		0,79	0,06	Bernoulli	1

Table A.5 *Additional information to figure 3.12. Cumulative fraction of beating embryoid bodies differentiated 0h after exposure to x-rays.*

Dose [Gy]	Days of Different.	Fraction of beating EB	Error	Error Type	Number of Experiments
0	10	0,99	0,01	SEM	3
1		0,73	0,08	SEM	2
3		0,35	0,06	SEM	2
6		0,01	0,01	Bernoulli	1
0	15	0,99	0,01	SEM	3
1		0,86	0,05	SEM	2
3		0,48	0,15	SEM	2
6		0,07	0,03	Bernoulli	1
0	21	0,99	0,01	SEM	3
1		0,91	0,03	SEM	2
3		0,66	0,09	SEM	2
6		0,60	0,05	Bernoulli	1
0	25	0,99	0,01	SEM	2
1		0,88	0,05	Bernoulli	1
3		0,78	0,10	SEM	2
6		0,81	0,04	SEM	2
0	30	0,99	0,01	SEM	2
1		0,96	0,03	Bernoulli	1
3		0,80	0,10	SEM	2
6		0,90	0,03	Bernoulli	1

Table A.6 *Additional information to figure 3.13. Cumulative fraction of beating embryoid bodies differentiated 72h after exposure to carbon ions.*

Dose [Gy]	Days of Different.	Fraction of beating EB	Error	Error Type	Number of Experiments
0	10	0,87	0,07	SEM	3
0.5		0,69	0,16	SEM	3
1		0,52	0,15	SEM	2
2		0,53	0,24	SEM	2
3		0,32	0,07	SEM	3
0	11	0,85	0,08	SEM	2
0.5		0,58	0,02	SEM	2
1		0,59	0,16	SEM	2
2		0,61	0,22	SEM	2
3		0,30	0,09	SEM	2
0	13	0,87	0,06	SEM	2
0.5		0,66	0,07	SEM	2
1		0,66	0,18	SEM	2
2		0,65	0,25	SEM	2
3		0,36	0,14	SEM	2
0	15	0,93	0,05	SEM	3
0.5		0,83	0,13	SEM	3
1		0,70	0,18	SEM	2
2		0,69	0,23	SEM	2
3		0,49	0,13	SEM	3
0	17	0,94	0,02	SEM	2
0.5		0,80	0,11	SEM	2
1		0,76	0,14	SEM	2
2		0,76	0,18	SEM	2
3		0,48	0,21	SEM	2
0	19	0,95	0,03	SEM	2
0.5		0,89	0,05	SEM	2
1		0,81	0,10	SEM	2
2		0,83	0,10	SEM	2
3		0,57	0,18	SEM	2
0	21	0,97	0,02	SEM	3
0.5		0,92	0,05	SEM	3
1		0,84	0,07	SEM	2
2		0,89	0,07	SEM	2
3		0,73	0,07	SEM	3
0	25	1,00	0,00	Bernoulli	1
0.5		1,00	0,00	Bernoulli	1
3		0,82	0,04	Bernoulli	1
0	30	1,00	0,00	Bernoulli	1
0.5		1,00	0,00	Bernoulli	1
3		0,89	0,03	Bernoulli	1

Table A.7 *Additional information to figure 3.14. Cumulative fraction of beating embryoid bodies differentiated 72h after exposure to x-rays.*

Dose [Gy]	Days of Different.	Fraction of beating EB	Error	Error Type	Number of Experiments
0	10	0,81	0,12	SEM	3
0.5		0,81	0,08	SEM	2
1		0,78	0,09	SEM	2
2		0,91	0,07	SEM	2
3		0,83	0,10	SEM	3
6		0,85	0,05	Bernoulli	1
0	11	0,77	0,13	SEM	2
0.5		0,85	0,06	SEM	2
1		0,81	0,08	SEM	2
2		0,97	0,01	SEM	2
3		0,84	0,14	SEM	2
0	13	0,83	0,08	SEM	2
0.5		0,89	0,03	SEM	2
1		0,86	0,03	SEM	2
2		0,98	0,02	SEM	2
3		0,86	0,11	SEM	2
0	15	0,90	0,06	SEM	3
0.5		0,90	0,04	SEM	2
1		0,86	0,03	SEM	2
2		0,98	0,02	SEM	2
3		0,92	0,07	SEM	3
6		0,92	0,04	Bernoulli	1
0	17	0,86	0,05	SEM	2
0.5		0,90	0,04	SEM	2
1		0,86	0,03	SEM	2
2		0,98	0,02	SEM	2
3		0,92	0,06	SEM	2
0	19	0,86	0,05	SEM	2
0.5		0,93	0,01	SEM	2
1		0,89	0,01	SEM	2
2		0,98	0,02	SEM	2
3		0,94	0,04	SEM	2
0	21	0,91	0,05	SEM	3
0.5		0,93	0,01	SEM	2
1		0,89	0,01	SEM	2
2		0,98	0,02	SEM	2
3		0,96	0,03	SEM	3
6		0,94	0,03	Bernoulli	1
0	25	1,00	0,00	Bernoulli	1
3		1,00	0,00	Bernoulli	1
0	30	1,00	0,00	Bernoulli	1
3		1,00	0,00	Bernoulli	1

Table A.8 *Additional information to figure 3.15. Size of embryoid bodies and fraction of beating embryoid bodies after exposure to carbon ions and x-rays (differentiation initiation at 0h).*

Dose [Gy]	Radiation	Size of EB	Error	Error Type	Number of Experiments
0	carbon ions	11,31	0,74	SEM	2
0.5		9,35	2,37	SEM	2
3		3,68	0,06	SEM	2
0	x-rays	12,42	1,04	SEM	2
1		10,39	0,87	SEM	2
3		7,55	2,47	SEM	2
6		3,66	1,44	SD	1

Table A.9 *Additional information to figure 3.16. Size and beating fraction of embryoid bodies after exposure to carbon ions and x-rays (differentiation initiation at 72h).*

Dose [Gy]	Radiation	Size of EB	Error	Error Type	Number of Experiments
0	carbon ions	14,11	1,67	SEM	3
0.5		9,00	1,80	SEM	3
1		8,14	1,30	SEM	2
2		6,62	0,31	SEM	2
3		5,20	0,32	SEM	3
0	x-rays	13,96	3,36	SD	1
3		7,84	1,66	SD	1

Table A.10 *Additional information to figure 3.17. Relationship between initial cell number and fraction of beating embryoid bodies after exposure to carbon ions (differentiation initiation at 72h).*

Dose [Gy]	Days of Different.	Cell number	Fraction of beating EB	Error	Error Type	Number of Experiments
0	10	500	0,88	0,07	Bernoulli	1
		750	0,87	0,07	SEM	3
		850	0,79	0,08	Bernoulli	1
	11	500	0,88	0,07	Bernoulli	1
		750	0,85	0,08	SEM	2
		850	0,79	0,08	Bernoulli	1
	13	500	0,88	0,07	Bernoulli	1
		750	0,87	0,06	SEM	2
		850	0,92	0,06	Bernoulli	1
	15	500	0,88	0,07	Bernoulli	1
		750	0,93	0,05	SEM	3
		850	0,92	0,06	Bernoulli	1
	17	500	0,88	0,07	Bernoulli	1
		750	0,94	0,02	SEM	2
		850	0,92	0,06	Bernoulli	1
	19	500	0,92	0,06	Bernoulli	1
		750	0,95	0,03	SEM	2
		850	0,92	0,06	Bernoulli	1
	21	500	0,92	0,06	Bernoulli	1
		750	0,97	0,02	SEM	3
		850	0,96	0,04	Bernoulli	1
2	10	500	0,42	0,10	Bernoulli	1
		750	0,53	0,24	SEM	2
		850	0,83	0,08	Bernoulli	1
	11	500	0,50	0,10	Bernoulli	1
		750	0,61	0,22	SEM	2
		850	0,83	0,08	Bernoulli	1
	13	500	0,54	0,10	Bernoulli	1
		750	0,65	0,25	SEM	2
		850	0,87	0,07	Bernoulli	1
	15	500	0,54	0,10	Bernoulli	1
		750	0,69	0,23	SEM	2
		850	0,87	0,07	Bernoulli	1
	17	500	0,58	0,10	Bernoulli	1
		750	0,76	0,18	SEM	2
		850	0,87	0,07	Bernoulli	1
	19	500	0,63	0,10	Bernoulli	1
		750	0,83	0,10	SEM	2
		850	0,87	0,07	Bernoulli	1
	21	500	0,67	0,10	Bernoulli	1
		750	0,89	0,07	SEM	2
		850	0,91	0,06	Bernoulli	1

Table A.11 *Additional information to figure 3.19. Cell death in embryoid bodies after exposure to x-rays, 0h experiments.*

Dose [Gy]	Days after Expsoure	Mean Value [%]	Error [%]	Error Type	Number of Experiments
0	1	13,13	0,72	SEM	3
1		17,34	1,61	SEM	2
3		19,17	6,57	SEM	2
6		35,90	1,88	Poisson	1
10		48,15	2,29	Poisson	1
0	3	39,07	15,25	SEM	3
1		27,62	1,61	SEM	2
3		31,35	2,35	SEM	2
6		37,89	1,89	Poisson	1
10		76,24	2,78	Poisson	1
0	5	35,52	4,51	SEM	3
1		43,82	18,91	SEM	2
3		48,35	22,53	SEM	2
6		22,39	1,39	Poisson	1

Table A.12 *Additional information to figure 3.20. Cell death in embryoid bodies after exposure to carbon ions, 72h experiments.*

Dose [Gy]	Days after Expsoure	Days of Different.	Mean Value [%]	Error [%]	Error Type	Number of Experiments
0	4	1	10,95	1,87	SEM	3
0.5			15,11	1,05	Poisson	1
2			13,23	2,26	SEM	3
3			9,51	0,96	Poisson	1
0	6	3	38,31	3,32	SEM	3
0.5			38,45	1,94	Poisson	1
2			38,48	1,45	SEM	3
3			39,77	1,81	Poisson	1
0	8	5	41,97	1,80	Poisson	1
0.5			25,25	1,40	Poisson	1
2			34,44	1,76	Poisson	1
3			42,36	2,05	Poisson	1

B List of abbreviations

BMP	Bone morphogenetic protein
BSA	Bovine serum albumin
cAct	Cardiac α-actin
CCD (camera)	Charged coupled device
CT	Computed tomography
cTrop-I	Cardiac troponin I
cTropT2	Cardiac troponin T
DAPI	4',6-diamidino-2-phenylindole
DDR	DNA damage response
DMSO	Dimethyl sulfoxide
DSB	Double strand break
EBs	Embroyid bodies
ECC	Embryonic carcinoma cell
ECL	Enhanced chemiluminscence
ECVAM	European Centre for the Validation of Alternative Methods
EDTA	Ethylenediaminetetraacetic acid
EdU	5-ethynyl-2'-deoxyuridine
EMT	Epithelial-to-mesenchymal transition
EPI	Epiblast
ESC	Embryonic stem cell
EST	Embryonic stem cell test
FCS	Foetal calf serum
FGF	Fibroblast growth factor
FITC	Fluorescein isothiocyanate
FSC	Forward scatter
Gapdh	Glyceraldehyde 3-phosphate dehydrogenase
Hcn4	Hyperpolarisation-activated, cyclic nucleotide-gated channel
hESC	Human embryonic stem cell
HR	Homologues Recombination

HRP	Horseradish Peroxidase
ICM	Inner Cell Mass
ICRP	International Commission on Radiological Protection
ICRU	International Commission on Radiation Units
LET	Linear energy transfer
LIF	Leakaemia inhibitory factor
MEF	Mouse embryonic fibroblast
mESC	Mouse embryonic stem cell
Myh7	Myosin Heavy Chain-β
NHEJ	Non-homologues end joining
Oct-3/4	Octamer binding transcription factor)-3/4
PE	Plating Efficiency
PE	Primitive Endoderm
PGC	Primordial Germ Cells
RBE	Relative Biological Effectiveness
REACH	Registration, Evaluation, Authorisation and Restriction of Chemicals
ROS	Reactive Oxygen Species
SIS18	*Schwerionensynchrotron* (Heavy Ion Synchrotron)
SOBP	Spread Out Bragg-Peak (also: extended Bragg-Peak)
Sox2	SRY-box 2
SSBR	Single-strand Break Repair
SSC	Side scatter
StZG	*Stammzellgesetz* (German Stem Cell Act)
TE solution	Trypsin-EDTA solution
TE	Trophectoderm
TGFβ	Transforming growth factor β
ZGA	Zygote Genome Activation
β-Myh	Myosin Heavy Chain-β

C List of materials

C.1 Chemicals

Acetic acid (Merck)

Acetone (LS Labor Service GmbH)

Acrylamide (SIGMA Aldrich)

APS (SIGMA Aldrich)

BSA (SIGMA Aldrich)

CASYTON solution (Schaerfe System)

DAPI (Serva)

DMEM, FG0435 (BIOCHROM AG)

DMSO (Roth)

ECL-Plus (Pierce)

EDTA (Roth)

Ethanol (AppliChem)

Formaldehyde 37% (Merck)

Gelatine (Merck)

Glycine (AppliChem)

Hoechst 33 342 (SIGMA Aldrich)

Leukaemia inhibitory factor, ESGRO (Millipore)

Methanol (Merck)

Methyleneblue solution, Loeffler (Merck)

Na3VO4 (SIGMA Aldrich)

NaCl (SIGMA Aldrich)

NaF (AppliChem)

NEAA (BIOCHROM AG)

NP-40 (SIGMA Aldrich)

$PBS^{-/-}$ Dulbecco, w/o calcium and magnesium (BIOCHROM)

Penicillin/Streptomycin (BIOCHROM AG)

PMSF (AppliChem)

Potassium hydroxide (Merck)

Protease Inhibitor Cocktail, Complete (Roche)

SDS (AppliChem)

TEMED (AppliChem)

Tris-HCl (AppliChem)

Triton-X-100 (Merck)

Tween 20 (SIGMA Aldrich)

VectaShield Antifade (Vector Laboratories)

C.2 Solutions, buffers and gels

β-mercaptoethanol working solution

5 ml $PBS^{-/-}$

3.5 µl β-Mercaptoethanol

BSA solution

0.4% BSA in $PBS^{-/-}$

1% BSA in $PBS^{-/-}$

DAPI solution

100 µg/ml DAPI in $PBS^{-/-}$

1 µg/ml DAPI in $PBS^{-/-}$

0.1 µg/ml DAPI in $PBS^{-/-}$

Hoechst 33 342 solution

10 µg/ml Hoechst 33 342 in $PBS^{-/-}$

3x Loeffler's Methyleneblue solution

30% Methyleneblue

9% Potassium hydroxide solution (0.1%)

5% Methanol

in ultrapure water

Paraformaldehyde solution

(3.7% in $PBS^{-/-}$)

RIPA buffer

50 mM Tris-HCl [pH 7.4]

150 mM NaCl

1% NP-40

0.25% Triton-X-100

1 mM EDTA

1 mM PMSF

1 mM Na3VO4

1 mM NaF

1x Protease Inhibitor Cocktail

SDS-PAGE gel

3.9% Tris-HCl [pH 8.8]

0.1% SDS

12% Acrylamide

0.04% TEMED

0.1% APS

in ultrapure water

SDS running buffer

40 mM Glycine
120 mM Tris-HCl
0.1% SDS
in ultrapure water

TBST

20 mM Tris-HCl [pH 7.5]
500 mM NaCl
0.05% Tween 20
in ultrapure water

TE solution PAN Biotech

0.05% Trypsin
0.02% EDTA

Transfer buffer

192mM Glycine
25mM Tris-HCl
0.1% SDS
20% Methanol
in ultrapure water

Triton-X-100 solution

0.5% Triton-X-100 in $PBS^{-/-}$

C.3 Cell culture media

Complete medium

500 ml	DMEM
90 ml	FCS (serum A, heat-inactivated)
5 ml	NEAA
5 ml	L-glutamine
5 ml	Penicillin and streptomycin
6.1 ml	β-Mercaptoethanol working solution

Cryo medium

13 ml	Complete Medium
5 ml	FCS (serum A, heat-inactivated)
2 ml	DMSO

C.4 Tested sera

Serum A: Biochrom AG, catalogue number: S 0115, LOT number: 0565 L

Serum B: Biochrom AG, catalogue number: S 0613 / S 0615, LOT number: 0892 T

Serum C: Biochrom AG, catalogue number: S 0613 / S 0615, LOT number: 0397 L

C.5 Consumables

15 ml tube (TPP)

24-well tissue culture plates (BIOCHROM AG)

50 ml tube (Greiner)

96-well Fast Thermal Cycling Plates (Life Technologies)

Cell counter vials (Schaerfe System)

Cell scraper (TPP)

Chamber slides, 2 chambers (Nalge Nunc International)

Cover slip, 24 x 46 mm (Roth)

Cryo vials, Cellstar CryoS (Greiner)

ECL Film, Amersham HyperflimTM (GE Healthcare)

Glass slides, 76 x 26 mm (Roth)

Pestle 1.5 ml (Argos Technologies)

Petri dish, bacterial, 90 mm (Greiner)

PVDF membranes (Millipore)

Reaction tubes, 0.5/1.5/2 ml (Eppendorf)

Tissue culture flasks, 12.5/25 cm^2 (Falcon)

C.6 Antibodies

Alpha tubulin, from rabbit (abcam)

Anti-rabbit IgG, HRP-linked, from donkey (GE Healthcare)

Anti-rabbit IgG, TexasRed-labelled, from sheep (abcam)

Cardiac troponin I, from rabbit (abcam)

C.7 Primers

cAct, Mm_Actc1_1_SG (QIAGEN)

cTropT2, Mm_Tnn2_1_SG (QIAGEN)

Eef2, Mm_Eef2_2_SG (QIAGEN)

Gapdh, Mm_Gapdh_3_SG (QIAGEN)

Gata4, Mm_Gata4_1_SG (QIAGEN)

Hcn4, Mm_Hcn4_2_SG (QIAGEN)

Myh7, Mm_Myh7_2_SG (QIAGEN)

Nanog, Mm_Nanog_1_SG (QIAGEN)

Oct-3/4, Mm_Pou5f1_1_SG (QIAGEN)

Sox2, Mm_Sox2_1_SG (QIAGEN)

C.8 Kit systems

Alkaline Phosphatase Kit (SIGMA Aldrich)
Click-iT EdU Flow Cytometry Assay Kit (Invitrogen)
Click-iT EdU Imaging Kit (Invitrogen)
FITC Active Caspase-3 Apoptosis Kit (BD Pharmingen)
High Capacity RNA-to-cDNA Kit (Applied Biosystems)
MasterPure RNA Purification Kit (Epicentre)

C.9 Devices

Autoclave, Autoklav EL (Tuttnauer)
CCD microscope camera, JAI M300 (Stemmer Imaging)
Centrifuge, Heraeus Fresco21 (Thermo Fisher Scientific)
Centrifuge, Rotina 380 R (Hettich)
Developer, Curix60 (AGFA)
Dosimeter, SN4 (PTW Freiburg)
Electrical cell counter, CASY TT Cell Counter (Schaerfe System)
Flow cytometer, BD FACSCANTO II (BD)
Fluorescence microscope, BX61 (Olympus)
Freezing container, Cryo 1°C (NALGENE)
Incubator (Binder)
Light microscope (Leica)
Liquid nitrogen container, Locator 8 Plus (Thermolyne)
Multipipette tray (VWR)
Sterile working bench, Herasafe HSP12 (Heraeus)
Ultrasound sonicator, Bioruptor TM Ucd-200 (Diagenode)
Water bath, ISOTEMP 215 (Fisher Scientific)
X-ray tube, Isovolt DS1 (Seifert)

C.10 Software

FACSDiva 6.0 (BD)

Isis 5.0 (Metasystems)

mFISH (Metasystems)

OriginPro 8G (OriginLab)

Bibliography

Adams, MJ., PH. Hardenbergh, LS. Constine, and SE. Lipshultz. 2003. "Radiation-associated Cardiovascular Disease." *Critical Reviews in Oncology/hematology* 45.

Andreuccetti, P., O. Carnevali, L. Dini, C. Falugi, S. Filosa, K. Kalthoff, and R. Viscuso. 2010. "Biologia dello Sviluppo." *McGraw-Hill Companies, 2nd edition, Milano*.

Annerén, C. 2008. "Tyrosine Kinase Signalling in Embryonic Stem Cells." *Clinical Science* 115.

Azimzadeh, O., H. Scherthan, H. Sarioglu, Z. Barjaktarovic, M. Conrad, A. Vogt, J. Calzada-Wack, F. Neff, M. Aubele, C. Buske, MJ. Atkinson, and S. Tapio. 2011. "Rapid Proteomic Remodeling of Cardiac Tissue Caused by Total Body Ionizing Radiation." *Proteomics* 11.

Baharvand, H., A. Piryaei, R. Rohani, A. Taei, MH. Heidari, and A. Hosseini. 2006. "Ultrastructural Comparison of Developing Mouse Embryonic Stem Cell- and in Vivo-derived Cardiomyocytes." *Cell Biology International* 30.

Balls, M.. 2002. "The Use of Scientifically-Validated In Vitro Tests for Embryotoxicity." *Report on the 17th meeting of the ECVAM Scientific Committee (ESAC) 2001*.

Banach, K., MD. Halbach, P. Hu, J. Hescheler, and U. Egert. 2003. "Development of Electrical Activity in Cardiac Myocyte Aggregates Derived from Mouse Embryonic Stem Cells." *American Journal of Physiology. Heart and Circulatory Physiology* 284.

Baruscotti, M., A. Bucchi, C. Viscomi, G. Mandelli, G. Consalez, T. Gnecchi-Rusconi, N. Montano, K. Rabello Casali, S. Micheloni, A. Barbuti, and D. DiFrancesco. 2011. "Deep Bradycardia and Heart Block Caused by Inducible Cardiac-specific Knockout of the Pacemaker Channel Gene Hcn4." *Proceedings of the National Academy of Sciences of the United States of America* 108.

Bert, C., R. Engenhart-Cabillic, and M. Durante. 2012. "Particle Therapy for Noncancer Diseases." *Medical Physics* 39.

ten Berge, D., W. Koole, C. Fuerer, M. Fish, E. Eroglu, and R. Nusse. 2008. "Wnt Signaling Mediates Self-organization and Axis Formation in Embryoid Bodies." *Cell Stem Cell* 3.

Boheler, KR., J. Czyz, D. Tweedie, Y. Huang-Tian, SV. Anisimov, and AM. Wobus. 2002. “Differentiation of Pluripotent Embryonic Stem Cells Into Cardiomyocytes.” *Circulation Research* 91.

Bradford, MM. 1976. “A Rapid and Sensitive Method for the Quantitation of Microgram Quantities of Protein Utilizing the Principle of Protein-Dye Binding.” *Analytical Biochemistry* 72.

Bruneau, BG. 2002. “Transcriptional Regulation of Vertebrate Cardiac Morphogenesis.” *Circulation Research* 90.

Buesen, R., E. Genschow, B. Slawik, A. Visan, H. Spielmann, A. Luch, and A. Seiler. 2009. “Embryonic Stem Cell Test Remastered: Comparison Between the Validated EST and the New Molecular FACS-EST for Assessing Developmental Toxicity in Vitro.” *Toxicological Sciences* 108.

Buggisch, M., B. Ateghang, C. Ruhe, C. Strobel, S. Lange, M. Wartenberg, and H. Sauer. 2007. “Stimulation of ES-cell-derived Cardiomyogenesis and Neonatal Cardiac Cell Proliferation by Reactive Oxygen Species and NADPH Oxidase.” *Journal of Cell Science* 120.

Bundesamt fuer Strahlenschutz. 2001. “Umweltradioaktivitaet und Strahlenbelastung: Teil IV: Strahlenexposition durch medizinische Massnahmen.” *Bundesamt fuer Strahlenschutz, Salzgitter, Germany*.

Bundesamt fuer Strahlenschutz. 2009. “Strahlenthemen - Schwangerschaft und Strahlenschutz.” *Bundesamt fuer Strahlenschutz, Salzgitter, Germany*.

Bundesministerium der Justiz. 2008. “Stammzellgesetz - StZG 2002.” *Bundesministerium der Justiz, Berlin, Germany*.

Buonanno, M., SM. de Toledo, D. Pain, and EI. Azzam. 2011. “Long-Term Consequences of Radiation-Induced Bystander Effects Depend on Radiation Quality and Dose and Correlate with Oxidative Stress.” *Radiation Research* 175: 405–415.

Campo-Paysaa, F., F. Marlétaz, V. Laudet, and M. Schubert. 2008. “Retinoic Acid Signaling in Development: Tissue-specific Functions and Evolutionary Origins.” *Genesis* 46.

Chambers, I., D. Colby, M. Robertson, J. Nichols, S. Lee, S. Tweedie, and A. Smith. 2003. “Functional Expression Cloning of Nanog, a Pluripotency Sustaining Factor in Embryonic Stem Cells.” *Cell* 113.

Chen, P., B. Joung, T. Shinohara, M. Das, Z. Chen, and S. Lin. 2010. “The Initiation of the Heart Beat.” *Circulation Journal* 74.

Choi, YY., BG. Chung, DH. Lee, A. Khademhosseini, JH. Kim, and SH. Lee. 2010. "Controlled-Size Embryoid Body Formation in Concave Microwell Arrays." *Biomaterials* 31.

Choppin, GR., J. Liljenzin, and J. Rydberg. 2002. "Radiochemistry and Nuclear Chemistry - Chapter 7: Radiation Effects on Matter." *Elsevier, 3rd edition*.

Ciccia, A., and SJ. Elledge. 2010. "The DNA Damage Response: Making It Safe to Play with Knives." *Molecular Cell* 40.

Cucinotta, FA., and M. Durante. 2006. "Cancer Risk from Exposure to Galactic Cosmic Rays: Implications for Space Exploration by Human Beings." *The Lancet Oncology* 7.

Denissova, NG., CM. Nasello, PL. Yeung, JA. Tischfield, and MA. Brenneman. 2012. "Resveratrol Protects Mouse Embryonic Stem Cells from Ionizing Radiation by Accelerating Recovery from DNA Strand Breakage." *Carcinogenesis* 33.

Desmarais, JA., MJ. Hoffmann, G. Bingham, ME. Gagou, M. Meuth, and PW. Andrews. 2012. "Human Embryonic Stem Cells Fail to Activate CHK1 and Commit to Apoptosis in Response to DNA Replication Stress." *Stem Cells* 33.

Ding, L., M. Shingyoji, F. Chen, A. Chatterjee, K. Kasai, and DJ. Chen. 2005. "Gene Expression Changes in Normal Human Skin Fibroblasts Induced by HZE-Particle Radiation." *Radiation Research* 164.

Dinsmore, J., J. Ratliff, T. Deacon, P. Pakzaban, D. Jacoby, W. Galpern, and O. Isacson. 1996. "Embryonic Stem Cells Differentiated In Vitro as a Novel Source of Cells for Transplantation." *Cell Transplantation* 5.

Doerr, H., and V. Meineke. 2011. "Acute Radiation Syndrome Caused by Accidental Radiation Exposure - Therapeutic Principles." *BMC Medicine* 9.

Doetschman, TC., H. Eistetter, M. Katz, W. Schmidt, and R. Kemler. 1985. "The in Vitro Development of Blastocyst-derived Embryonic Stem Cell Lines: Formation of Visceral Yolk Sac, Blood Islands and Myocardium." *Journal of Embryology and Experimental Morphology* 87.

Durante, M. 2003. "Potential Applications of Biomarkers of Radiation Exposure in Nuclear Terrorism Events." *Physica Medica* XIX.

Durante, M., and FA. Cucinotta. 2008. "Heavy Ion Carcinogenesis and Human Space Exploration." *Nature Reviews. Cancer* 8.

Durante, M., and JS. Loeffler. 2010. "Charged Particles in Radiation Oncology." *Nature Reviews. Clinical Oncology* 7.

Elmore, S. 2007. “Apoptosis: A Review of Programmed Cell Death.” *Toxicologic Pathology* 35.

European Commission. 2002. “Effects of In Utero Exposure to Ionising Radiation During the Early Phases of Pregnancy - Proceedings of a Scientific Seminar Held in Luxembourg on 5 November 2001.” *European Communities, Luxembourg*.

European Union. 2006. “Regulation (EC) No 1907/2006 of the European Parliament and of the Council.” *Official Journal of the European Union*.

Evans, M. J., and M. H. Kaufman. 1981. “Establishment in culture of pluripotent cells from mouse embryos.” *Nature* 292.

Fonoudi, H., M. Yeganeh, F. Fattahi, Z. Ghazizadeh, H. Rassouli, M. Alikhani, BA. Mojarad, H. Baharvand, GH. Salekdeh, and N. Aghdami. 2013. “ISL1 Protein Transduction Promotes Cardiomyocyte Differentiation from Human Embryonic Stem Cells.” *PloS One* 8.

Franken, NA., HM. Rodermond, J. Stap, J. Havemann, and C. van Bree. 2006. “Clonogenic Assay of Cells In Vitro.” *Nature Protocols* 1.

Fuchs, C., M. Scheinast, W. Pasteiner, S. Lagger, M. Hofner, A. Hoellrigl, M. Schultheis, and G. Weitzer. 2011. “Self-Organization Phenomena in Embryonic Stem Cell-Derived Embryoid Bodies: Axis Formation and Breaking of Symmetry During Cardiomyogenesis.” *Cells Tissues Organs* 195.

Fuchs, Y., and H. Steller. 2011. “Programmed Cell Death in Animal Development and Disease.” *Cell* 147.

Gassmann, M., J. Fandrey, S. Bichet, M. Wartenberg, HH. Marti, C. Bauer, RH. Wenger, and H. Acker. 1996. “Oxygen Supply and Oxygen-dependent Gene Expression in Differentiating Embryonic Stem Cells.” *Proceedings of the National Academy of Sciences of the United States of America* 93.

Gilbert, SF. 2006. “Developmental Biology.” *Sinauer Associates, 8th edition, Sunderland, MA*.

Gittenberger-de Groot, AC., MM. Bartelings, MC. Deruiter, and RE. Poelmann. 2005. “Basics of Cardiac Development for the Understanding of Congenital Heart Malformations.” *Pediatric Research* 57.

Goodhead, DT. 1999. “Mechanisms for the Biological Effectiveness of high-LET Radiations.” *Journal of Radiation Research* 40 Suppl.

Goodhead, DT. 2009. “Understanding and Characterisation of the Risks to Human Health from Exposure to Low Levels of Radiation.” *Radiation Protection Dosimetry* 137.

Groebe, K., K. Hayess, M. Klemm-Manns, G. Schwall, W. Wozny, M. Steemans, AK. Peters, C. Sastri, P. Jaeckel, W. Stegmann, H. Zengerling, R. Schoepf, S. Poznanovic, TC. Stumann, A. Seller, H. Spielmann, and A. Schrattenholz. 2010. "Protein Biomarkers for in Vitro Testing of Embryotoxicity Research Articles." *Journal of Proteome Research* 9.

Hahnel, AC., DA. Rappolee, JL. Millan, T. Manes, CA. Ziomek, NG. Theodosiou, Z. Werb, RA. Pedersen, and GA. Schultz. 1990. "Two Alkaline Phosphatase Genes Are Expressed During Early Development in the Mouse Embryo." *Development* 110.

Hall, EJ., and AJ. Giaccia. 2006. "Radiobiology for the Radiologist." *Lippincott Williams & Wilkins, 6th edition, Philadelphia, PA*.

Hei, T., H. Zhou, Y. Chai, B. Ponnaiya, and VN. Ivanov. 2011. "Radiation Induced Non-targeted Response: Mechanism and Potential Clinical Implications." *Current Molecular Pharmacology* 4.

Helm, A., S. Luft, P. Hessel, D. Pignalosa, M. Durante, P. Layer, D. Pollet, and S. Ritter. 2011. "Embryonic Stem Cell Derived Cardiomyocytes: A Model System to Study Cardiac Effects of Heavy Ion Exposure." *GSI Scientific Report 2010*.

Hendry, JH, SL Simon, AWojcik, M. Sohrabi, W. Burkart, E. Cardis, D. Laurier, M. Tirmarche, and I. Hayata. 2009. "Human Exposure to High Natural Background Radiation: What Can It Teach Us About Radiation Risks?" *Journal of Radiological Protection□: Official Journal of the Society for Radiological Protection* 29.

Hirai, H. 2011. "Regulation of Embryonic Stem Cell Self-renewal and Pluripotency by Leukaemia Inhibitory Factor." *Biochemical Journal* 438.

Hlatky, L., RK. Sachs, M. Vazquez, and MN. Cornforth. 2002. "Radiation-induced Chromosome Aberrations: Insights Gained from Biophysical Modeling." *BioEssays□: News and Reviews in Molecular, Cellular and Developmental Biology* 24.

ICRP. 2003. "Biological Effects After Prenatal Irradiation (Embryo and Fetus)." *Annals of the ICRP, ICRP Publication 90, Pergamon*.

ICRU. 2011a. "Quantification and Reporting of Low-Dose and Other Heterogeneous Exposures" *Journal of the ICRU 11 2011, ICRU Report No. 86*.

ICRU. 2011b. "Fundamental Quantities and Units for Ionizing Radiation (Revised)" *Journal of the ICRU 11 2011, ICRU Report No. 85*.

European Commission. 2002. "Effects of In Utero Exposure to Ionising Radiation During the Early Phases of Pregnancy - Proceedings of a Scientific Seminar Held in Luxembourg on 5 November 2001." *European Communities, Luxembourg*.

Karbanová, J., and J. Mokrý. 2002. “Histological and Histochemical Analysis of Embryoid Bodies.” *Acta Histochemica* 104.

Keller, G.. 2005. “Embryonic Stem Cell Differentiation: Emergence of a New Era in Biology and Medicine.” *Genes & Development* 19.

Kerr, JFR., AH. Wyllie, and AR. Currie. 1972. “Apoptosis: A Basic Biological Phenomenon with Wide-Ranging Implications in Tissue Kinetics.” *British Journal of Cancer* 26.

Kouskoff, V., G. Lacaud, S. Schwantz, HJ. Fehling, and G. Keller. 2005. “Sequential Development of Hematopoietic and Cardiac Mesoderm During Embryonic Stem Cell Differentiation.” *Proceedings of the National Academy of Sciences of the United States of America* 102.

Kumar, A., K. Crawford, L. Close, M. Madison, J. Lorenz, T. Doetschman, S. Pawlowski, J Duffy, J. Neumann, J. Robbins, GP. Boivin, BA. O'Toole, and JL. Lessard. 1997. “Rescue of Cardiac Alpha-actin-deficient Mice by Enteric Smooth Muscle Gamma-actin.” *Proceedings of the National Academy of Sciences of the United States of America* 94.

Kurosawa, H. 2007. “Methods for Inducing Embryoid Body Formation: In Vitro Differentiation System of Embryonic Stem Cells.” *Journal of Bioscience and Bioengineering* 103.

Kuske, B., PY. Pulyanina, and NI. zur Nieden. 2012. “Embryonic Stem Cell Test: Stem Cell Use in Prediciting Developmental Cardiotoxicity and Osteotoxicity.” *Methods in Molecular Biology* 889.

Van Laake, LW., D. Van Hoof, and CL. Mummery. 2005. “Cardiomyocytes Derived from Stem Cells.” *Annals of Medicine* 37.

Lee, LMY., C. Leung, WWC. Tang, H. Choi, Y. Leung, and PJ. Mccaffery. 2012. “A Paradoxical Teratogenic Mechanism for Retinoic Acid.” *Proceedings of the National Academy of Sciences of the United States of America* 109.

Leist, M., S. Bremer, P. Brundin, J. Hescheler, A. Kirkeby, K. Krause, P. Poerzgen, M. Puceat, M. Schmidt, A. Schrattenholz, NB. Zak, and H. Hentze. 2008. “The Biological and Ethical Basis of the Use of Human Embryonic Stem Cells for in Vitro Test Systems or Cell Therapy.” *ALTEX* 25.

Luft, S. 2011. “Untersuchung zur Wirkung von locker- und dicht-ionisierender Strahlung auf pluripotente embryonale Stammzellen der Maus.” *Diploma Thesis, Technische Universitaet Darmstadt*.

Luft, S., A. Helm, P. Hessel, D. Pignalosa, S. Brons, P.G. Layer, M. Durante, and S. Ritter. 2013a. "Impact of Ionizing Radiation on the Potency State of Murine Embryonic Stem Cells." *GSI Scientific Report 2012* (in press).

Luft, S., D. Pignalosa, E. Nasonova, O. Arrizabalaga, A. Helm, M. Durante, and S. Ritter. 2013b. "Densely Ionizing Radiation Does Not Affect Pluripotency and Genomic Stability of D3 Mouse Embryonic Stem Cells." *Toxicology and Applied Pharmacology* (submitted).

Maltsev, VA., J. Rohwedel, J. Hescheler, and AM. Wobus. 1993. "Embryonic Stem Cells Differentiate in Vitro into Cardiomyocytes Representing Sinusnodal, Atrial and Ventricular Cell Types." *Mechanisms of Development* 44.

Mansergh, FC., CS. Daly, AL. Hurley, MA. Wride, SM. Hunter, and MJ. Evans. 2009. "Gene Expression Profiles During Early Differentiation of Mouse Embryonic Stem Cells." *BMC Developmental Biology* 5.

Martin, GR. 1981. "Isolation of a Pluripotent Cell Line from Early Mouse Embryos Cultured in Medium Conditioned by Teratocarcinoma Stem Cells." *Developmental Biology* 78.

Maser, RS., and RA. DePinho. 2002. "Connecting Chromosomes, Crisis, and Cancer." *Science* 297.

Masui, S., Y. Nakatake, Y. Toyooka, D. Shimosato, R. Yagi, K. Takahashi, H. Okochi, et al. 2007. "Pluripotency Governed by Sox2 via Regulation of Oct3/4 Expression in Mouse Embryonic Stem Cells." *Nature Cell Biology* 9.

Materna, M., A. Helm, P. Hessel, J. Friess, C. Thielemann, D. Pignalosa, W. Maentele, M. Durante and S. Ritter. 2013. "First Electrophysiological Studies on Mouse Embryonic Stem Cell-Derived Cardiomyocytes." *GSI Scientific Report 2012* (in press).

Medema, RH., and L. Macůrek. 2012. "Checkpoint Control and Cancer." *Oncogene* 31.

Messana, JM., NS. Hwang, J. Coburn, JH. Elisseeff, and Z. Zhang. 2008. "Size of the Embryoid Body Influences Chondrogenesis of Mouse Embryonic Stem Cells." *Journal of Tissue Engineering and Regenerative Medicine* 2.

Miura, M. 2011. "Active Participation of Cell Death in Development and Organismal Homeostasis." *Development, Growth & Differentiation* 53.

Mobley, S., JM. Shookhof, K. Foshay, M. Park, and GI. Gallicano. 2010. "PKG and PKC Are Down-Regulated During Cardiomyocyte Differentiation from Embryonic Stem Cells: Manipulation of These Pathways Enhances Cardiomyocyte Production." *Stem Cells International* 2010.

Molkentin, JD. 2000. “The Zinc Finger-containing Transcription Factors GATA-4, -5, and -6. Ubiquitously Expressed Regulators of Tissue-specific Gene Expression.” *The Journal of Biological Chemistry* 275.

Mullen, EM., P. Gu, and AJ. Cooney. 2007. “Nuclear Receptors in Regulation of Mouse ES Cell Pluripotency and Differentiation.” *PPAR Research* 2007.

Munro, TR. 1970. “The Relative Radiosensitivity of the Nucleus and Cytoplasm of Chinese Hamster Fibroblasts.” *Radiation Research* 42.

Muenter, MW., M. Wengenroth, G. Fehrenbacher, D. Schardt, A. Nikoghosyan, M. Durante, and J. Debus. 2010. “Heavy Ion Radiotherapy During Pregnancy.” *Fertility and Sterility* 94.

Murry, CE., and G. Keller. 2008. “Differentiation of Embryonic Stem Cells to Clinically Relevant Populations: Lessons from Embryonic Development.” *Cell* 132.

Nagaria, P., C. Robert, and FV. Rassool. 2012. “DNA Double-strand Break Response in Stem Cells: Mechanisms to Maintain Genomic Integrity.” *Biochimica Et Biophysica Acta* 1830.

Newhauser, WD., and M. Durante. 2011. “Assessing the Risk of Second Malignancies After Modern Radiotherapy.” *Nature Reviews. Cancer* 11.

Ng, ES., RP. Davis, L. Azzola, EG. Stanley, and AG. Elefanty. 2005. “Forced Aggregation of Defined Numbers of Human Embryonic Stem Cells into Embryoid Bodies Fosters Robust, Reproducible Hematopoietic Differentiation.” *Blood* 106.

Niwa, H. 2001. “Molecular Mechanism to Maintain Stem Cell Renewal of ES Cells.” *Cell Structure and Function* 26.

Niwa, H. 2010. “Mouse ES Cell Culture System as a Model of Development.” *Development, Growth & Differentiation* 52.

Nowotschin, S., and AK. Hadjantonakis. 2011. “Cellular Dynamics in the Early Mouse Embryo: From Axis Formation to Gastrulation.” *Current Opinions in Genetics & Development* 20.

Oron, E., and N. Ivanova. 2012. “Cell Fate Regulation in Early Mammalian Development.” *Physical Biology* 9.

Pampfer, S., and C. Streffer. 1988. “Prenatal Death and Malformations After Irradiation of Mouse Zygotes with Neutrons or X-rays.” *Teratology* 37.

Pease, S., and RL. Williams. 1990. “Formation of Germ-Line Chimeras from Embryonic Stem Cells Maintained with Recombinant Leukemia Inhibitory Factor.” *Experimental Cell Research* 190.

Pennsylvania Patient Safety Advisory. 2008. “Diagnostic Ionizing Radiation and Pregnancy: Is There a Concern?” *Pennsylvania Patient Safety Advisory* 5.

Pera, MF., and PPL. Tam. 2010. “Extrinsic Regulation of Pluripotent Stem Cells.” *Nature* 465.

Preda, MB., A. Burlacu, and M. Simionescu. 2013. “Defined-Size Embryoid Bodies Formed in the Presence of Serum Replacement Increase the Efficiency of the Cardiac Differentiation of Mouse Embryonic Stem Cells.” *Tissue and Cell* 45.

Quiat, D., KA. Voelker, J. Pei, NV. Grishin, RW. Grange, R. Bassel-Duby, and EN. Olson. 2011. “Concerted Regulation of Myofiber-specific Gene Expression and Muscle Performance by the Transcriptional Repressor Sox6.” *Proceedings of the National Academy of Sciences of the United States of America* 108.

Rai, R., CCL. Wong, T. Xu, NA. Leu, DW. Dong, C. Guo, KJ. McLaughlin, JR. Yates, and A. Kashina. 2008. “Arginyltransferase Regulates Alpha Cardiac Actin Function, Myofibril Formation and Contractility During Heart Development.” *Development* 135.

Ratnapalan, S., N. Bona, and G. Koren. 2003. “Ionizing Radiation During Pregnancy.” *Canadian Family Physician* 49.

Rebuzzini, P., D. Pignalosa, G. Mazzini, R. Di Liberto, A. Coppola, N. Terranova, P. Magni, CA. Redi, M. Zuccotti, and S. Garagna. 2012. “Mouse Embryonic Stem Cells That Survive Γ-rays Exposure Maintain Pluripotent Differentiation Potential and Genome Stability.” *Journal of Cellular Physiology* 227.

Ritter, S., E. Nasonova, M. Scholz, W. Kraft-Weyrather, and G. Kraft. 1996. “Comparison of Chromosomal Damage Induced by X-rays and Ar Ions with an LET of 1840 keV/Micrometer in G1 V79 Cells” *International Journal of Radiation Biology* 69.

Rohwedel, J., K. Guan, C. Hegert, and AM. Wobus. 2001. “Embryonic Stem Cells as an in Vitro Model for Mutagenicity, Cytotoxicity and Embryotoxicity Studies: Present State and Future Prospects.” *Toxicology in Vitro* 15.

Roos, WP., and B. Kaina. 2006. “DNA Damage-induced Cell Death by Apoptosis.” *Trends in Molecular Medicine* 12.

Rossant, J., and PPL. Tam. 2009. “Blastocyst Lineage Formation, Early Embryonic Asymmetries and Axis Patterning in the Mouse.” *Development (Cambridge, England)* 136.

Sauer, H., G. Rahimi, J. Hescheler, and M. Wartenberg. 1999. “Effects of Electrical Fields on Cardiomyocyte Differentiation of Embryonic Stem Cells.” *Journal of Cellular Biochemistry* 75.

Schardt, D., T. Elsaesser, and D. Schulz-Ertner. 2010. “Heavy-ion Tumor Therapy: Physical and Radiobiological Benefits.” *Reviews of Modern Physics* 82.

Scholz, G., I. Pohl, E. Genschow, M. Klemm, and H. Spielmann. 1999. “Embryotoxicity Screening Using Embryonic Stem Cells in Vitro: Correlation to in Vivo Teratogenicity.” *Cells, Tissues, Organs* 165.

Scholz, G., and H. Spielmann. "Embryonic Stem Cell Test (EST)" *INVITTOX* no 113, ECVAM DB-ALM: *INVITTOX protocol*. 2002.

Scholz, M. 2003. “Effects of Ion Radiation on Cells and Tissues.” *Advances in Polymer Science* 162.

Seiler, AEM., and H. Spielmann. 2011. “The Validated Embryonic Stem Cell Test to Predict Embryotoxicity in Vitro.” *Nature Protocols* 6.

Serrano, L., L. Liang, Y. Chang, L. Deng, C. Maulion, S. Nguyen, and JA. Tischfield. 2011. “Homologous Recombination Conserves DNA Sequence Integrity Throughout the Cell Cycle in Embryonic Stem Cells.” *Stem Cells and Development* 20.

Shah, DJ., RK. Sachs, and DJ. Wilson. 2012. “Radiation-induced Cancer: a Modern View.” *The British Journal of Radiology* 85.

Sharma, S., PG. Jackson, and J. Makan. 2004. “Cardiac Troponins.” *Journal of Clinical Pathology* 57.

Shigematsu, N., J. Fukada, T. Ohashi, O. Kawaguchi, and T. Kawata. 2012. “Nuclear Disaster After the Earthquake and Tsunami of March 11.” *The Keio Journal of Medicine* 61.

Singh, AK., D. Siingh, and RP. Singh. 2011a. “Impact of Galactic Cosmic Rays on Earth’s Atmosphere and Human Health.” *Atmospheric Environment* 45.

Singh, M., P. Chaudhry, and E. Asselin. 2011b. “Bridging Endometrial Receptivity and Implantation: Network of Hormones, Cytokines, and Growth Factors.” *The Journal of Endocrinology* 210.

Smith, K., and S. Dalton. 2011. "Myc Transcription Factors: Key Regulators Behind Establishment and Maintenance of Pluripotency." *Regenerative Medicine* 5.

Sokolov, MV., and RD. Neumann. 2012. "Human Embryonic Stem Cell Responses to Ionizing Radiation Exposures: Current State of Knowledge and Future Challenges." *Stem Cells International* 2012.

Spitz, DR., EI. Azzam, and D. Gius. 2004. "Metabolic Oxidation/Reduction Reactions and Cellular Responses to Ionizing Radiation: A Unifying Concept in Stress Response Biology." *Cancer and Metastasis Reviews* 23.

Stewart, CL., P. Kaspar, LJ. Brunet, H. Bhatt, I. Gadi, F. Koentgen, and SJ. Abbondanzo. 1992. "Blastocyst Implantation Depends on Maternal Expression of Leukaemia Inhibitory Factor." *Nature* 359.

Stieber, J., S. Herrmann, S. Feil, J. Loester, R. Feil, M. Biel, F. Hofmann, and A. Ludwig. 2003. "The Hyperpolarization-activated Channel HCN4 Is Required for the Generation of Pacemaker Action Potentials in the Embryonic Heart." *Proceedings of the National Academy of Sciences of the United States of America* 100.

Streffer, C. 2006. "Transgenerational Transmission of Radiation Damage: Genomic Instability and Congenital Malformation." *Journal of Radiation Research* 47 Suppl B.

Takaoka, K., and H. Hamada. 2012. "Cell Fate Decisions and Axis Determination in the Early Mouse Embryo." *Development* 139.

Tam, PPL., and DAF. Loebel. 2007. "Gene Function in Mouse Embryogenesis: Get Set for Gastrulation." *Nature Reviews. Genetics* 8.

Tanaka, SS., Y. Kojima, YL. Yamaguchi, R. Nishinakamura, and PPL. Tam. 2011. "Impact of WNT Signaling on Tissue Lineage Differentiation in the Early Mouse Embryo." *Development, Growth & Differentiation* 53.

Tardiff, JC., TE. Hewett, SM. Factor, KL. Vikstrom, J. Robbins, LA. Leinwand. 2000. "Expression of the β (Slow)-isoform of MHC in the Adult Mouse Heart Causes Dominant-negative Functional Effects." *American Journal of Physiology. Heart and Circulatory Physiology* 278.

Teklenburg, G., M. Salker, C. Heijnen, NS. Macklon, and JJ. Brosens. 2010. "The Molecular Basis of Recurrent Pregnancy Loss: Impaired Natural Embryo Selection." *Molecular Human Reproduction* 16.

Theunissen, PT., and AH. Piersma. 2012. "Innovative Approches in the Embryonic Stem Cell Test." *Frontiers in Bioscience* 17.

Theunissen, PT., JL. Pennings, DA. van Dartel, JF. Robinson, JC. Kleinjans, and AH. Piersma. 2013. "Complementary Detection of Embryotoxic Properties of Substances in the Neutral and Cardiac Embryonic Stem Cell Tests." *Toxicological Sciences* 132.

Thielen, H. 2012. "The Fukushima Daiichi Nuclear Accident - An Overview." *Health Physics* 103.

Thomson, JA. 1998. "Embryonic Stem Cell Lines Derived from Human Blastocysts." *Science* 282.

Thomson, M., SJ. Liu, L. Zou, Z. Smith, A. Meissner, and S. Ramanathan. 2011. "Pluripotency Factors in Embryonic Stem Cells Regulate Differentiation into Germ Layers." *Cell* 145.

Tichy, ED. 2011. "Mechanisms Maintaining Genomic Integrity in Embryonic Stem Cells and Induced Pluripotent Stem Cells." *Experimental Biology and Medicine* 236.

Toumadje, A., K. Kusumoto, A. Parton, P. Mericko, L. Dowell, G. Ma, L. Chen, DW. Barnes, and JD. Sato. 2003. "Pluripotent Differentiation in Vitro of Murine ES-D3 Embryonic Stem Cells." *In Vitro Cellular & Developmental Biology. Animal* 39.

Verheij, M., and H. Bartelink. 2000. "Radiation-induced Apoptosis." *Cell and Tissue Research* 301.

Wagner, M., and MAQ. Siddiqui. 2007. "Signal Transduction in Early Heart Development (I): Cardiogenic Induction and Heart Tube Formation." *Experimental Biology and Medicine* 232.

Weber, U., and G. Kraft. 2009. "Comparison of Carbon Ions Versus Protons." *Cancer Journal* 15.

Wei, H., OJ. Juhasz, J. Li, YS. Tarasova, and KR. Boheler. 2005. "Embryonic Stem Cells and Cardiomyocyte Differentiation: Phenotypic and Molecular Analyses." *Journal of Cellular and Molecular Medicine* 9.

Weissenborn, U., and C. Streffer. 1988. "The One-cell Mouse Embryo: Cell Cycle-dependent Radiosensitivity and Development of Chromosomal Anomalies in Postradiation Cell Cycles." *International Journal of Radiation Biology* 54.

Weyrather, WK., S. Ritter, M. Scholz, and G. Kraft. 1999. "RBE for carbon track-segment irradiation in cell lines of differing repair capacity." *International Journal of Radiation Biology* 75.

White, J., and S. Dalton. 2005. "Cell Cycle Control of Embryonic Stem Cells." *Stem Cell Reviews* 1.

Williams, J., and WH. McBride. 2011. "After the Bomb Drops: A New Look at Radiation-induced Multiple Organ Dysfunction Syndrome (MODS)." *International Journal of Medical Sciences* 87.

Williams, RL., D. Hilton, S. Pease, TA. Willson, CL. Stewart, DP. Gearing, EF. Wagner, D. Metcalf, NA. Nicola, and NM. Gough. 1988. "Myeloid Leukaemia Inhibitory Factor Maintains the Developmental Potential of Embryonic Stem Cells." *Nature* 366.

Wilson, KD., N. Sun, M. Huang, WY. Zhang, AS., Z. Li, SX. Wang, and JC. Wu. 2010. "Effects of Ionizing Radiation on Self Renewal and Pluripotency of Human Embryonic Stem Cells." *Cancer Research* 70.

Wittig, A., and R. Engenhart-Cabillic. 2011. "Cardiac Side Effects of Conventional and Particle Radiotherapy in Cancer Patients." *Herz* 36.

Wobus, AM., H. Holzhausen, P. Jaekel, and J. Schoeneich. 1984. "Characterization of a Pluripotent Stem Cell Line Derived from a Mouse Embryo." *Experimental Cell Research* 152.

Wobus, AM., and KR. Boheler. 2005. "Embryonic Stem Cells: Prospects for Developmental Biology and Cell Therapy." *Physiological Reviews* 85.

Wobus, AM., and P. Loeser. 2011. "Present State and Future Perspectives of Using Pluripotent Stem Cells in Toxicology Research." *Archives of Toxicology* 85.

Wolbarst, AB., AL. Wiley, JB. Nemhauser, DM. Christensen, and WR. Hendee. 2010. "Medical Response to a Major Radiologic Emergency: A Primer for Medical and Public Health Practitioners." *Radiology* 254.

Ying, QL., J. Nichols, I. Chambers, and A. Smith. 2003. "BMP Induction of Id Proteins Suppresses Differentiation and Sustains Embryonic Stem Cell Self-renewal in Collaboration with STAT3." *Cell* 115.

Yu, J., and JA. Thomson. 2008. "Pluripotent Stem Cell Lines." *Genes & Development* 22.

Zaffran, S., and M. Frasch. 2002. "Early Signals in Cardiac Development." *Circulation Research* 91.

Zhou, P., A. He, and WT. Pu. 2012. "Regulation of GATA4 Transcriptional Activity in Cardiovascular Development and Disease." *Current Topics in Developmental Biology* 100.

Zwaka, TP., and JA. Thomson. 2005. "A Germ Cell Origin of Embryonic Stem Cells?" *Development* 132.

Acknowledgements

This PhD study has been performed at the biophysics department of GSI Helmholtzzentrum für Schwerionenforschung in Darmstadt, Germany and Technische Universität Darmstadt from February 2010 until April 2013. The work was supported by the graduate school HGS-HIRe and ProCardio (Euratom, 7th Framework Programme no. 295823).

First of all, I would like to thank Prof. Marco Durante, my *Doktorvater*, for giving me the opportunity to perform my PhD thesis in the Biophysics department under his supervision. I especially want to thank him for the motivation and the ease I always felt after data discussions with him. Ti ringrazio di cuore per tutto! Anche per la lettera in cui avevi scritto che sono un contadino di Odenwald che comunque sa comunicare con gli stranieri.

I cordially thank Prof. Paul Layer, my co-referee from the TUD for his professional support during our PhD meetings and for giving me the opportunity to learn the work with embryonic stem cells in his group.

Very special thanks go to my supervisor Dr. Sylvia Ritter for helpful discussions and her permanent support in all kind of issues during the time of my thesis. Herzlichen Dank für Alles! Auch, für die entgegengebrachte Geduld, denn meine „Odenwälder Art", wie du sie gerne nennst, war nicht immer leicht für dich.

Ich danke herzlichst Petra Hessel, die mir tatkräftig, erfahren und mit viel Elan bei der Auswertung der Proben half und immer hilfsbereit war!

Ha sido una suerte y alegria grande poder haber trabajado con Dr. Onetsine Arrizabalaga de Mingo. Me has ayudado mucho, con profesionalidad, con entusiasmo y muy importante, con tu amistad! Muchas gracias por todo! Eskerrik asko!

Ringrazio di tutto cuore la Dr. Diana Pignalosa, collega, amica, consigliera (anche se secondo te non ho mai fatto quello che mi hai consigliato ☺), che mi ha aiutato tanto e che mi ha sempre motivato!

Herzlichst möchte ich auch Sabine Luft danken, die, wann immer Hilfe nötig war zur Seite stand und Doktorandenfreud und –leid mit mir teilte.

I would also like to thank the rest of our sub-group, Dr. Nerea Paz Gandiaga (that helped with microscopic analysis and motivated me always, eskerrik asko!), Dr. Elena Nasonova, Simon Frank and Dr. Ryonfa Lee (that unfortunately has left us to England) for the support and the nice atmosphere.

Thanks go to PD Dr. Michael Scholz and Dr. Thomas Friedrich for the technical support in the radiation experiments using the accelerator. I would like to thank Thomas also for his ideas concerning the mathematical modelling.

Dr. Emanuele Scifoni, la persona piu umane e pura che mai ho incontrato, lo ringrazio cordialmente per il suo valido contributo per il modello matematico e per tutto. Sei un grande!

Einen riesigen Dank möchte ich Dr. Anja Heselich aus der AG Layer aussprechen, die mich bereits auf vielen Etappen meiner „Karriere“ seit Anfang an professionell und freundschaftlich unterstützt hat und die sicher nicht ganz unschuldig an meiner Berufswahl war. Ich hoffe, dass wir auch weiterhin die Gelegenheit zur Zusammenarbeit haben werden!

Apart from the help one can experience directly connected to the work, there is always a contribution of persons on another, a social level, which is definitely not less important. The space here is not enough to do all of them justice but I would like to mention some people, that in their very individual ways especially contributed to this work and my life.

Primo, il mio carissimo amico Walter. Senza il tuo impatto in questi anni la maggioranza delle cose sarebbero state molto differenti, non scriverei oggi questo ringraziamento in quattro lingue e forse sarei ancora tedesco. Molte grazie per tutto, amico mio!

Jorge, que diria de te: scipio, fiel amigo e insustituible, mas que eso, mi hermano. Muchas gracias que me has sermoneado cuando lo necesitaba y que me has animado siempre cuando pasaba un bache! Has contribuido a esto mas de lo que piensas.

Samu, mi amigo, te agradezco las conversaciones en la maquina de cafe y por la confianza que me has dado siempre cuando estuve preocupado!

Francesco (Ciccio), che ha iniziato al GSI lo stesso giorno e nel mio stesso ufficio, ti ringrazio per tutto, amico mio!

Grazie di cuore anche a te, Palmina, la “pazza di Sessauronica”, il sole di Napoli, splendendo anche nella grigia Germania, che sempre sapevi rinfrancarmi!

Fabio ed Alessia, cari amici, i “nonni”, che sfortunatamente ci lasciano per ritornare in Sicilia, mille grazie di cuore a voi! Ci siete stati sempre per me. Mi mancherete!

Thanks to all my friends, in Darmstadt and Odenwald or meanwhile far away, from different nations, on whose support I could always count!

Einen enormen Dank möchte ich meiner Familie, ganz besonders meinen Eltern aussprechen! Ohne eure Unterstützung hätte ich weder studieren noch promovieren können! Den allerherzlichsten Dank!

Related reports and publications

Helm, A., S. Luft, P. Hessel, D. Pignalosa, M. Durante, P. Layer, D. Pollet, and S. Ritter. 2011. "Embryonic Stem Cell Derived Cardiomyocytes: A Model System to Study Cardiac Effects of Heavy Ion Exposure." *GSI Scientific Report 2010*.

Helm, A., D. Pignalosa, M. Durante, P. Layer, D. Szypkowski, and S. Ritter. 2012. "Embryonic Stem Cell Derived Cardiomyocytes: A Model System to Study Cardiac Effects of Heavy Ion Exposure." *GSI Scientific Report 2011*.

Luft, S., A. Helm, D. Pignalosa, P. Hessel, M. Durante, P. Layer, and S. Ritter. 2012. "Radiation Response of Pluripotent Stem Cells Derived From Early Mouse Embryos." *GSI Scientific Report 2011*.

Luft, S., A. Helm, P. Hessel, D. Pignalosa, S. Brons, P.G. Layer, M. Durante, and S. Ritter. 2013. "Impact of Ionizing Radiation on the Potency State of Murine Embryonic Stem Cells." *GSI Scientific Report 2012* (in press).

Luft, S., D. Pignalosa, E. Nasonova, A. Helm, O. Arrizabalaga, M. Durante, and S. Ritter. 2013. "Densely Ionizing Radiation Does Not Affect Pluripotency and Genomic Stability of D3 Mouse Embryonic Stem Cells." *Toxicology and Applied Pharmacology*: (submitted).

Materna, M., A. Helm, P. Hessel, J. Friess, C. Thielemann, D. Pignalosa, W. Maentele, M. Durante and S. Ritter. 2013. "First Electrophysiological Studies on Mouse Embryonic Stem Cell-Derived Cardiomyocytes." *GSI Scientific Report 2012* (in press).

Materna, M., A. Helm, M. Durante, W. Maentele, and S. Ritter. 2012. "First Electrophysiological Studies on Mouse Embryonic Stem Cell-Derived Cardiomyocytes." *GSI Scientific Report 2011*.

Ehrenwörtliche Erklärung

Ich erkläre hiermit ehrenwörtlich, dass ich die vorliegende Arbeit entsprechend den Regeln guter wissenschaftlicher Praxis selbstständig und ohne unzulässige Hilfe Dritter angefertigt habe.

Sämtliche aus fremden Quellen direkt oder indirekt übernommenen Gedanken sowie sämtliche von Anderen direkt oder indirekt übernommenen Daten, Techniken und Materialien sind also solche kenntlich gemacht. Die Arbeit wurde bisher bei keiner anderen Hochschule zu Prüfungszwecken eingereicht.

Darmstadt, den 30.04.13

Curriculum Vitae

Personal Data

Name	Alexander Helm
Address	Wingertsgasse 7, 64407 Fränkisch-Crumbach
Date of birth	29.04.1985
Place of birth	Erbach im Odenwald
Nationality	German

Education and Work Experience

1991-1995	Basic primary school, Rodensteinschule Fränkisch-Crumbach
1995-2004	Secondary school, Georg-August-Zinn-Schule, Reichelsheim
21.06.2004	Abitur
2005-2009	Studies of biotechnology at University of Applied Sciences, Darmstadt
15.12.2009	Diploma (Dipl.-Ing. (FH))
Since 02/2010	Ph.D. studies in biology at Technische Universität Darmstadt and GSI Helmholtzzentrum für Schwerionenforschung, Darmstadt, Supervisor: Prof. Dr. Marco Durante